ABSTRACT

Title of Document:	THE POTENTIAL OF NATURAL, PHOTOSYNTHETIC PIGMENTS TO IMPROVE THE EFFICIENCY OF DYE-SENSITIZED SOLAR CELLS Grenergy Eran Barnoy, Mark Conley, A. Stephen Gan, Yoni Gefen, Jana Lovell, Katherine Mann, Adin Shuchatowitz, Christine Tobin
Directed By:	Dr. Joseph Sullivan, PhD. Department of Plant Science and Landscape Architecture.

Current photovoltaic cells incorporate silicon or synthetic dyes; however, these cells are expensive and the dyes are toxic. Our project used natural, photosynthetic pigments to sensitize an alternative design solar cell, the dye-sensitized solar cell (DSSC). Research has shown that plant pigments are suitable sensitizers for these cells but there is presently no good rationale to determine which pigment combinations may be most effective. Our research goal was to develop and test an absorption index for pigment selection that would increase the output of DSSCs. Our results demonstrated a positive correlation between spectral absorption of the sensitizing dye and power output of the cell. Certain pigment combinations were more effective sensitizers based on combined absorption capabilities, but resolving the mechanisms of the exact relationship requires further research and likely further development of the algorithm used to choose optimal pigment combinations.

THE POTENTIAL OF NATURAL, PHOTOSYNTHETIC PIGMENTS TO IMPROVE THE EFFICIENCY OF DYE-SENSITIZED SOLAR CELLS

By

Eran Barnoy, Mark Conley, A. Stephen Gan, Yoni Gefen, Jana Lovell, Katherine Mann, Adin Shuchatowitz, Christine Tobin

"Thesis submitted in partial fulfillment of the requirements of the Gemstone Program, University of Maryland, 2011".

Advisory Committee:
Dr. Joseph Sullivan, Chair
Dr. Daniel Falvey
Dr. Raymond Adomaitis
Dr. Sheryl Ehrman
Mr. Jeff Gilbert

ACKNOWLEDGEMENTS

Support for this research was provided by the Gemstone Program, a grant from the Howard Hughes Medical Institute Undergraduate Science Education Program, funding from the Department of Plant Science and Landscape Architecture, and a grant from the Atlantic Coast Conference Inter-Institutional Academic Collaboration. We are especially grateful to the individuals who have helped make our research possible, such as Dr. William Kenworthy, Dr. Daniel Falvey, Dr. Brian Borak, and our team librarian, Nedelina Tchangalova. We would like to thank Dr. Joseph Sullivan for his guidance as he mentored our team through the research process. Finally, we would like to express our gratitude to Dr. Michael Grätzel for meeting with us and sharing his knowledge with us. His research on dye-sensitized solar cells inspired our study.

TABLE OF CONTENTS

LIST OF TABLES

LIST OF FIGURES

LIST OF EQUATIONS

1. INTRODUCTION

1.1. Energy Crisis

> "Now, to protect our planet, now is the time to change the way we use energy. Together, we must confront climate change by ending the world's dependence on fossil fuels, by tapping the power of new sources of energy like the wind and sun, and calling upon all nations to do their part."
>
> - President Barack Obama, April 2009

1.1.1. Climate Change

In the past century, human activity has created undeniable and unprecedented climate changes. The global average surface temperature has increased by 0.6°C over the past century, leading to a 10% decrease in the extent of snow cover, widespread retreat of mountain glaciers, and a 40% decline in Arctic sea-ice thickness (Figure 1.1) (*1*). With extensive melting of glaciers and ice, the global average sea level has risen almost 0.2 meters in the past century alone (*2*). Further, in the past 15 years, the sea level has risen at double the rate experienced over the past century (*2*).

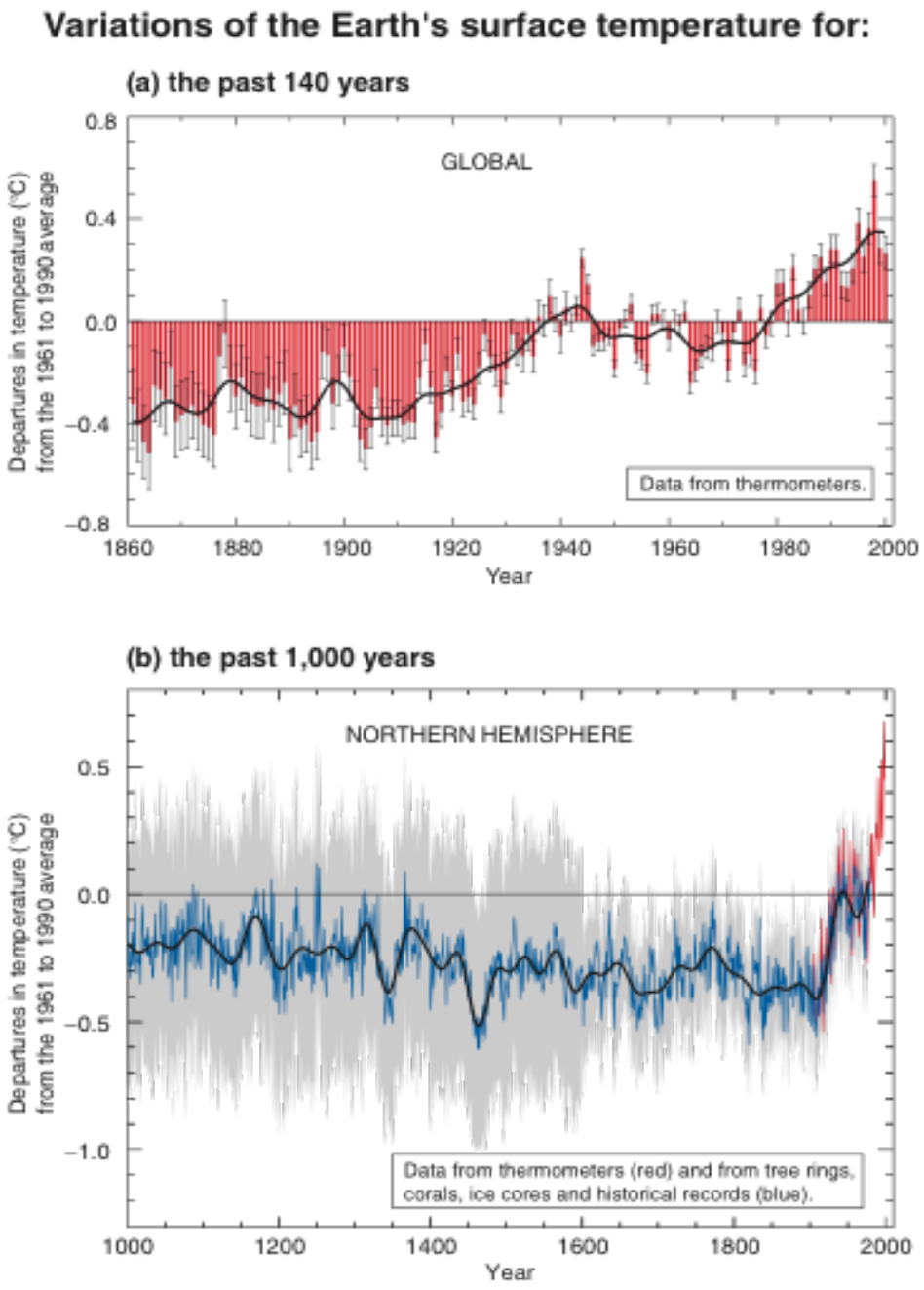

Figure 1.1: Variations of the Earth's surface temperature over the last 140 years and the last millennium. (a) The red bars show the Earth's surface temperature year-by-year and the black line shows the Earth's surface temperature according to decade. Global average surface temperature has increased by 0.6±0.2°C. (b) The blue curve represents variations of the average surface temperature of the Northern Hemisphere year by year and the black curve shows the 50 year average variations of the average surface temperature of the Northern Hemisphere for the past 1000 years (*1*).

The warming of the Earth's surface and subsequent rising sea levels cannot be attributed to natural forces alone. Although the energy emitted from the sun follows an 11-year cycle with steady increases and decreases, there is no net increase in the energy absorbed at the top of the Earth's atmosphere (*2*). Thus, small increases in the sun's energy cannot be culpable for large increases in the global surface temperature. Instead, human activity continues to be the primary contributor to global warming (*2*). Global warming is attributed to positive radioactive forcing largely induced by increases in greenhouse gases including carbon dioxide, methane, and nitrous oxide (Figures 1.2 and 1.3) (*2*). Since 1750, atmospheric levels of carbon dioxide have increased by almost 31% and continue to rise at unparalleled rates. The burning of fossil fuels has contributed to almost 75% of the anthropogenic emissions of carbon dioxide in the past 20 years (*1*). Over the past decade, global emissions of carbon dioxide have increased to a growth rate of 3.3% per year, compared to a 1.3% per year growth rate in the 1990s (*2*).

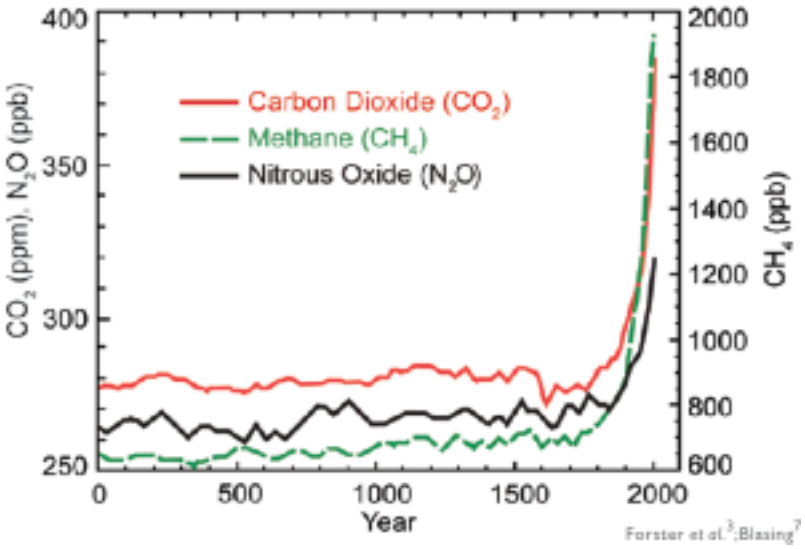

Figure 1.2. Greenhouse Gas Concentrations. Changes in three of the most important atmospheric trace gasses over the past two thousand years (2).

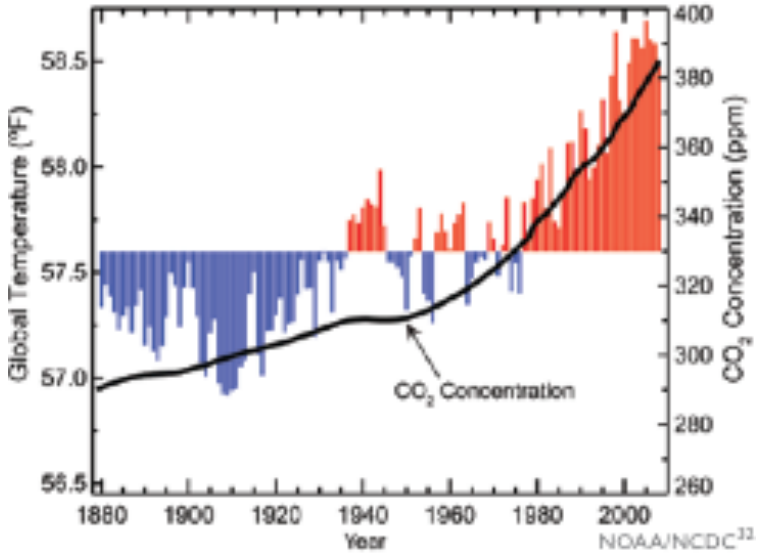

Figure 1.3. Global Temperature and Carbon Dioxide. The relationship between atmospheric CO_2 concentration and departure from mean global temperature average. Red bars indicate temperature above and blue bars indicate temperatures below the average temperature for the period 1901-2000. The black line shows atmospheric carbon dioxide concentration in parts per million (*2*).

In addition to likely increases in global temperatures in response to increases in CO_2 and other trace gases, there may be a suite of other potentially negative effects on the earth. For example, as oceans absorb more carbon dioxide, seawaters become less alkaline in an irreversible process of ocean acidification. The acidification of ocean waters has negatively affected many oceanic species and ecosystems that rely on calcification for survival (*2*). Increased carbon dioxide emissions have also altered precipitation patterns, with notable increases in precipitation in eastern North America, southern South America, and northern Europe in the past century (*2*). Moreover, extreme natural events, like heat waves, regional droughts, and hurricanes, have become more common in the past 50 years (*2*).

Recent projections of the long term effects of increasing carbon dioxide emissions and warmer temperatures predict changes in precipitation and sea level on a global scale. Precipitation is projected to increase in northern areas and decrease in southern regions of

Earth, and heavy precipitation will likely increase in the wettest regions. The intensity of Atlantic hurricanes and cold-season storms is predicted to increase in the 21st century. Heat waves will continue to increase in intensity, frequency, and duration. As the global surface temperature rises, melting of Arctic sea ice is likely to continue to increase (Figure 1.4). The 2007 assessment by the IPCC predicts global sea levels will rise 8 inches to 2 feet by the end of the 21st century. Other models predict that, with increased carbon dioxide emissions, sea levels will rise 3 to 4 feet by the end of the century (*2*).

Greenland and Antarctica contain the largest ice sheets in the world. Increased melting of these ice sheets, resulting in decreased ice volume, is contributing to rising sea levels. In the event that the entire Greenland Ice Sheet melted completely, worldwide sea level could rise almost 20 feet. The Antarctic Ice Sheet is divided into two parts, the West Antarctic Ice Sheet and the East Antarctic Ice Sheet. Global sea levels would increase by 16 to 20 feet with complete melting of the West Antarctic Sheet and 200 feet with the melting of the East Antarctic Sheet (*2*).

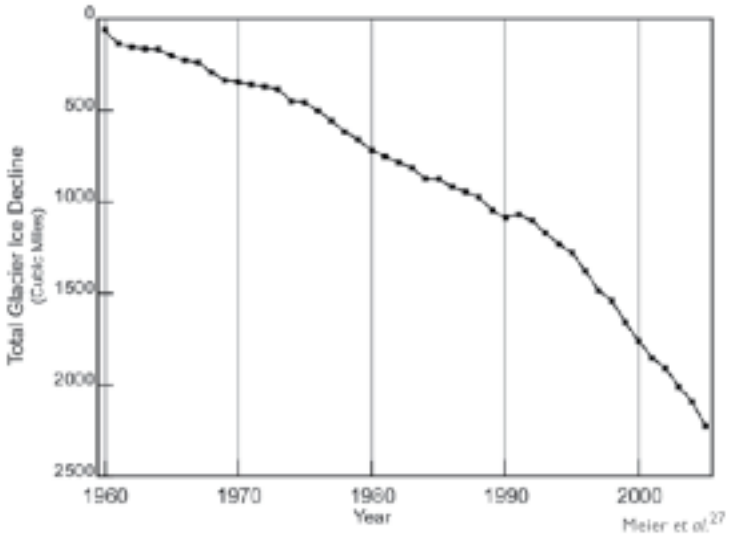

Figure 1.4. Cumulative decrease in global glacier ice since 1960 (*2*).

1.1.2. Fossil Fuels

Since the beginning of the industrial era in the mid-1700s, the atmospheric carbon dioxide concentration has risen exponentially due largely to the burning of fossil fuels and biomass (see Figure 1.3) (*2*). By 1951, petroleum surpassed coal in annual U.S. consumption, and by 1960 (Figure 1.5), the import of petroleum became necessary for continued consumption (*3*). Between 1950 and the 1973, U.S. oil consumption doubled, eventually reaching 33% of global oil consumption, even though the U.S. comprised only 6% of the global population (*4*). By 1973, the U.S. was importing 6.3 million barrels of petroleum each day and becoming more dependent on foreign oil (*3*).

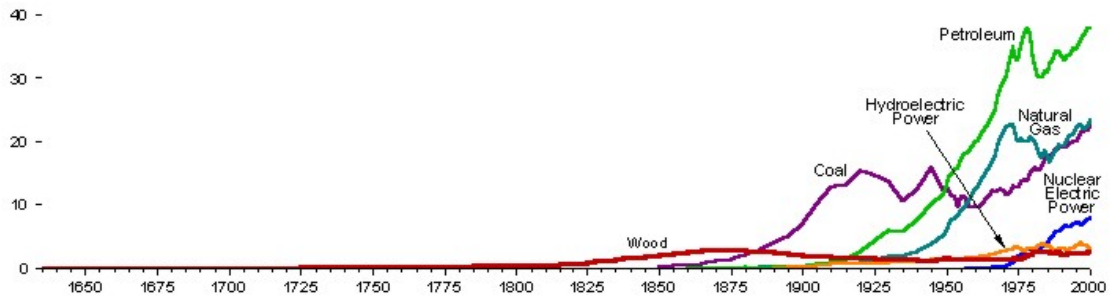

Figure 1.5. Energy consumption by source, 1635-2000 (Quadrillion BTU) in the United States (*3*).

1.1.3. 1973 OPEC Oil Embargo

In addition to the environmental effects induced by rising levels of carbon dioxide and use of fossil fuels, the increasing demand for a limited supply of petroleum has led to political and international turmoil. The growing reliance on imported fossil fuels was first exposed by the oil crisis that occurred from 1973 to 1974. In 1973, the members of the Organization of Petroleum Exporting Countries (OPEC) sanctioned an oil embargo against the United States (*4*). The embargo quickly caused gas prices at the pump to quadruple and crude oil prices to increase almost ten times in the U.S. (*5*).

The embargo was particularly detrimental because, in addition to dependence on foreign oil, the United States was confronted with growing oil consumption along with diminishing domestic oil reserves. The initial effects were worsened by price controls sanctioned by the U.S. government. The price controls lowered the price of old oil and increased the price of newly discovered oil, inadvertently eliminating old oil from the market and creating "artificial scarcity" of available oil (*4*).

In response to the effects of the embargo, the U.S. government initiated Project Freedom to promote domestic energy independence. Though the oil embargo was lifted in March of 1974, only six months after it was initiated, the effects of the embargo lingered. President Richard Nixon appointed William Simon the official "Energy Czar" and created the Department of Energy in 1977 to help reduce oil consumption (*4*). Since the oil crisis of 1973, research in alternative energies has intensified with a goal to alleviate dependence on fossil fuels. Nevertheless, by 1975, U.S. petroleum consumption began to increase again, reaching 18.8 million barrels per day in 1978 and 19.4 million barrels per day in 2000, with 10 million barrels being imported daily (*3*).

1.1.4. Deepwater Horizon Oil Spill

Beyond the political issues that arise with consistent reliance on petroleum and other fossil fuels, the environmental and social impact of fossil fuels further complicates their use. Particularly, the drilling and transportation of oil is frequently hampered by environmentally catastrophic spills, notably the 1989 Exxon Valdez spill off the coast of Alaska and, most recently, the Deepwater Horizon disaster in the Gulf of Mexico. In both situations, countless gallons of oil spilled into the world's waters, wreaking havoc on fragile ecosystems. In the summer of 2010, an explosion in an offshore rig operated

by British Petroleum (BP) created a leak that soon began releasing 5,000 barrels of oil a day into the Gulf. Estimates indicate that up to 7 million barrels of crude oil emptied into the Gulf before the leak was finally capped almost 3 months following the initial accident (*6*).

That oil spill has negatively affected the fishing and tourism economies in states adjacent to the Gulf of Mexico (*7*). On May 24, 2010, U.S. Commerce Secretary issued a "fishery disaster" in Gulf States including Louisiana, Mississippi, and Alabama due to the economic impact of the spill. The effects of the spill on wildlife have yet to be accurately determined. The Unified Area Command issued its first Consolidated Fish and Wildlife Collection Report on May 30, 2010. Of 1,746 dead and living birds captured, 1,014 were covered in oil. The Exxon Valdez spill left 350,000 to 600,000 birds and thousands of other wildlife dead, and wildlife biologists estimate that similar numbers of casualties will ultimately result from the BP spill (*7*).

Following the initial public outcry and media frenzy over the oil spill, there is a lack of political or legislative action to prevent future catastrophes by alleviating reliance on fossil fuels. For example, *Time* magazine recently stated:

> "the carbon cap-and-trade bill, just being introduced to the Senate back in May, has died without a vote. The Presidential moratorium on new deepwater drilling was lifted early this fall, before the official government report on the causes of the spill even came out. Congress never managed to pass legislation that would have overhauled drilling safety, nor did it make any new laws that would have helped move the country off fossil fuels (*8*)."

Thus, despite the disastrous environmental and economical effects of the spill, deepwater oil drilling is able to continue in order to satisfy the U.S.'s dependence on oil.

1.1.5. Government Policy

Although reliance on fossil fuels has increased in the past century, a few recent laws have promoted independence from fossil fuels and the development of clean, alternative fuels. The Energy Policy Act of 1992 granted financial incentives for consumers of and companies that built clean-fuel vehicles (*9*). The Energy Policy Act of 2005 promoted energy conservation and efficiency, as well as encouraged the development and use of renewable alternative energies. It also provided tax incentives to businesses and individuals for reducing energy needs and using alternative fuels. Specifically, Title IX encouraged the development of advanced technologies such as biofuel production. The Energy Independence and Security Act of 2007, or the Clean Energy Act, further promoted the improvement of energy use and the development of alternative fuels. The law required the use of 36 billion gallons of ethanol by 2022 and designated a minimum corporate average fuel economy standard of 35 miles per hour by 2020. The 2007 Act allocated $240 million per year from 2008-2012 for research into carbon capture and sequestration and $200 million per year for research involving the capture and purification of carbon dioxide released from industry sources. It also created various efficiency standards for appliances, lighting, and motors. With increased government funding, more research and development projects have focused on improving the efficiency of current alternative fuels (*9*).

1.2. Alternative Fuels

1.2.1. Biofuels

In 2005, the use of renewable energy was 6.6% of total U.S. energy consumption, with biofuels comprising just 10% of all renewable energy use. The most common liquid forms of biofuels are bioethanol and biodiesel. Bioethanol is commonly produced from the fermentation of crops like sugarcane, corn, and sugar beets, while biodiesel is produced from vegetable oils, animal fats, or waste cooking oils (*10*). Both biofuels are environmentally beneficial because they are biodegradable, locally available, and their use does not contribute to a net increase in atmospheric carbon dioxide levels. Further, biodiesel contains less sulfur dioxide and aromatic compounds than conventional diesel. Biodiesel use also reduces carbon dioxide emissions by 14%, carbon monoxide emissions by 17.1%, and smoke density levels by 22.5% compared with diesel to produce the same amount of energy. Ethanol is often used as a gasoline additive, reducing petroleum consumption for transportation. Similarly, biodiesel can be readily substituted for conventional diesel fuel in diesel engines (*11*).

However, because biofuels are largely produced from crops, the environmental impact of their production must be considered. Extended production of biofuels can result in loss of cropland for food production and increased food prices, deforestation, biodiversity extinction, soil degradation by erosion, and water depletion (*12*). Further, fossil fuels are required to produce fertilizer for the crops, and the fertilizer can release nitric oxide and other components with high Global Warming Potential into the environment (*12*). For example, the high levels of nitrogen used in corn production and fertilization requires large energy inputs and leads to increased nitrogen run-off. Thus,

the large-scale production of ethanol from corn may not have a positive impact on total carbon emissions and can exacerbate existing water problems because of increased nitrogen release to the environment (*13*).

Moreover, the production of high-quality fuel ethanol requires energy input of almost 80% of the energy value of ethanol. Compared to gasoline, ethanol production is energetically more costly in all regions except Brazil, where sugar cane is plentiful (*10*). Further, both bioethanol and biodiesel production are limited by high input cost of production. Feedstock accounts for 66% and 75-80% of the total operating costs of bioethanol and biodiesel production, respectively (*10*). In developed countries, the production cost of biofuels is up to three times higher than that of petroleum. Ultimately, due to their expensive cost, biofuels cannot compete effectively with conventional fuels in the U.S.

1.2.2. Wind Energy

Wind energy has increasingly been used as a source of alternative energy since the capacity of wind energy has continued to rise. By the end of 2009, worldwide capacity reached 159,213 MW, with a growth rate of 31.7% in wind power in that year alone. The typical generating capacity for wind turbines is 20-35% (*14*). Since most countries meet the standards for the wind levels required for wind energy, wind energy remains a feasible alternative internationally (*15*).

However, the potential of wind energy to become a major contributor to current energy consumption is limited by several factors. The efficiency of wind energy is affected by wind availability and the size of the turbine system (*14*). During times of low wind levels, the generating capacity of turbines declines. For example, wind plants

cannot generate enough energy to match demand in the winter and summer months, since electricity use is high but wind levels are low (*14*).

Other factors further prevent wind energy from being an effective competitor of fossil fuels. Wind energy, at its cheapest, can cost only four cents per kilowatt-hour, but this cost achievement is only possible through the latest wind turbine models (*15*). In addition, in order to generate sufficient power and prevent wake interaction effects, large numbers of wind turbines must be spaced adequately over large areas of land (*15*). But, the public is concerned about the construction and use of wind turbines because of unpleasant noise and aesthetics, which interferes with land requirements (*15*). Wind power also requires a suitable infrastructure to connect wind power plants to existing electricity systems. In the absence of a functional network, the cost of implementation rises with the construction of expensive lines and substations (*15*).

Although wind power does not produce emissions harmful to the environment, wind turbines, which require large rotating blades, have been shown to have significant negative ecological effects, primarily on local animals. Noticeable bird and bat fatalities have occurred due to wind turbines, raising concern about potential population impacts on particular species (*16*).

Many studies have asserted that one of the major advantages of wind energy is the short energy payback time of wind turbines (*15*). However, a recent 2009 study has found that the methods used to determine payback time are unreliable and show variability in their results (*14*). The current trend in wind energy technology is to increase the size of turbines and, in effect, increase the output of the turbines. However,

larger turbine sizes lead to an increase in the quantity of materials and energy required for turbine manufacture without a sufficient increase in energy yield (*14*).

1.2.3. Wave Energy

Since the 1970s, interest and research concerning the potential of wave energy has increased. Wave energy is most feasible in areas near long oceanic coastlines, although recent models are focusing on offshore developments to increase the availability of wave energy to inland areas. Wave energy is more advantageous than wind energy because it has a higher energy density and is more predictable (*17*).

While research into an array of different models continues, concerns about the utilization of wave energy swell. Wave energy is primarily limited by variance in wave power, ranging from day to day, season to season, and year to year (*18*). In order to generate waves sufficient to produce a useful source of energy, strong winds must be present. Wave power further depends on the local climate, the amount of solar energy transferred to waves, and the distance and duration of the winds (*18*). Although wave energy is influenced by several uncontrollable factors, no control back-up systems exist for when wave power declines.

The ecological impact of offshore renewable energy developments additionally restricts the potential of wave energy. Offshore developments can have ecological footprints ranging from several to more than fifty square kilometers of water (*19*). These ecological effects are further expounded when developments are located adjacent to each other. Thus, before offshore generators can be constructed, additional research must be conducted to examine the effects on marine habitats. Yet, field research in marine

environments is limited because it is "costly and requires advanced underwater technologies" (*17*).

1.2.4. Nuclear Technology

According to estimates by the International Atomic Energy Agency, nuclear energy accounted for 13 to 14 percent of the global electricity demand in 2009 (*20*). However, the percentage of global nuclear electricity production has declined over the past decade due to the shutdown of large nuclear reactors (Figure 1.6). In 2008, nuclear energy contributed 13.5 percent to world electricity production compared to 16.7 percent in 2000 (*21*). By December 2009, 436 reactors remained out of the 444 running in 2002 (*21*). There has been little growth in nuclear technology due to the cost of nuclear power compared to coal and natural gas, declining investment in research and development, and reduction in the workforce. In addition, nuclear power is limited by the rising costs of nuclear plants operations, the cost of nuclear waste management, and unfavorable electricity cost comparisons with coal and natural gas. Since 2003, the construction costs for nuclear plans have risen exponentially. A 2003 study conducted by the Massachusetts Institute of Technology concluded that nuclear power is not an economically competitive choice, as it is more expensive than both coal and natural gas (Figure 1.7) (*21*).

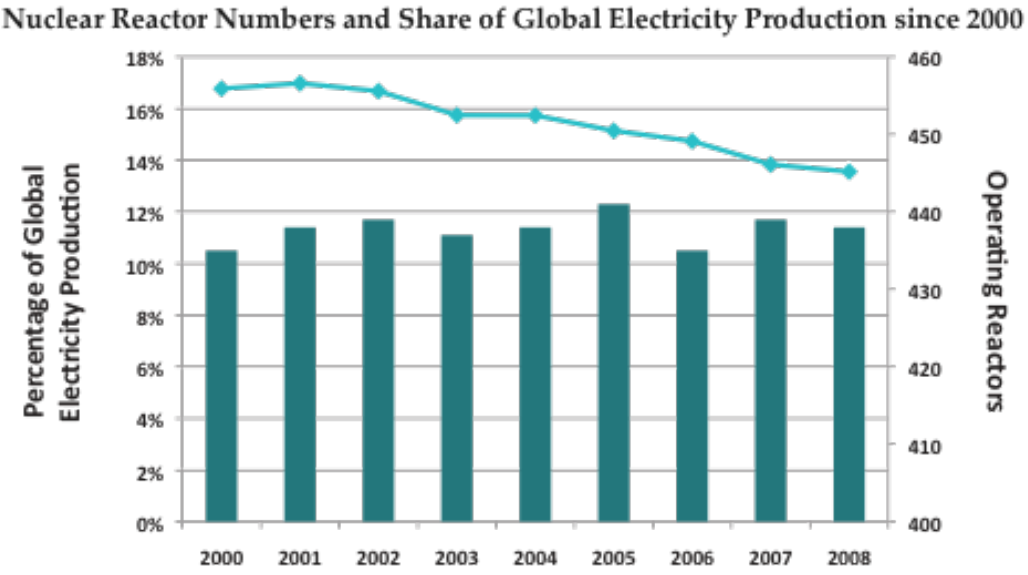

Figure 1.6. The blue line depicts the number of operating nuclear reactors since 2000. The green bars represent the nuclear percentage of global electricity production each year between 2000 and 2008 (21).

Costs of Electric Generation Alternatives

	Over-night Cost	Fuel Cost	Base Case	With carbon charge $25/ton CO_2	With same cost of capital as coal/gas
	$/kW	$/million BTU	¢/kWh	¢/kWh	¢/kWh
2003 (2002 USD)					
Nuclear	2,000	0.47	6.7	n/a	5.5
Coal	1,300	1.20	4.3	6.4	n/a
Gas	500	3.5	4.1	5.1	n/a
2009 (2007 USD)					
Nuclear	4,000	0.67	8.4	n/a	6.6
Coal	2,300	2.60	6.2	8.3	n/a
Gas	850	7.00	6.5	7.4	n/a

Figure 1.7. Costs of nuclear, coal, and gas energy sources compared in 2003 and 2009. (*21*).

Additionally, the use of fission and fusion technology is limited by safety hazards, including the environmental release of radioactive nuclides. Before nuclear technology can be effectively employed, safety issues must be addressed. Radioactive waste must be disposed of in underground repositories that "afford efficient containment so to prevent

the escape of radioactive species to the biosphere" (*22*). However, plans for the development of repositories often met with opposition, as in the proposed site at Yucca Mountain in Nevada that was halted due to political resistance (22).

Foreign relation issues further exacerbate the research in and availability of nuclear technology. Fuel and some by-products from Nuclear power generation can potentially be used to produce nuclear weapons and must be adequately regulated. President Barack Obama recently asserted the necessity to secure nuclear material within four years in order to ensure global security from nuclear attack (*23*). Before nuclear power can be exploited as a useful source of energy, President Obama calls for a global ban on nuclear testing and a "new framework for civil nuclear cooperation, including an international fuel bank, so that countries can access peaceful power without increasing the risk of proliferation" (*23*). Even with international cooperation, the threat of nuclear terrorism persists as nuclear technology continues to be sold in the black market.

1.3: Solar Energy

Solar energy has the largest potential of all the alternative energies. However, due to the high cost of photovoltaics, solar energy's leading technology, harnessing solar energy is out of reach for most of the population. Solar energy has been utilized for millennia and studied in depth for centuries. In the last two centuries, photovoltaics have jumped from hypothesis to reality, and in the last fifty years, spurred by oil crises and the development of nanotechnology, solar energy is now a $7.5 billion industry growing at a rate of 35–40% per annum (*24*).

In comparison to the other alternative and renewable energies, no other type of energy is as renewable, available, or primary as solar energy. Man has been able to harness solar energy to heat buildings and water since the time of the Romans in the first century A.D. Horace de Saussure developed the first solar collector used for cooking in 1767 and modern photoelectric theories began in 1839 when Edmond Becquerel discovered the photovoltaic effect (*25*). In 1883 Charles Fritts created the first solar cell made with selenium, and in 1905 Albert Einstein published his papers on the Theory of Relativity and the Photoelectric Effect, which explained Max Planck's discovery of black body radiation (*25, 26*). Einstein won the Nobel Prize for these papers in 1921. In 1954, scientists at Bell Laboratories developed the silicon photovoltaic cell of the same design used today (*27*).

Several factors must be understood in order to comprehend the development of solar energy technology for uses ranging from heating Roman baths to providing energy for satellites two-thousand years later. These factors include the process of harnessing the sun's energy, the legislative and technical developments leading to our modern solar energy industry, and the obstacles that the industry faces now and in the future.

1.3.1 The Sun

The sun is the principal source of energy for Earth (*24*). In *The Problem of Increasing Human Energ*y, originally published in Century Illustrated Magazine in June 1900, Nikola Tesla repeatedly emphasized the importance of harnessing the sun's energy. Even at that time he realized our need for energy-driven processes,

> "that all the objects about us are manufactured by machinery: the water we use is lifted by steam-power, the trains bring our breakfast from distant localities; the elevators in our dwelling and our office building, the cars that carry us there, are

> all driven by power, in all daily errands, and in our very life-pursuit, we depend upon it" (*28*).

Due to this reliance on machinery and the vast potential of technological developments, Tesla instructed that, "whatever our resources of primary energy may be in the future, we must, to be rational, obtain it without consumption of any material" (*28*). The chief way to produce energy without consuming material is through the sun. Tesla believed in the sun's potential so greatly that he poetically wrote,

> "First let us ask: Whence comes all the motive power? […] All this energy emanates from one single center, one single source—the sun. The sun is the spring that drives all. The sun maintains all human life and supplies all human energy. Another answer we have now found to the above great question: To increase the force accelerating human movement means to turn the uses of man more of the sun's energy" (*28*).

The sun indirectly provides the energy for essentially all life on earth through photosynthesis and heat, and thus has continually been given scientific interest and consideration. Even over one hundred years ago, science knew that harnessing the power of the sun is essential to support human development.

The sun provides the Earth with all the energy necessary for life. The sun constantly provides 120,000 terawatts (TW) of radiation on the surface of the Earth (*24*). In comparison, the entire world consumes 13 TW of power. Thus, the sun's energy is "far exceeding human needs even in the most aggressive energy demand scenarios." As the "Earth's natural power source," the sun provides an "energy stream far more potent than present-day human technology can achieve" (*24*). The power of the sun is so great that "covering 0.16% of the land on Earth with (only) 10% efficient solar conversions systems would provide 20 TW of power, nearly twice the world's consumption rate of fossil energy and the equivalent of 20,000 1-GW_e nuclear fission plants" (*24*). While it is

clear that there are vast amounts of solar energy available and that solar technology holds great potential, the hurdles of solar technology are also great, beginning with harnessing the energy itself.

1.3.2. Harnessing Solar Energy

Though Tesla did not know the exact method for harnessing solar energy in 1900, he knew that "an inexhaustible source of power would be opened up by the discovery of some efficient method of utilizing the energy of the rays" (*28*). Solar energy can be harnessed through solar electric, solar fuel, and solar thermal systems.

Solar electric technology is the most common form of solar energy and consists of photovoltaic cells, often simply called solar cells. Solar fuel consists of any fuel made by the sun, "converting solar photons into chemical fuel" (*29*). Solar fuel systems include fuels made by the natural processes of photosynthesis and microbial anaerobic fermentation such as biomass and biofuels, as well as fuels produced by the metabolic pathways of genetically modified organisms like algae and *E. coli*. Artificial photosynthesis and non-biologically based photoelectrochemical conversion also create fuels by harnessing the power of the sun.

Solar thermal systems utilize heat from the sun through concentrated sunlight. After being concentrated with mirrors, sunlight in towers can reach 1500° C or greater (*29*). Solar thermal systems include solar water heating, heat engines, and thermo-chemical water splitting. Solar water heating is used to heat water around the globe, and heat engines can be used to drive steam engines and solar thermal electricity plants. Solar electricity generated from these steam engines produce the "cheapest solar electricity" (*29*). Thermo-chemical water splitting, which involves a reaction that is

thermodynamically very unfavorable, is possible using the high temperatures of sunlight generated by solar thermal systems (*29*).

While solar thermal and fuel systems do provide viable and useful forms of energy, recent developments in nanotechnology have provided the opportunity for improvements to solar electrics and their efficiency of converting sunlight into useable energy.

1.4. Photovoltaic Technology

1.4.1. The Beginning

Daryl Chapin, Calvin Fuller, and Gerald Pearson began working on the first photovoltaic cell at Bell Laboratories in 1952. Initially Chapin was instructed to design a cell to replace "traditional dry cell batteries, which worked fine in mild climates, (but) degraded too rapidly in the tropics and ceased to work when needed" (*27*). Early experiments with selenium solar cells achieved low conversion efficiencies, or the percent of incident light striking a solar cell that is converted into useable electrical power.

Pearson instructed Chapin to change his material to silicon after Pearson himself discovered the benefits of the "introduction of impurities necessary to transform silicon from a poor to a superior conductor," meaning combining other elements into silicon to allow it to better carry a current (*27*). With these adjustments, this silicon cell reached 6% conversion efficiency, but did not reach its calculated potential of 23% due to effects of the chemical instability of the lithium-doped silicon (*27*).

With the silicon cell's failure to reach its full potential, research was temporarily abandoned. Then, Bell's competitor, RCA, developed the atomic battery that generates power from strontium-90, now "classified as one of the more hazardous constituents of nuclear waste" (*27*). With pressure to "produce something newsworthy," Fuller increased the efficiency of his solar cells by cutting silicon into strips and using arsenic and boron to produce a p-n junction close to the surface of the silicon (*27*).

By 1954 Bell Laboratories had a finished product. Although it still did not reach the 23% optimal conversion efficiency, the New York Times stated that "the construction of the first solar module to generate useful amounts of power marks 'the beginning of a new era, leading eventually to the realization of one of mankind's most cherished dreams—the harnessing of the almost limitless energy of the sun for the uses of civilization'" (*27*). This is the same design currently used today in the silicon solar cell.

1.4.2. How Photovoltaic Cells Work

Photovoltaic cells are semiconductors that capture solar energy in the form of photons and release these as electron flow or electrical power (Figure 1.8). The wave-particle model of light describes light as consisting "of discrete particle-like packets of energy called photons" (*24*). The available energy of a given photon is a function of its frequency, so all photons do not contain the same amount of energy. The energy available is usually measured in electron volts (eV), and the energy within the visible spectrum (ranging in wavelengths from about 400 nm to about 700 nm) varies from about 3.0 eV to 1.8 eV (*24*). However, the peak irradiance present on the surface of the earth lies in the region of the solar spectrum at about 2.4-2.2 eV (500-550 nm) with the number of photons present dropping off dramatically at the shorter, but more energetic

wavelengths. In order to maximize photoconversion, it is important for a photovoltaic cell to absorb light at the higher energy levels as well as across the entire visible spectrum since the total energy depends on the energy of each photon and the number of photons reaching the cell (*30*).

The first reaction in a photovoltaic cell occurs when a photon from the sun (or other light source) strikes the photovoltaic cell. This photon can pass through the cell, be reflected away, or be absorbed. In order to induce the photoelectric effect that converts light energy into electrical energy, the photon must be absorbed (*30*). Thus, the semiconductor in the photovoltaic cell only absorbs photons carrying at least a given minimum energy. This energy is defined as the minimum energy required to elevate the energy of the outer valence electron across the band gap, or energy state where no electron exists, to the next higher conductive level or energy state. In this way, only photons with energies above the band gap are absorbed (*24*). Silicon, the semiconductor used in conventional solar cells absorbs only electrons with energy greater than 1.1 eV (32). There are two layers of the semiconductor as seen in Figures 1.8 and 1.9.

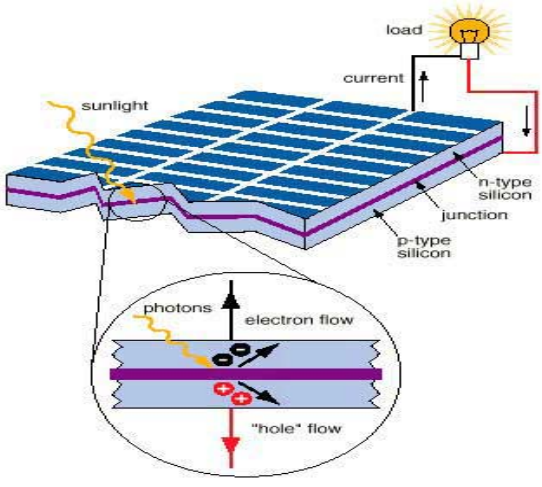

Figure 1.8. Generation of electric current in a traditional solar cell. The sunlight hits the semiconductor, which excites an electron, creating an electron hole causing a separation of charges and subsequently electron flow, or current (31).

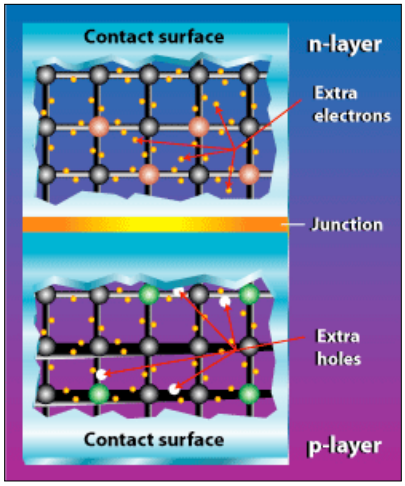

Figure 1.9. N (negative) and P (positive) layers of photovoltaic cell (33).

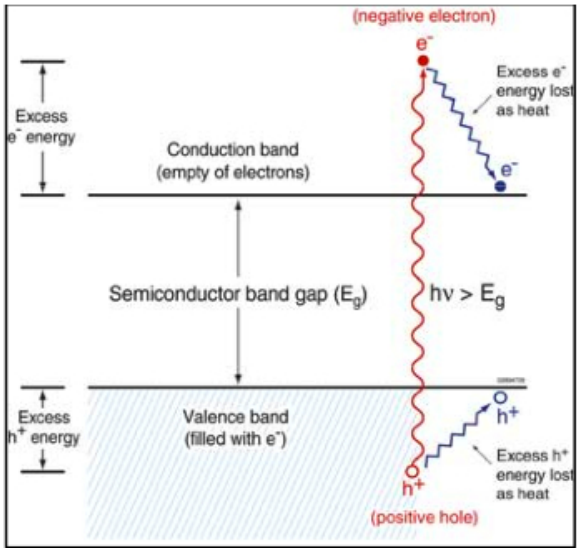

Figure 1.10. When a semiconductor absorbs the energy of a photon, excited electrons move from the valence to the conduction band (24).

The energy of the electrons ("e-" in the figure) in the valance level (lower electron in the figure) and next higher energy conductive level (upper portion of Figure 1.10) is called a band, and more importantly, the energy difference between these levels is called a band gap. Therefore, for a photon to be effective in inducing a current it must contain energy equivalent to that required to cross the band gap and reach the conductive level.

When a photon of sufficient energy is absorbed by the valence electron, the energy is transferred precisely into that electron elevating its energy to the "excited" state of the conductive level, which was previously empty of excess electrons. Once electrons are in the conduction band, they are bound to their atoms more loosely. This reduction in the energy binding the electron to the atom means that, although the atom maintains its neutral charge, the electron can more readily move from the atom to a nearby atom and so produce a current and a voltage.

During the construction of a photovoltaic cell, each layer of the semiconductor is 'doped' with another element in order to change the ability of the semiconductor to conduct electricity. Doping is the "process of adding impurities to the silicon, (and) is used to increase the activity of free electrons." A layer of semiconductor that has been doped to contain more electrons in the conduction band than the pure semiconductor is called an n-layer, where the "n" refers to the negative charge carried by the electrons (not the atoms). A layer of semiconductor doped to contain fewer electrons in the conduction band than the pure semiconductor has a greater number of "holes", or positions of a lack of electrons in the conduction band that thus have a positive charge, and is so called the p-layer (*24*). Neither layer is electrically charged, but the two layers sandwiched next to each other form what is called a p-n junction. In the p-n junction there is a separation of charge, which induces an electric field. This electric field provides voltage which helps push the current of photon-excited electrons through the field and eventually creates electricity as described above (*30*). Doping silicon with phosphorous provides the silicon with excess electrons to serve as the n-layer, and doping with boron provides the silicon with excess holes to serve as the p-layer (*31*).

The entire process of converting light to electrical energy as described is for inorganic photovoltaic cells primarily. In addition to these inorganic photovoltaic cells, the same general concept of photon-excited electrons, with slight variations, applies to other types of photovoltaic cells called organic and dye-sensitized solar cells. In organic semiconductors, the electrons and holes "are initially bound to each other in pairs called excitons, (which) must be broken apart in order to separate the electrons and holes to generate electricity" (*24*). The reaction in dye-sensitized solar cells is more complex, and will be described in the next section as well as in the literature review.

1.4.3. Uses of Photovoltaic Cells

In 1955 Western Electric began to sell licenses for silicon photovoltaic technologies. Some of their products included computer punch card decoder devices and dollar bill changers, all powered through photovoltaics (*25*). The first solar heated office building was designed around the same time by architect Frank Bridges. For the next two decades, scientific developments continually increased the conversion efficiency of silicon solar cells. Finally, in the 1970s, Eliot Berman, with help from Exxon, increased the efficiency to cost ratio and brought the price of solar electricity from $100/watt to $20/watt (*25*).

According to the U.S. Department of Energy Solar Timeline, commercialization of solar energy in the 1950s and 1960s failed. However, during this same period, NASA pioneered the use of solar cells using photovoltaics to power devices in satellites. In 1958 the Vanguard I used a photovoltaic array that generated more than one watt to power its radios (*25*). By 1978, NASA's Lewis Research Center developed a 3.5-kilowatt photovoltaic (PV) system, and the Department of Energy was created in 1977

along with the National Renewable Energy Laboratory (NREL) (*25*). According to the Department of Energy, solar energy "became the accepted energy source for space applications and remains so today" (*25*). Other modern applications include lighthouses, solar powered calculators, and of course solar panels for homes and buildings. While these applications are of fairly small scale, photovoltaics are also currently a major part of renewable electric plants.

NREL's 2000 Technical Report on the Renewable Electric Plant Information System (REPiS) describes the REPiS database and the contributions of each type of renewable energy. In 1999, photovoltaics contributed 90 MW from 866 units (*34*). In the 1980s the government installed large photovoltaic systems, but more recently, smaller and more numerous systems have been implemented. In the late 1990s when this report was written, the United States' economy was on the rise, which allowed expensive photovoltaic energy to emerge as a viable alternative energy source. The production of solar energy has risen from essentially zero (0) to 15,000 kW between 1980 and 2000 (Figure 1.11).

In most production schemes, increased production leads to decreased per-unit cost. The prices of PV modules have followed this trend: "for every doubling of the total cumulative production of PV modules worldwide, the price has dropped by approximately 20%," this is referred to as the '80% learning curve' (*24*). In 1997 President Bill Clinton announced an initiative to have 1 million solar roofs installed by 2010 through public-private partnerships (*34*). Therefore the use of solar energy to produce electricity appeared to increase dramatically by the turn of the century.

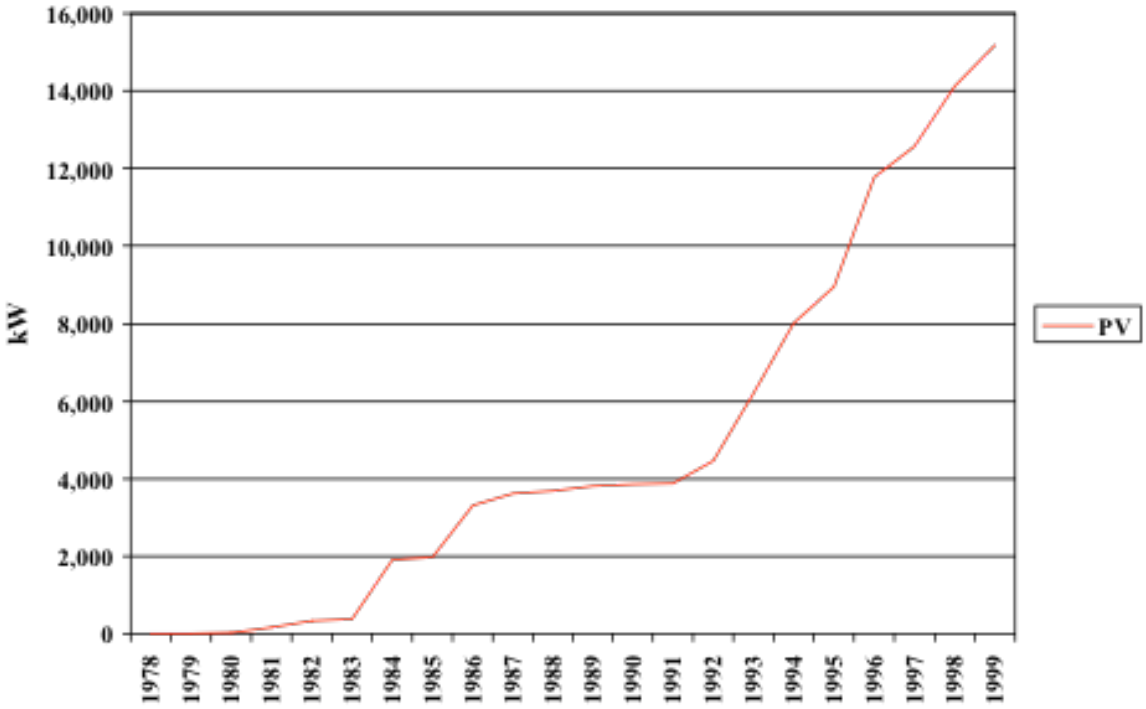

Figure 1.11. Kilowatts of power generated by photovoltaics from 1978-1999 (34).

1.4.4. Problems with Photovoltaic Cells

While the use of photovoltaic technology has increased and the cost has decreased immensely since the 1970s, the cost of electricity generated by photovoltaics needs to be reduced further if its use is to become more widespread. Specifically, according to the Report of the Basic Energy Sciences Workshop on Solar Energy Utilization by the U.S. DOE in 2005, the price must decrease by a factor of 15 to 25 to approach $\$.40/W_p$ (*24*), given in units of dollars per Watts of power produced. In 1976 the cost of photovoltaic modules was $\$70/W_p$, and in 2003 it was $\$3.50/W_p$. The balance of system (BOS) costs, or the costs associated with all parts of a PV system except for the solar modules themselves, for a grid-tiled PV system is $\$2.50/W_p$. In order to consider the total cost of energy and not just power (electricity) production, both module and BOS costs must be

considered. Using this unit, the cost per kilowatt-hour of solar electricity costs have dropped from $3.65/kWh in 1976 to $.30/kWh in 2003. However, in order to be economically feasible and competitive, the cost of solar energy needs to approach $.05/kWh (*24*). This is not projected to occur for 20 to 25 more years, and this projection is possible only with an increased rate of research in the field. Currently, silicon-based photovoltaic cells make up more than 99% of today's photovoltaic production (*24*). Their high cost (due to the need for high-purity silicon) is limiting the contribution of photovoltaics to energy production (*35*).

Increasing solar cell efficiency without substantially increasing costs is another means to improve the cost-to-efficiency ratio and potentially boost the contribution of solar cells to global energy production. William Shockley and Hans Quiesser established the efficiency limit of single junction photovoltaic cells at 31% in 1961. However, the highest efficiency achieved by silicon crystal solar cells is 25% in the laboratory and 18% in commercial applications (*29*).

The Department of Energy in the Solar Energy Utilization Report calls for,

> "basic research…to not only maintain the existing technology path and learning curve in support of evolution, but to also produce a revolution to dramatically change the slope of the historical learning curve and produce dramatic reductions in the PV module cost-to-efficiency ratio. The goal is to reduce the cost per peak watt by a factor of about 15-25 relative to present systems through the use of new designs, materials, and concepts for solar electricity production, and to do so more quickly than would be accomplished by staying on the existing learning curve—thereby materially impacting global energy supply in 10-15 years rather than by the mid-21st century "(*24*).

It is clear that research efforts need to increase in order to increase solar cell efficiency. As illustrated previously, technological advancements and increases in use and production of solar cells will also certainly continue to cyclically decrease their cost

of production and the utilization of new materials may lower all the surrounding costs included in the BOS. These two factors—efficiency and cost of materials—are the chief motivators behind the increasing number of alternative photovoltaic designs that have been developed in the last two decades.

1.4.5. Alternative Designs of Photovoltaic Cells

The conventional silicon crystalline photovoltaic cell, a single junction photovoltaic cell, is presently the best commercial solar cell. Other single junction photovoltaic cells are nanocrystalline silicon, gallium arsenide, dye-sensitized and organic solar cells. No single junction solar cell has yet surpassed the crystalline silicon conversion efficiency of 25% in the laboratory. As of 2007, gallium arsenide solar cells have also reached 25%, while dye-sensitized solar cells have reached 10% conversion efficiency and are made of much less expensive material than conventional silicon solar cells (*29*).

In addition to single junction cells, there are also multijunction solar cells. While single junction solar cells are thermodynamically restricted to a maximum conversion efficiency of 31% due to the Shockley-Queisser limit, multijunction solar cells have a potential 66% conversion efficiency limit. Multijunction solar cells can be flexible and lightweight, and have reached a laboratory best of 32% conversion efficiency. In addition, multijunction cells can also increase the absorption to a larger portion of the solar spectrum through the use of multiple absorbing materials separated in the multiple cells. Single junction photovoltaic cells combined with concentrated sunlight have achieved 28% conversion efficiency in the laboratory and have a thermodynamic limit of 41% (29). While developments in nanotechnology have allowed for such designs as the

quantum-dot solar cells to increase the conversion efficiency of solar cells, there is currently no way to attach wires to nanocrystals, so no laboratory results have been reported for carrier multiplication solar cells (*29*).

While these commonly reported figures show impressive efficiencies for multijunction photovoltaic cells, we must also consider cost. According to Chen et al. (2007) at the International Conference on Advance Manufacture (ICAM): "'high conversion efficiency' and 'low manufacturing cost' are the two key points for the popularization of solar cells" (*26*). While multijunction and traditional silicon solar cells achieve the highest conversion efficiency, they fail to have a low manufacturing cost. Amorphous solar cells are less expensive, but have not achieved high conversion efficiencies (*26*).

Einstein's 1905 mathematical explanation of the photoelectric effect depicted how electrons emitted in solar energy capture depend only on the frequency of incoming light (*26*). In terms of solar cells, this means that "the spectral absorption and emission of incident light will influence the measurements of efficiency for solar cells" (*26*). Therefore, increasing the absorption spectrum of the cells should directly increase electricity generated and, in turn, increase efficiency. Taking light absorption capabilities into account, the three most important factors to consider in the development of a successful type of solar cell are (1) overall efficiency, (2) cost of materials, and (3) light absorption. A novel type of solar cell, the dye-sensitized solar cell (DSSC) addresses these three facets and has the potential to be the front-runner of solar technology.

1.4.6. The Dye-Sensitized Solar Cell

Invented by Michael Grätzel in 1991, the DSSC is made of relatively affordable and readily available resources. However, the achieved efficiencies to date are only about 10% in the laboratory. As of 2009, the certified record efficiency of dye-sensitized solar cells was 11.1%, and suggested lifetimes exceeding 10 years (*36*). The implementation of light-absorbing dyes provides another opportunity to increase efficiency by expanding the absorption spectra and to reduce costs (*26*).

Since its advent in the early 1990s, the DSSC has developed into a promising addition to solar technology that makes use of low-cost and abundant materials. The cells are flexible, lightweight, transparent, and bifacial, meaning they have less reliance on the angle of incident light. Dye-sensitized solar cells operate using a mechanism that mimics photosynthesis and separates light absorption and charge generation (*37*). A molecular dye, known as the sensitizer, absorbs photons and uses the energy of its own excited electrons to excite electrons to the TiO_2 semiconductor. During the process of photosynthesis in plants, chlorophyll absorbs photons of incident light exciting its electrons to a higher energy state. These electrons then undergo a series of oxidation-reduction reactions that ultimately reduce $NADP^+$ to NADPH and produce a trans-membrane proton gradient or membrane potential. This indirect production of energy from the absorbed photon is used to generate ATP. The DSSC is the first photovoltaic system to mimic natural photosynthesis (*37*).

In recent years, DSSC technology has progressed and DSSC modules have begun to enter the commercial market. Dr. Michael Grätzel's original DSSC design has remained relatively constant, despite some modifications, which will be discussed in the

following chapter (*37*). Although efficiency has improved over the years, dye-sensitized solar cells remain more costly than traditional silicon solar cells and less efficient. One of the most important parts of the DSSC is also one of the most expensive—the sensitizer. Costly synthetic dyes are most frequently used although organic dyes and plant pigments have also been employed as sensitizers for DSSCs (*38*). Using plant pigments to sensitize DSSCs is a low-cost, non-toxic, and natural alternative to synthetic dyes, but further research on pigment sensitizers is necessary. Because the sensitizer must absorb light to generate the charge, the sensitizer must have high light absorbance across a large range of wavelengths. Although there may not be a single pigment that can act as a highly efficient sensitizer, it is possible that a combination of pigments could provide the absorbance necessary to increase the efficiency of a DSSC. In fact, some research has demonstrated a synergistic effect of two sensitizing pigments, meaning the absorption spectra of two pigments combined to increase light absorption and increase the incident photon to current conversion efficiency of the solar cell (*38, 39*). An added benefit of natural pigments is that they can be extracted directly from plants, whereas dyes must be synthesized using costly procedures.

Our research focuses on developing an optimal combination of natural pigments to use as a DSSC sensitizer. The ultimate goal of our project is to determine whether the use of natural plan pigments can improve the efficiency and lower the cost of DSSCs. If so, then this may lower the effective cost of DSSCs and make solar energy more available, affordable, and usable.

1.5. Our Research

1.5.1. Research Question

Our primary research question is: Which combinations of plant pigments will most effectively sensitize a DSSC in terms of increased output? Since testing all plant pigments and all possible pigment combinations is not practical our research sub-question is: Can we determine and then use an index of the absorption spectra of various sensitizing dyes to predict the pigment combination that will lead to the highest cell electrical output and conversion efficiency?

1.5.2. Hypotheses

A dye-sensitized photovoltaic cell sensitized with a specific pigment, or combination of pigments, will yield a higher conversion efficiency and voltage output than a cell sensitized with another combination of pigments. Theoretically, the output of the cells will vary based on the combined effect of pigments' light absorption properties. By spectrophotometrically analyzing pigments' absorption spectra and measuring cell output, our team will evaluate the relationship between a given pigment mixture's absorbance and cell electrical output. Essentially, we expect if a cell can absorb more light, its electrical output will be greater. The null hypothesis is that any particular predetermined concentration of natural plant pigments will not produce an energy conversion efficiency and voltage output significantly different from any other pigment concentration used on our cells.

2. LITERATURE REVIEW

2.1. Michael Grätzel and the Dye Sensitized Solar Cell

2.1.1. Development of the Dye-Sensitized Solar Cell

Vlachopoulos, Liska, Augustynski, and Grätzel created the first incarnation of a DSSC in 1988 using a titanium sheet covered with a fractal TiO_2 film (*40*). A yellow ruthenium dye was used as the sensitizer and a platinum wire was inserted into a beaker of electrolyte as the counter electrode. At the sensitizer's absorption maximum wavelength, the device converted over 60% of the photons into electric energy with an overall conversion efficiency in sunlight between 1 and 2% (*40*). Grätzel's lab then significantly expanded on these initial findings to develop a low-cost solar cell with a much higher efficiency.

O'Regan and Grätzel developed a photovoltaic cell based on a transparent, porous film of TiO_2 particles coated with a sensitizing dye (*41*). DSSCs consist of an electrode, coated with TiO_2, a dye, and a counter electrode, coated with platinum catalyst. Light absorption in dye-sensitized solar cells is separated from charge carrier transport. Nanoparticles of TiO_2 are deposited onto a glass electrode and then coated with sensitizing dye. Dye molecules absorb the photons of incident light, causing electron injection into the TiO_2 semiconductor. These electrons diffuse toward the glass electrode and travel through a wire to the counter electrode, creating an electrical circuit. The electrons then attach to iodine molecules, which diffuse across the electrolyte and return to the dye molecules. A graphic representation of the components of the DSSC as well as summary of the reactions involved in the functioning of the DSSC are shown in Figures 2.1 ad 2.2, respectively.

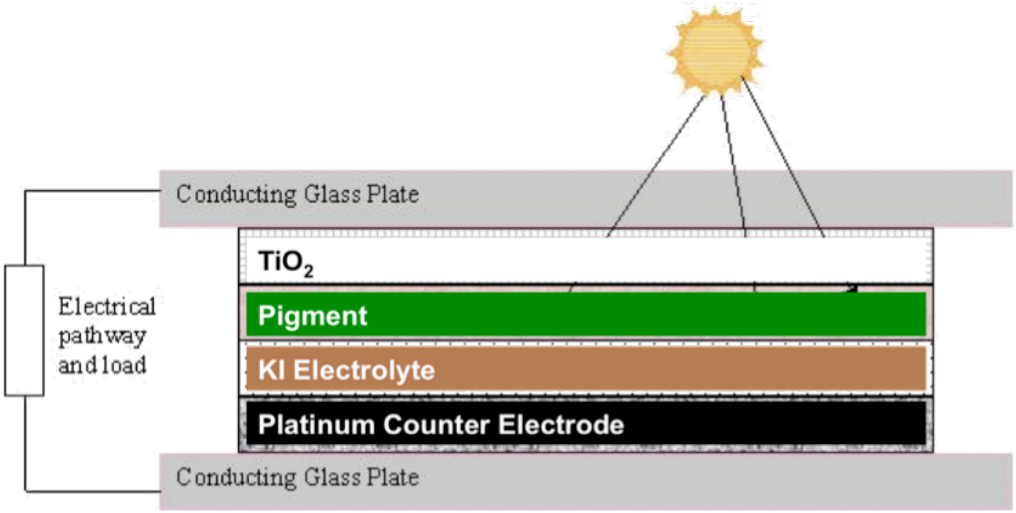

Figure 2.1. Side view representation of the components of a DSSC.

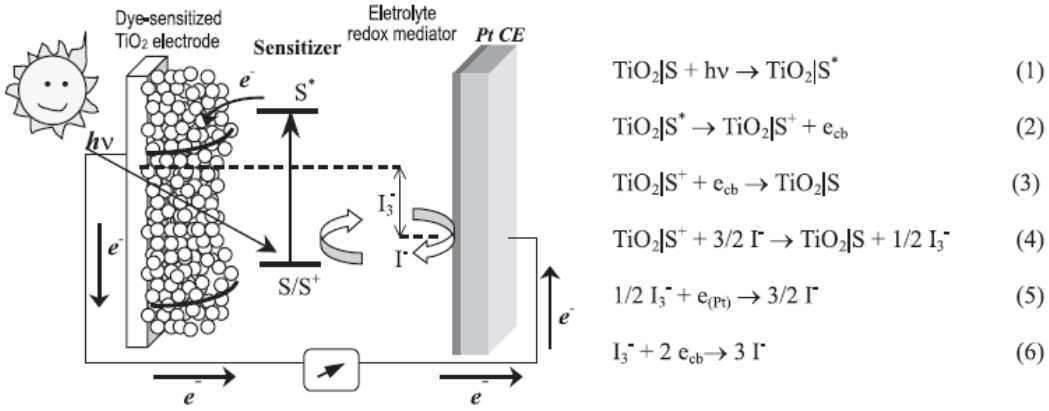

Figure 2.2. Schematic representation of a DSSC and the reactions associated with light absorption and charge transport. S denotes the sensitizer, or dye, I^-/I_3^- is the charge mediating electrolyte, and Pt CE denotes the platinum-coated counter electrode (*42*).

This revolutionary type of photovoltaic cell is modeled after plants, which also separate the two parts of energy conversion as they function to process solar energy. The light-to-electric energy conversion efficiency of the DSSC in this landmark study was 7.1-7.9% in simulated solar light and 12% in diffuse sunlight (*41*). Grätzel patented his DSSC in 1990 (US Patent 4,927,721), and by 2003, scientists overall registered more than 800 patents (*42*).

2.1.2. Principles of Operation of DSSCs

The dye-sensitized solar cell differs from other solar cells in two primary ways. First, light absorption and charge transport are separated. Light absorption occurs in the dye sensitizer and charge transport occurs in the TiO_2 and electrolyte. This separation allows for low carrier recombination, or back reaction of injected electrons, and a high tolerance for impurities (*43*). The efficiency of the cell depends heavily on the kinetics of electron transfer. The rate of electron injection must be higher than the decay of the excited state of the dye, and the rate of reduction of the oxidized sensitizer must be higher than the rate of recombination of the injected electrons with the dye cation. In addition, the reaction at the counter electrode must regenerate the charge-mediating electrolyte quickly enough so that the step does not become rate limiting. Once the sensitizer has been regenerated, the cell has transformed light into electric energy without permanently changing its chemical structure. A graphic representation of the components of the DSSC as well as summary of the reactions involved in the functioning of the DSSC is shown in Figures 2.1 ad 2.2, respectively.

The second major unique feature of DSSCs involves the novel use of a mesoscopic junction. Charge generation takes place only at the interface between the dye, TiO_2, and electrolyte. Grätzel was able to increase the efficiency of his cell by an order of magnitude by taking advantage of the large surface area of the porous TiO_2 film deposited onto the glass surface (*41*). The surface area of the porous TiO_2 allows the applied dye to seep in and form hundreds of monolayers for maximal absorption of light. A single monolayer would only weakly absorb light because the area of one dye molecule

is larger than its optical cross section. The multi-layered structure closely resembles the stacked thylakoid vesicles in chloroplasts, which harvest light via chlorophyll (*37*).

The mesoporous nature of the TiO_2 film also allows the liquid electrolyte to seep into the pores of the TiO_2. The deep penetration of the dye into the T_iO_2 increases the contact between the dye molecules, the TiO_2, and the electrolyte. When light strikes the cell, a dye molecule is excited and an electron is injected at an extremely high rate (i.e., on the order of femtoseconds) into the TiO_2 semiconductor. The conduction band of the oxide allows for rapid electron conduction. The time required for electrons to cross a 10 μm TiO_2 film is 10 ms, and this rate of transfer is even more rapid than electron transfer across a photosynthetic membrane in plants (*37*). Therefore, the TiO_2 is essential for optimal light absorption by providing a framework for multiple dye layers. TiO_2 is also essential for charge transport from the mesoscopic dye/TiO_2/electrolyte junction toward the anode. Figure 2.3 shows a scanning electron micrograph of the TiO_2 film (*37*).

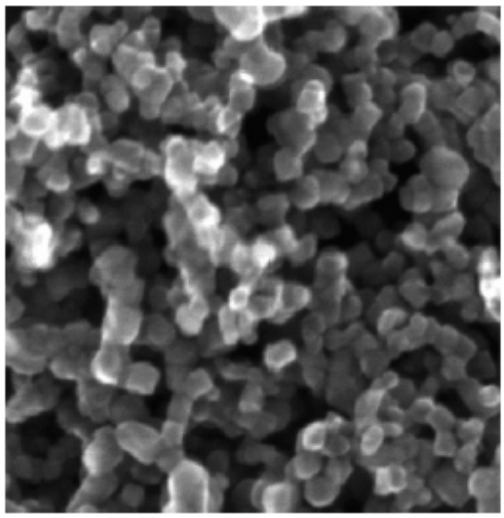

Figure 2.3. Scanning electron micrograph of TiO2 film. Average particle size is 20 nm (*37*).

2.1.3. Recent Developments in DSSC Technology and Commercialization

Despite being a promising next step in solar energy generation, the efficiency of the DSSC has yet to reach standards high enough to make it commercially viable to compete with PV solar cells or other sources of energy. The efficiency (η) of a solar cell is given by the following equation:

$$\eta = \frac{J_{sc} * V_{oc} * FF}{P_m} \qquad (40)$$

Equation 2.1. Solar cell efficiency.

where J_{sc} is the short circuit current, V_{oc} is the open current voltage, FF is the fill factor, and P_m is the total solar power incident on the cell. The FF in the equation is relatively constant, where typical values for the fill factor range from 0.75 to 0.85. P_m is based on solar irradiance but would change over geographic and temporal scales and for use with an artificial source of irradiance. Therefore, the principal way to adjust the efficiency of the cell is to increase either the J_{sc} or V_{oc}, so most developments in the technology of DSSCs aim to improve these variables (*44*).

Dr. Michael Grätzel, winner of the 2009 Balzan Prize and 2010 Millennium Technology Prize, discussed the most recent developments in DSSC technology at his Balzan Lecture at the Carnegie Institution for Science in Washington, D.C. on November 3, 2010 (*45*). Notable milestones for DSSC technology occurred in 2005, when DSSCs were scaled up to modules by researchers in Israel, and in 2009, when DSSCs began to be commercially produced by G24 Innovations (G24i) located in Cardiff, Wales. G24i collaborated with Grätzel to mass produce DSSC-powered phone chargers, universal remotes, lamps, and indoor modules (*46*). G24i backpacks and bicycle panniers integrated with DSSCs are able to provide power for charging small electronics such as

iPods, cell phones, and GPS devices. The "Grätzel Solar Bag" and "G-pack", shown in Figure 2.4, are two products offered by G24i (*46*).

Figure 2.4. The Grätzel Solar Bag (left) and the G-pack (right) produced by G24i are capable of harvesting energy from sunlight and charging small electronics on the go (*46*).

Grätzel discussed the unique aspects of DSSC technology that give it great potential for success in global markets (*45*). DSSCs are bifacial, allowing them to capture light from any angle, and are translucent, making them perfect for integration into buildings or homes as façades or windows. They are less sensitive to the angle of incidence of light and also have increased efficiency in higher temperatures compared to traditional silicon solar cells (*45*). Also, DSSCs can be made to appear different colors, which means an energy-harvesting façade can also be aesthetically pleasing.

The original design of the DSSC, developed by Grätzel in the early 1990s, has remained relatively constant despite modifications and improvements. Although DSSCs have unparalleled potential for commercial success, the future of DSSC technology will depend on increasing efficiency and lowering cost. Grätzel stated that the price of solar energy needed to decrease to 5 cents/ kW-hr in order to be viable for widespread use (*45*). Currently, a Grätzel Solar Bag sells for $124.95 and the G-pack sells for $99.95

before shipping costs (*46*). Large scale projects for homes and buildings using DSSCs would be extremely costly and only affordable for the wealthiest "green" consumers.

Research has increased to improve many aspects of these solar cells, with the main goal of decreasing cost. Researchers have studied ways to improve all parts of the DSSC, including the electrolyte, TiO_2, and catalyst. However, one of the most important parts of the DSSC is also the most expensive—the dye.

2.2. Specifications and Modifications of DSSCs

2.2.1. Size of the DSSC

There is a significant difference between the size of solar cells studied in a research laboratory and those that are actually applicable on a large scale. Most studies involving DSSCs focused on small cells, less than 1 cm^2. However, recent advances in technology have led to the ability to test larger modules that would make DSSCs competitive with other major forms of energy.

Lenzmann and Kroon (2007) studied the effect of DSSC size without considering stability, and found that efficiency decreased with DSSC size (Figure 2.5) (*43*).

Surface area (cm^2)	η (%)
<1 cm^2	11.2
0.219	11.1
1.004	10.4
1.31	10.1
2.36	8.2
26.5 (submodule)	6.3

Figure 2.5. A comparison between cell active surface area and top recorded efficiencies (η) as of 2007 (43).

It should also be noted that the last entry, a cell with the largest active area of 26.5 cm^2, is roughly the size of what can be considered a "submodule," which is the beginning of large scale production (*43*). A cell this size has only achieved a recorded efficiency slightly greater than half of the highest recorded efficiency for DSSCs (*43*). As the active area of a DSSC is increased by a few square centimeters, the overall resistance of the glass grows, causing a high series resistance for the solar cell module and a low fill factor. As the area of the DSSC increases, more energy was lost as heat due to this resistance (*47*).

Lee et al. (2007) also studied how a varying size in the DSSC tested corresponded to a change in efficiency recorded, and they found more evidence of larger cells achieving lower efficiencies than their smaller counterparts (*47*). In their research, they compared 25 cm^2 cells (15.12 cm^2 active area) with 1.2 cm^2 cells (36mm^2 active area). The measured open circuit voltages of both sizes were equal, but the short-circuit current density and fill factor both decreased by over 5% in the larger 25 cm^2 cell (*47*).

Although it seems that smaller cells yield higher efficiencies and better results, Park et al. (2007) examined an important aspect regarding DSSC size that helped advocate for further study into larger cells (*48*). They found that an overestimation of cell efficiency was enhanced in small cells and concluded that the overestimation decreased as the active area increased. This suggested that a larger cell provided more accurate results. When considering an assembly of solar modules, only the light hitting the front of the cells is relevant, and so, such overestimations are not applicable for eventual real-world applications. To truly get a dependable reading from smaller DSSCs,

some kind of masking is required to cover the edges of the cell and make sure that only the light incident on the front surface is the light providing electricity (*48*).

Dai et al. called for a need to shift research to the development of larger cells as they reiterated how already by 2007, a record efficiency of 11.14% was achieved with cells of active area less than 0.3 cm^2, while cells significantly over 1 cm^2 only displayed a record 8.18% efficiency. Even this record 8.18% efficiency was achieved by a DSSC with an area of only 2.36 cm^2. As Dai et al. said, to properly commercialize DSSCs, they need to be scaled up (*49, 50*).

However, scaling up to larger cells is not simple and new details must be accounted for that do not appear in smaller cells. Small cells can be made with conductive glass and no collective electrode, but for cells around a size of 10 cm by 10 cm, efficiency without such an electrode comes out to less than 1%. Dai et al. worked with modules at a size of 15 cm by 20 cm (187.2 cm^2 active area) each, and managed to produce from each module a short current between 2 and 3 A, an open circuit voltage of about 0.7 V, and a fill factor between 55 and 60% (*50*). Overall, these modules mostly displayed a photoelectric conversion efficiency around 5-6%, with averages of 7.4% efficiency for an active area of 10.2 cm^2, 5.9% efficiency for 187.2 cm^2, and 6.2% efficiency for 1497.6 cm^2 (*49*). Although these output values were not as high as those achieved by the best small cells, they are still significant, especially when taking into account the overestimation in efficiency that arises in smaller cells. It is clear that more research is needed on the technological aspects of increasing cell sizes.

2.2.2. Types of glass

Continuing with the constituents of any DSSC, another component that contributes to the net efficiency of the cell is the type of glass used for the outer layers. These layers of the cells are the ones exposed directly to the environment and hold the rest of the parts carrying out the functions of the cells. Since the glass plates are in contact with the inner elements, they play a role in their connection to the cell as an electrical component that interacts with the generated energy and could potentially affect its output. The glass used for DSSCs is made to be conductive so that it can aid in the collection of free electrons produced and help transfer the current out of the cell. In addition, since the glass plates are the outer boundaries of the cell, any incoming light must travel through the glass. Thus, the optical properties of the glass are critical to the cells functioning. The glass must be highly transparent in the absorbing region of the sensitizers in order to excite electrons within the DSSC.

The current typical practice is to place the TiO_2 on glass plates that are coated with a thin layer of fluorine-doped tin or tin-doped indium oxide (FTO or ITO). The FTO or ITO are conductive, and so can make the glass plates serve as electrodes that help collect electric charge produced within the cell. Both types of coatings are very transparent throughout the visible spectrum (they are more absorbent in ranges closer to UV radiation), making them well suited for the main part of the Sun's output (*42*).

Besides allowing light to enter the cell, the glass electrode also takes part in the overall circuit created by the cell, and the main parameter that affects the circuit is the resistivity of the glass, or its resistance per unit area. In general, a higher resistivity leads to a higher series resistance within the solar cell, which in turn decreases the overall

performance of the cell in terms of electrical output. Both FTO and ITO coatings share a typical resistivity of between 10-20 Ω/cm^2. However, the resistivity of glass-ITO electrodes increases significantly as temperature rises and this effect is not observed in FTO covered glass (*42*).

Another variation on ITO glass is a flexible electrode, polyethylene terephthalate coated with tin-doped indium oxide (PET-ITO), which is cheaper, lighter, and less limited by its shape than regular ITO. However, temperature becomes even more of an issue since at the same time PET-ITO requires that a lower temperature be used for binding TiO_2, and this lower binding temperature causes less TiO_2 to stick to the electrode. Some treatments help the TiO_2 stick better, but they result in a lower stability of the DSSC. Longo and De Paoli showed that flexible electrodes also create a higher series resistance than glass electrodes, so the final series resistance in FTO glass reaches around 35-50 Ω versus about 400 Ω for the PET-ITO. Due to this difference, despite the relatively same open current voltage displayed by both flexible and glass electrodes, flexible cells produced about 10 times less photocurrent (*42*).

In terms of their interaction with the rest of a DSSC, ITO and FTO glass cannot serve alone. The surface of these transparent glass electrodes allows for poor kinetics in the reduction of triiodide to iodide, and the process at their surface is very slow. Catalysts such as platinum are much better for the reaction, and so covering the glass plates aids the overall solar cell (*42*). In addition to lowering the efficiency of a cell, glass also poses the potential risk of breaking. Metal is a conceivable replacement for the back electrode of a DSSC since it is cheaper and would provide a longer lifetime for the cell than glass. Also, with metal's higher conductivity, a metal electrode would provide

less resistance and so increase efficiency. However, glass is believed to not react with the corrosive Iodine electrolyte as metal does and it is still the most commonly used electrode. Toivola et al. (2006) tested various substances and found that platinum-treated FTO glass was the more efficient than any metal electrode tested. They also tried using plastic substrates to replace glass ones, but the glass cells performed much better than any plastic. Until the metal and plastic process is optimized, glass is still the best choice for substrate and electrode (*51*).

It seems that in general, FTO is a better choice for coating than ITO due to its independence on temperature. Although flexible electrodes could be cheaper and more versatile, they result in a lower output and again display temperature dependence. In most studies, the commonly used glass is FTO coated glass and the common resistivity is similar to that of TEC15-type glass (glass with 15 Ω/cm^2 resistivity). The TEC15 is cheaper than the other viable option, TEC8 (8 Ω/cm^2), and is still of a quality fit to make a good solar cell (*42, 47, 50, 51*). The few instances when a lower resistivity glass (such as TEC8 or TEC10) has been used were in studies that considered other parameters of the glass. One example is with Park et al. who considered the effect of the electrode thickness on the cell performance and they wanted to reduce other possible contributions to efficiency from the glass as much as possible (*48*). While several innovations in glass are underway at the present, it appears that FTO coated, TEC15 glass for DSSCs is still the norm used in current research. Further research is needed to improve the performance of the glass in DSSCs.

2.2.3. Review of Reaction Components: Electrode, Catalyst, and Electrolyte

The type of glass used and size of the cell affect the ability to gather energy by a DSSC, but a cell's ability to produce energy depends on the components that directly affect the main photochemical reaction. As explained previously, the main chemical reaction in a DSSC involves the photon of light, the sensitized electrode or photoelectrode, the counter electrode, the catalyst, and the electrolyte. The photoelectrode consists of TiO_2 bound to glass and sensitized by dye. The counter electrode is coated with the catalyst for the chemical reaction. The electrolyte assists as the redox mediator in the chemical reaction (*36*).

The reaction starts as the photon is absorbed by the dye, which injects an electron into the TiO_2. Then, the electron moves through the TiO_2 to the film plated glass. Since the dye has just lost an electron, it has been oxidized. To regain an electron (in order to keep the reaction going), iodide (I^-) reduces the dye and becomes triiodide (I_3^-). The triiodide moves to the counter electrode, where it is reduced back to iodide for use in another round of the chemical cycle. The catalyst coated on the counter electrode increases the kinetics of the reaction (*52*).

Since these components of the cell help maintain and speed up the photochemical reaction that produces electrical energy, improvements in these components can lead to drastic increases in DSSC efficiency. Additionally, the use of lower priced materials while maintaining efficiency could potentially decrease the cost to efficiency ratio. Such replacements could make DSSCs and solar energy technology more affordable, available, and ultimately more popular. The following is a review of previous research that has addressed the standard features and adaptations of the photoelectrode, catalyst, and

electrolyte—the key factors in the driving chemical reaction, as pathways to an improved DSSC.

2.2.4. The Photoelectrode

Kay and Grätzel (1996) described the photoelectrode of the DSSC as a conductive glass plate "coated with a porous layer of a wide band gap semiconductor, usually TiO_2, which is sensitized for visible light by an absorbed dye (*52*)." This paper was published so early that the cells described were not even called DSSCs, but instead were called "low cost photovoltaic modules based on dye sensitized nanocrystalline titanium dioxide and carbon powder (*52*)." Kay and Grätzel applied colloid TiO_2 by the doctor-blading method (using a rod pressed against the surface to spread across the surface) to the conductive side of glass with SnO_2 film. Then, the glass coated in TiO_2 was heated to 450°C (*52*). Next, the glass coated in TiO_2 was soaked in sensitizing dye to complete the photoelectrode. This process is standard to most DSSCs. Since Kay and Grätzel, before the term 'DSSC' was even in use, TiO_2 has always been used as the photoelectrode. As revealed by an extensive literature review, there have been very few changes to the semiconductor in the last fifteen years. Most experiments affecting the photoelectrode have dealt with changing the sensitizer of the electrode: the dye. Otherwise, the main developments in the photoelectrode have only involved the use of different types of TiO_2. The studies of the dye will be discussed later in this literature review.

TiO_2 has been used as the semiconductor in DSSCs since their inception because of its low cost, excellent semiconducting properties, and already widespread use as a white colorant in toothpastes and paints (*52*). From the beginning of the reaction (photon absorption) to the end of the cycle (redox), TiO_2 is a good semiconductor.

In the beginning of the excitation cycle, due to the high refractive index of TiO_2, light is able to scatter throughout the photoelectrode, allowing for maximum absorption. Next, electron injection is supported by TiO_2's conduction band, which is slightly below the excited state energy level of many dyes. TiO_2 then sufficiently shields that injected electron due to its high dielectric constant, which prevents the electron from interacting prematurely with the dye instead of the electrode. TiO_2 is also stable under extreme conditions, such as high temperatures, in photoelectrochemical cells (*52*).

Different types of TiO_2 can affect the abilities of a cell. Kang et al. (2008) recommended using TiO_2 nanorods instead of TiO_2 nanoparticles (*53*). Nanorods result in improved charge transport, and induce a longer lifetime for the electron in the photoelectrode due to necking of the rods in a unique 3D network. Due to the increased surface area of nanorods over nanoparticles, the initial conversion efficiency of nanorod-based DSSCs is 3.32% compared to that of nanoparticle-based DSSCs at 1.97%. Nanorod-based DSSCs also have a higher overall conversion efficiency in an environment of increasing salt concentration. The conversion efficiency of nanorod-based DSSCs remained constant while the conversion efficiency of nanoparticle-based DSSCs decreased with increasing salt concentrations. These results led to the conclusion that nanorod-based DSSCs performed better in extreme environments and overall than nanoparticle-based DSSCs (*53*).

While we will be changing the sensitizer in DSSCs, we will not be changing the semiconductor component of the photoelectrode. Though Kang et al. recommended using TiO_2 nanorods rather than nanoparticles, nanoparticles are more affordable and currently the most readily available form of TiO_2 from the common suppliers of DSSC

kits. For DSSC construction, the doctor-blading method for applying TiO_2, recommended by Kay and Grätzel and supported by most researchers since the 1990s, is both cheap and reliable.

2.2.5. The Counter Electrode and Catalyst

The counter electrode has been subject to much more experimentation than the electrode. The basis of modifications to the counter electrode has been through modifications to the catalyst. Platinum is the primary catalyst used, but carbon catalysts are a significantly lower priced option. Carbon is much more readily available, as opposed to platinum which is a precious metal that is not abundantly available (*35*). Thus far, DSSCs incorporating platinum catalysts have always had higher initial efficiency in comparison to DSSCs incorporating carbon catalysts. However, recent studies have found modified-structure carbon catalysts provide higher long-term efficiency.

2.2.5.a. Platinum as the Catalyst

In 1996 Kay and Grätzel acknowledged that platinum "has been the preferred material for the counter electrode since it is an excellent catalyst for triiodide reduction (*52*)." The primary focuses of research on the platinum catalyst are the methods of preparation, methods of application, and thickness.

Khelashvili et al. (2006) compared multiple types of platinum preparation methods (*54*). Sputtering, thermal deposition, electrochemical reduction, and chemical deposition were all measured through transmission electron microscopy, x-ray diffraction, x-ray photoelectron spectroscopy, and x-ray absorption near edge structure

analysis. Based on electrochemical performance, they concluded that hydrogen reduction is the best method for platinum preparation (*54*).

Fang et al. (2004) studied the effect of thickness of the platinum film on DSSC performance (*55*). Platinum is one of the most expensive components of the DSSC. Using the smallest possible layer of platinum is essential to lowering the cost of DSSCs overall. Platinum was deposited in thicknesses ranging from 0 nm to 415 nm based on sputtering time. After analysis of grain size, porosity, conductivity, sheet resistance, and overall DSSC performance, platinum thicknesses of 2 nm and 415 nm provide the highest energy conversion efficiency due to the lowest sheet resistance of the counter electrode (*55*).

There are a variety of methods of platinum application to the glass of the counter electrode. One of the most common, screen-printing, is also one of the simplest. Burnside et al. (2000) tested the application of screen-printing for coating both the electrode with TiO_2 and the counter electrode with catalyst. The screen-printing method provides even and consistent layers of pastes. This method also allows for quick and easy, automated fabrication of DSSCs (*56*).

2.2.5.b. Carbon as the Catalyst

One of the most appealing features of DSSCs over conventional silicon solar cells is their low cost. Cost of DSSCs can be reduced immensely by lowering the cost of the most expensive component: the platinum catalyst. In comparison to other catalysts, though it is efficient, platinum "has the disadvantage of being very expensive." Additionally, commercially mass producing DSSCs require a substantial amount of platinum "which is not abundantly available (*35*)." Platinum is both "extremely

expensive and also has the potential of corrosion by the iodide solution (*57*)." Kay and Grätzel also emphasized the concern "that a small amount of platinum might dissolve in the electrolyte by oxidation and complex formation with iodide/triiodide, e.g.., as PtI_4 or H_2PtI_6." These compounds would adversely affect the conversion efficiency of the cell (*52*).

Joshi et al. (2009) contended that "efforts are needed to search for an alternative material which is readily available, cost effective, and capable of showing comparable catalytic effects for tri-iodide, and carbon is such a material (*35*)." Kay and Grätzel (1996) also reached the same conclusion when looking for a catalyst that was low cost but could still "be well conducting and exhibit a low overvoltage for reduction of the redox couple (*52*)." They proposed using carbon as a "low cost alternative" because "it combines sufficient conductivity and heat resistance as well as corrosion resistance and electrocatalytic activity for triiodide reduction (*52*)."

Kay and Grätzel used the doctor-blading method to coat the counter electrode with graphite powder with 20% carbon black added (*52*). Fanis et al. (1998) and Kay and Grätzel (1996) also suggested using a graphite rod or soft lead pencil, as well as an open flame to apply the carbon layer (*52, 58, 59*). Nevertheless, problems with consistency and even coating have been experienced while using graphite rods or pencils as well as with open flame techniques.

Li et al. (2009) made carbon counter electrodes with organic binder free carbon slurry at low temperatures (*57*). Efficiency reached as high as 6.1%, which is "comparable," but not higher than counter electrodes coated in platinum. The significant achievement here is that Li et al. achieved these results while staying at low temperatures,

and previous research had only achieved results when cells were heated up to 450°C. High temperature requires additional energy and "limits the choice of substrates to heat-resistant materials, and they cannot be used for plastic substrates usually employed in flexible DSSCs" (*57*).

The most recent research in carbon catalysts has been done with carbon nanotubules. They have higher surface area than ordinary carbon and thus contribute to higher conversion efficiencies in DSSCs with liquid electrolytes due to increased contact between the electrolyte and the counter electrode (*60*).

Suzuki et al. (2002) compared three different types of nanocarbon materials: single wall carbon nanotubes (SWCNTs), nanohorns, and carbon filaments. The study also compared the three nanocarbon-coated counter electrodes to a platinum-coated counter electrode (*60*). The conventional platinum coated electrode achieved the highest conversion efficiency (5.4%). Of the three types of nanocarbon materials, only the SWCNT had a high conversion efficiency (4.5%) (60). Ramasamy et al. (2007) achieved 6.73% overall conversion efficiency with a nanocarbon counter electrode, which is comparable to the 7.26% conversion efficiency they achieved with conventional platinum (*61*).

Koo et al. (2006) compared the effect of different counter electrodes on DSSC efficiency over a period of five days (*62*). The three counter electrodes compared were prepared with a multi-wall carbon-nanotube film (~20-25 μm), a platinum film prepared by the sputtering method (~500 nm), and a platinum film prepared by the electro-deposition method (~5 nm). The films were applied by the doctor-blading method. This study reported that the DSSC with the carbon nanotube counter electrode had more

stability than those coated in platinum. Increased percent efficiency was also reported for the carbon-nanotube counter electrode, but only in the period from 24 hours to 5 days. According to figures in the paper, the efficiencies for all three electrodes were roughly equivalent in the first 24 hours. Additionally, while the platinum counter electrode performance decreased with time, there was "no significant change of impedance characteristics in the carbon-nanotube electrode" after 5 days (*62*).

Based on these results, the study concluded that a "DSSC having carbon-nanotube counter electrode has higher efficiency and more stability than those in the case of two platinum counter electrodes (*62*)." However, later studies still contended that carbon-nanotube counter electrodes are comparable to, but have not surpassed, the conversion efficiencies of platinum counter electrodes (*61*).

2.2.5c. Catalyst Conclusion

The choice of which catalyst to use, nanocarbon or platinum, is controversial. While nanocarbon is the low-cost option, platinum is the industry standard. Additionally, the initial conversion efficiencies of nanocarbon have not surpassed those of platinum. While carbon in the form of an open flame or a lead pencil is readily available and inexpensive, those methods of application are not automated and therefore leave room for errors and inconsistencies. The most successful form of the inexpensive element is nanocarbon material, which, in addition to still being experimental, is not currently readily available from the DSSC kit suppliers. For this study we have chosen the more expensive option because it is currently the most efficient and conventional. Since we are changing so many aspects of the cell, the catalyst is a factor where we would like to use the foremost and industry premier material. However, we acknowledge that using a

carbon counter electrode is an excellent and feasible way to improve the cost efficiency of DSSCs. In the future, when there is more industry support of and evidence for the use of nanocarbon materials as the counter electrode, a more cost efficient DSSC may be made with nanocarbon materials.

2.2.6. The Electrolyte

The reduction oxidation (redox) couple is the key component to DSSCs (*36*). Iodide (I^-) reduces the dye that has been oxidized by the incoming photon and becomes triiodide (I_3^-). Triiodide moves to the counter electrode and is reduced back into iodide. The iodide can then reduce the dye that has been newly oxidized by the second incoming photon. The cycle continues, dependent on the redox reactions occurring with the redox couple mediator (I^-/I_3^-). Because the electrolyte serves as the redox mediator, it is key to the functionality of the DSSC. According to Boschloo and Hagfeldt (2009) in their review of the iodide/triiodide redox mediator, "the photovoltage of the device depends on the redox couple because it sets the electrochemical potential at the counter electrode (*36*)." Kinetically, this is because the "driving force for dye regeneration reaction is given by the difference between" the energy states of the standard dye with the oxidized dye and iodide with diiodide (I_2^-) (*36*).

However, a few problems exist with this mediator. First, though the iodide/triiodide couple has an extremely large standard potential and the sensitizer has an extremely large oxidation potential, internal potential loss is also great, decreasing the efficiency. If we could gain only half of the internal potential loss, overall DSSC efficiencies above 15% might be achieved (*36*). Kay and Grätzel demonstrated that iodide is highly corrosive to most metals, limiting cell-to-cell connections. Additionally,

the conventional liquid electrolyte solution (with acetonitrile) has a relatively low boiling point of 82° C, which results in low stability of DSSCs under extreme conditions and requires hermetic sealing of the cell (*52*).

Regardless of these issues with the conventional electrolyte, Boschloo and Hagfeldt concluded "the iodide/triiodide couple will probably be unsurpassed as a redox mediator for dye-sensitized solar cells for some time to come." They also acknowledged that with "the growing ability to master the semiconductor/dye/electrolyte interface and control recombination reactions, we will be able to use alternative redox mediators…that have redox potentials up to .5 V more positive than that of iodide/triiodide (*36*)." The following literature review highlights the current research of both alternative redox mediators and the durability of the electrolyte solution and therefore the DSSC as a whole.

2.2.6.a. Alternative Redox Mediators

Bromide pseudohalides and selenocyanate based ionic liquid electrolytes have been developed (*36*). Selenocyanate-based ionic liquid electrolytes "gave very encouraging performance" (*36*). One-electron redox systems have also been investigated, using cobalt and copper in coordination with organic mediators like TEMPO (*36, 63*). Copper-iodide (CuI) as an inorganic hole-transport material had increased efficiency from 1% to 6%, but deteriorated quickly due to the property of iodide to degrade metals (*63*). Solid-state organic hole conductors are another possible substitute for the redox electrolyte couple. Yanagida et al. (2009) also described the fabrication of PEDOT poly (3, 4-ethyl-enedioxythiophene)-based DSSCs and in situ photoelectrochemical polymerization as alternatives for iodide-free DSSCs (*63*). New liquid crystal embedded

in polymer electrolytes composed of click polymers have also been developed that have relatively high conversion efficiencies of 4.7% (*64*). However, at this point, none of these electrolytes have surpassed the capabilities of the triiodide/iodide mediator.

2.2.6.b. Addressing Durability Issues: Gel Electrolytes

In addition to increasing efficiency of the redox couple, the second important factor in alternative electrolytes is durability. According to Wang et al. (2003), due to the electrolyte, "one of the main factors that has hampered widespread practical use of the DS(S)C is the poor thermostability encountered so far with these devices" (*65*). The principal solution to the problem of low-boiling point and thus low stability of the electrolyte solution is to create gelled electrolytes.

Kubo et al. (2001) studied the performance of DSSCs with gelled and liquid electrolytes. The study concluded that "gelation does not affect the conductivity of the electrolyte and that the conductivity increased with an increase of iodine in both gel electrolytes and liquid electrolyte" (*66*). In three separate studies, Wang et al. investigated solid-state DSSCs using amphiphilic ruthenium as a dye sensitizer and a polymer gel electrolyte (*65, 67, 68*). These studies addressed the issue that "the leakage of the liquid electrolyte…as well as corrosion of the platinum counter electrode by the triiodide/iodide couple have been suggested as some of the critical factors limiting the long-term performance of the DS(S)C, especially at elevated temperature (*68*)." There is no difference in the conversion efficiencies of the polymer gel electrolyte with iodide/triiodide created with silica nanoparticles in comparison with the standard, conventional liquid electrolyte, demonstrating "extraordinary stabilities of the device

under both thermal stress and soaking with light…rendering these devices viable for practical application" (*67, 68*).

2.2.6.c. Electrolyte Conclusion

Though the iodide/triiodide couple definitely has room for improvement, it is still currently the best electrolyte for DSSCs. It is also readily available, found in DSSC kits, and extremely affordable. We are not testing our DSSCs in high-temperature conditions, so we have chosen to use the conventional liquid iodide/triiodide electrolyte. In the future, if a superior alternative redox mediator is developed, it will greatly enhance the efficiency of DSSCs and should be employed if it continues to lower the cost to efficiency ratio.

2.2.7. Reaction Component Conclusion

Though many variations and adaptations of the chemical components of the DSSC have been developed, most are still in an experimental phase. Since we are drastically changing the sensitizer from that of the conventional DSSC, we have planned to minimize changes in other key chemical components like the catalyst, electrolyte, and semiconductor. However, in order to achieve the overarching goal of making solar energy more cost effective by simultaneously increasing efficiency and lowering cost, improved advances in the catalyst, electrolyte, and semiconductor must be incorporated into DSSC technology. We will keep the reaction components of the catalyst, electrolyte, and semiconductor constant, and vary the combination and concentration of the sensitizer: the photosynthetic pigments.

2.3. Photosynthesis

The greatest inspiration and original model for DSSCs comes from nature itself and the evolutionarily developed process of photosynthesis. DSSCs imitate photosynthesis through their own "photosynthetic" pigments. Although plants in nature are not perfect in their conversion of light to energy, the ability of their pigments to capture sunlight is very efficient and should be discussed in order to fully understand the process and capabilities of DSSCs.

Roughly speaking, photosynthesis is the process through which plants and a few other organisms use sunlight to create energy. More specifically, plants take in carbon dioxide and water, and, with the aid of sunlight, produce sugar and oxygen. Actually, this process is comprised of two primary reaction sequences. The first sequence is the light-dependent, or thylakoid reactions, where pigments in the plant cells absorb light and convert it to potential chemical energy in the form of ATP and NADPH. The second reactions are light-independent and take place in the stroma, but use the chemical potential energy created in the thylakoids to build carbohydrates. These carbohydrates can be used as packets of energy for the entire plant and essentially all ecosystems (69, 70). A plant's ability to transfer energy from light to ATP and NADPH is very efficient, at around 95-99%. However, the total energy that could be produced on a theoretical level if all light were absorbed is around 27% of the initial energy input (*71*). Overall, photosynthesis is not very efficient in terms of biomass production, yielding 3-5% of the energy captured, but light excitation and subsequent electron transfer is very efficient. It is this efficient, light-dependent reaction that can be utilized by humans through photovoltaic cells.

The principle of photosynthesis stems from the interaction of light with matter. When a photon, or a "particle" of energy, hits a molecule that is capable of absorbing energy at that wavelength, the energy of the photon is absorbed by an electron and the photon ceases to exist. The electron is then "excited," or boosted, to a more energetic level around the molecule (Figure 2.6). The electron excitation, however, is very brief so after a very short period of time, the excited electron loses this excitation energy in one of four ways. One option is for the electron to simply return to its original energy level, and in doing so emit the energy as either another photon of lesser energy than the original (fluorescence) or as heat, or as both another photon and heat. Alternatively, the excitation energy may be transferred to another molecule through resonance transfer or may be converted through photochemistry into potential chemical energy ultimately yielding reducing power in the form or NADPH or ATP (*69*).

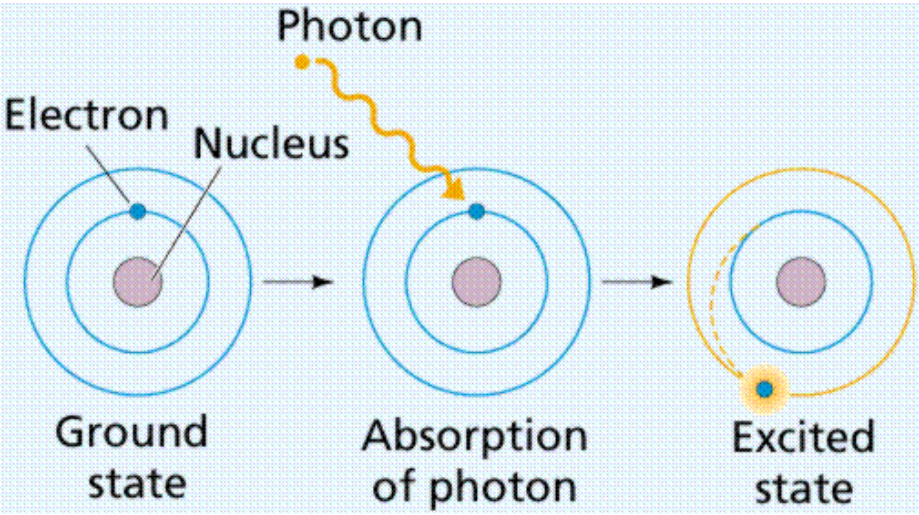

Figure 2.6. An electron is shown excited to a higher energy state, an excited state, after being struck by a photon (72).

In plant cells, photosynthesis occurs within the chloroplasts, which contain a variety of light-absorbing molecules called pigments. The main pigments found in green plants are chlorophylls a and b, and in fact, all photosynthetic cells contain some kind of

chlorophyll (*69*). There also exist accessory pigments, which include carotenoids (which split into two types: carotenes and xanthophylls) and phycobilins (which are found only in algae). The pigments in the chloroplasts are arranged into two structural groups called Photosystems I and II. Each photosystem is basically a cluster of pigments, with what are called "antenna pigments" at the edges and the "reaction center" at the center. The reaction center is simply a chlorophyll molecule and associated proteins anchored in the thylakoid membrane within the chloroplast. A photosystem starts functioning by having the antenna pigments absorb energy from sunlight. The energy may be transferred by resonance transfer to neighboring pigments that require light of either the same or less energy until it reaches the reaction center. The reaction center is where the energy of excited electrons is transferred into potential chemical energy via a sequence of oxidation-reduction reactions (Figure 2.7) (*69, 70*).

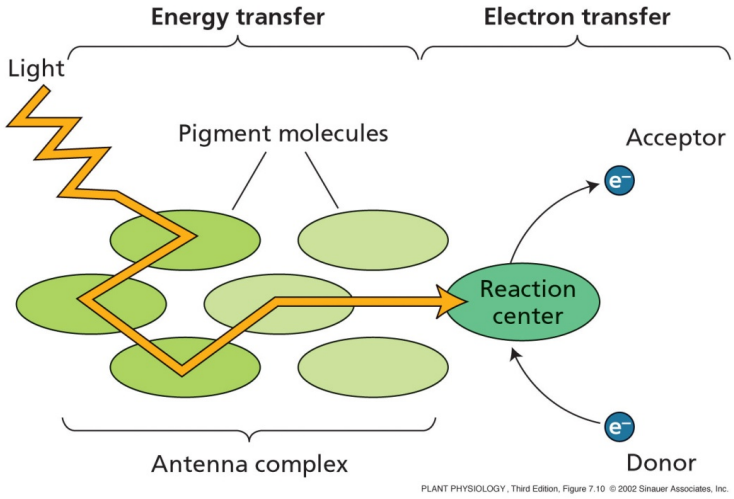

Figure 2.7. The functioning of a photosystem, where energy from light is carried among antenna pigment molecules until it makes its way to the reaction center, where it can then initiate a flow of electrons (71).

Photosystem I is a system with a high amount of the chlorophyll a pigment. Its reaction center is a molecule called P700, which is a chlorophyll molecule with attached proteins specialized to trap energy with a maximum absorbance at a wavelength of

around 700 nm (far red light). Photosystem II has a lower ratio of chlorophyll a to b than the first, and its reaction center is P680, another specialized chlorophyll and protein combination molecule whose peak absorbance is around 680 nm (red light). Both reaction centers, after receiving energy, release electrons that can then be transferred in a series of oxidation-reduction reactions.

The interaction between the two photosystems that eventually results in the creation of ATP and NADPH is a process called the "Z-scheme." As explained, a photon strikes pigments in Photosystem I, and the energy from the photon is transferred to the P700 molecule. The P700 loses electrons, which flow through a chain of electron carriers to an already existing, positively charged molecule called $NADP^+$. The negatively charged electrons are able to react with $NADP^+$ to create the product NADPH. Since P700 has lost electrons, it is left with an electron hole and a net positive charge. To fill this hole, an electron comes from Photosystem II via transporters and the cytochrome system protein complex (69). This electron comes from another photon striking Photosystem II at about the same time. Similar to Photosystem I, the energy from that photon makes its way to the Photosystem II reaction center, called P680. The P680 loses an electron that flows through a different chain of electron carriers to the hole that had been created in P700. The hydrolysis of a water molecule produces electrons that fill the electron holes formed in P680. Each transfer of electrons is energetically favorable, since the electrons start in an excited state with excess energy and reach a lower energy state by filling a hole. This process is often portrayed as a Z shape (on its side) with the rises and falls in energy levels of the electrons as they flow from water to fill a hole in

Photosystem II, from which an electron flows to fill a hole in Photosystem I, from which an electron flows to create usable energy (Figure 2.8) (*69, 71*).

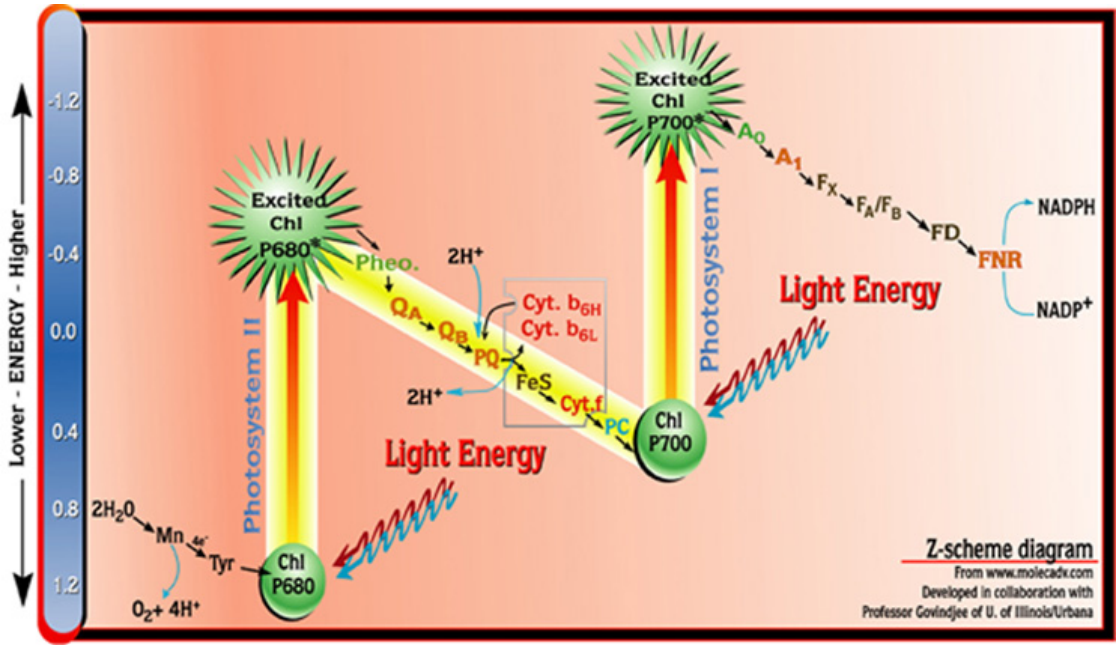

Figure 2.8. Another rendering of the Z-scheme, this time showing the energies of each state and how the electrons always flow to a position of lower energy except when light energy lifts them to an excited state (73).

Photosynthetic pigments are natural molecules whose primary function is to trap energy from sunlight and eventually convert it into a flow of electrons. They are found in all plants, and so they are very readily available in potentially large quantities. Plants have perfected photosynthesis over billions of years, and humans could use this natural technology to tap into the Sun's resources.

2.4. Individual Photosynthetic Pigments and Spectral Properties

The different pigments involved in photosynthesis vary in their spectral properties. Plants in nature make use of a myriad of pigments to capture a spectrum of light broader than any single pigment alone. By exploring the spectral properties of

various pigments, we are able to learn about their ability to capture different parts of the energy provided by the sun.

Not every photon can excite every electron in a light-absorbing molecule. Rather than being continuous, there is a discrete amount of energy between each level to which an electron can be excited. For this reason, only photons that have a certain wavelength (which governs the color of the light but is also related to energy) can be absorbed by a particular molecule (*69*). The color of a photosynthetic pigment is an indicator of what wavelengths the pigment can absorb, since the wavelengths that are not absorbed are usually reflected off the pigment and so give it the color we see. Thus, chlorophyll is green because it absorbs best in the red and blue range of the light spectrum. The two kinds of carotenoids, carotenes and xanthophylls, each get their colors from their own absorbance spectrum. Carotenes appear orange since they do not absorb blue light, and xanthophylls are yellow since they do not absorb light of the red spectrum. The construction of the light harvesting antennae leads to a broadened absorbance in the intact plant that is greater than the single pigment absorbance spectrum of the single pigments alone. Examples of some common photosynthetic pigment absorption spectra are shown in Figure 2.9. These spectra are made even broader when pigments interact with various proteins within chloroplasts (*70*).

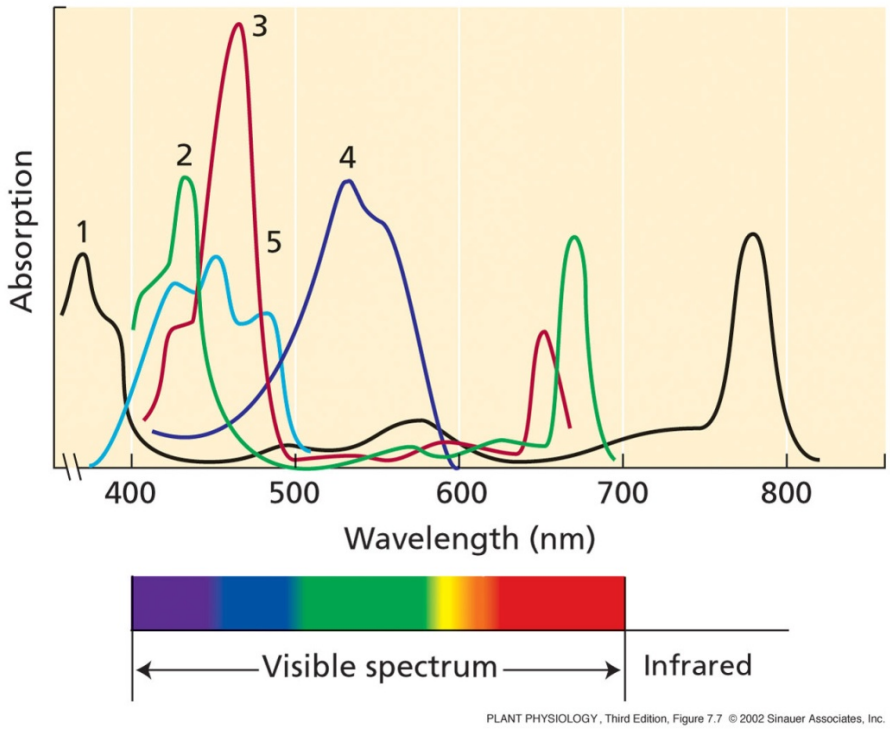

Figure 2.9. The absorbance spectra of various pigments. It can be seen here that each pigment has a peak absorbance at a different wavelength, and that the area under any one particular spectrum is not as great as the area under all of them combined (71).

Chlorophylls are naturally very efficient at absorbing light. In green plants in nature, chlorophyll serves as the major light-absorbing pigment. A photosynthetic action spectrum demonstrates which wavelengths of light cause photosynthesis to occur. For green plants, the action spectrum essentially follows the absorption spectrum of chlorophyll and, to a lesser extent, that of carotenoids (see Figure 2.10). Light that is captured by accessory pigments eventually has its energy transferred to chlorophyll molecules to be used in photosynthesis (*69, 70*).

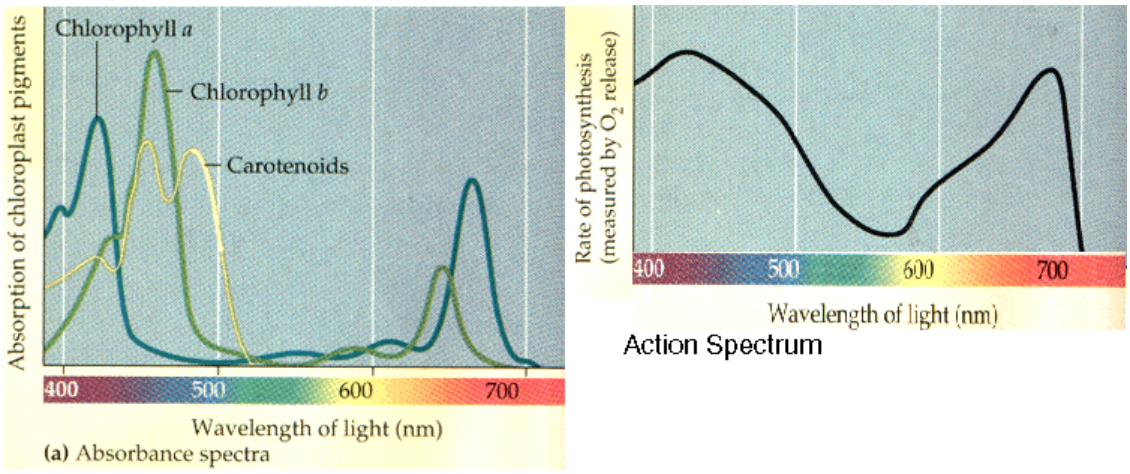

Figure 2.10. Here the absorption spectra of chlorophyll a, chlorophyll b, and certain carotenoids are overlapped and then placed beside the action spectrum of the photosynthesis in green plants to show how large a role chlorophyll plays in the determination of this spectrum (74).

Carotenoids aid the chlorophylls in two ways. First, carotenoids collect light that the chlorophyll does not absorb near the green part of the spectrum. As can be seen by their different colors, accessory pigments (like carotenes and xanthophylls) have absorption maxima at wavelengths different from those of chlorophyll, making them supplementary receptors of light to the chlorophyll. Accessory pigments capture incoming light that the chlorophyll cannot absorb (*69*). With this addition to the usable spectrum of light, a plant can utilize more of the incoming sunlight. The second role played by carotenoids is a form of defense, as carotenoids collect extra energy from the already excited chlorophyll and then dissipate it away as heat or in a series of biochemical reactions. For example, the xeazanthin cycle helps plants dissipate excess absorbed energy and minimize photoinhibition. This absorption of the excess energy prevents the formation of reactive oxygen species that may damage the plant (*70*).

Plants have naturally evolved to reach the composition of antennae complexes that maximize absorbance at their own unique environments. For example, plants vary tremendously quantitatively and qualitatively in the structure and composition of their

light harvesting complexes under shade and sun conditions. Therefore it seems likely that modifying pigments in DSSCs can improve their performance and efficiency as well. In our attempts to harvest energy from the sun, we can learn from plants and even make use of the pigments that they have already developed over billions of years for this sole purpose. By combining various different pigments, we can potentially at least imitate a process already found to be extremely efficient in nature.

2.5. Pigments and DSSCs

DSSCs incorporate pigments as the sensitizer with which they can absorb incoming sunlight and proceed with their process of turning that sunlight into viable energy. Most DSSCs in use today use artificial pigments, based on ruthenium and developed to capture as much light from the solar spectrum as possible. However, these artificial dyes are both expensive and toxic. Natural pigments could solve both of these issues, and it is this area that we wish to explore. Researchers have explored the possibilities of a variety of natural pigments as a replacement for the artificial sensitizers.

2.5.1. Individual Photosynthetic Pigments as Sensitizers for DSSCs

2.5.1.a. Chlorophyll Alone

As the source of energy capture, the sensitizer of a DSSC is a vital component that can be improved to raise the efficiency of DSSCs as a whole. Much research has been done with various dye electron sources to find sensitizers that would increase cell efficiency. Shortly after his ground-breaking paper, Michael Grätzel wrote a paper with

Andreas Kay in which they discussed TiO_2 solar cells sensitized with chlorophyll (Figure 2.11) and chlorophyll derivatives (*75*).

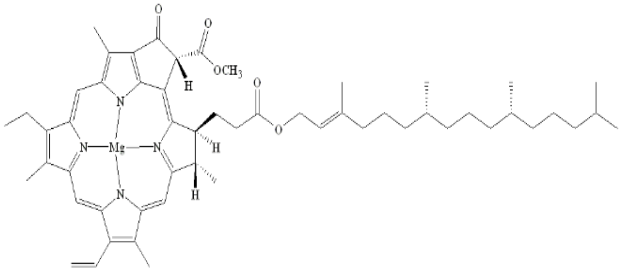

Figure 2.11. Molecular structure of chlorophyll (76).

When bound to TiO_2, the normal chlorophyll absorption peaks broadened (Figure 2.12) and Grätzel attributed this broadening to the polar interactions of the TiO_2 with the polar moieties of the chlorophyll a molecule and the higher concentration of chlorophyll that aggregates on the limited cell surface area. Gräztel and Kay concluded that while chlorophyll derivatives have shown a high photocurrent quantum yield comparable with the efficiency of natural photosynthesis, their practical use as a sensitizer is limited by their low energy conversion efficiency (*75*).

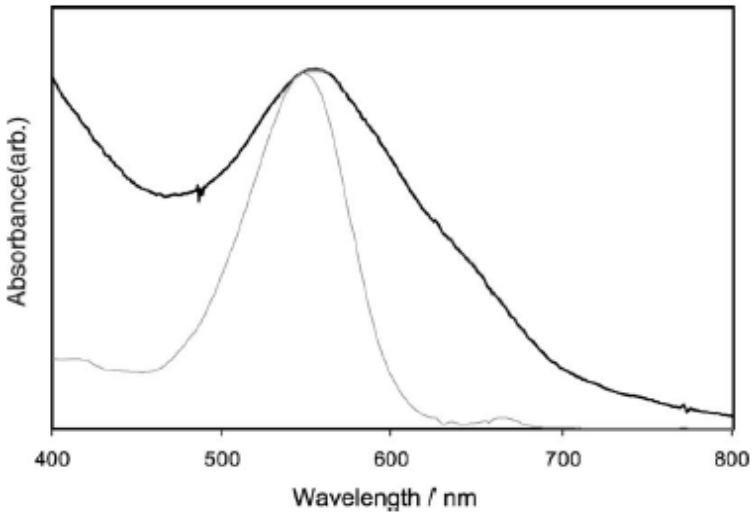

Figure 2.12. An example of widening of an absorbance spectrum when the dye is bound to the TiO2. Though this example is of fruit extract, the same thing occurs with all pigments (77).

An additional problem with using chlorophyll comes from its photostability as explained by the physical chemistry involved in electron excitation. When an electron absorbs energy, it is excited to a higher energy level from the ground state ($S_0 \rightarrow S_1$) and then releases this excess energy through radiation as it decays to its ground state. This process occurs very quickly in the order of magnitude of picoseconds. Occasionally, a vibrational energy sub-state of a lower energy level is close enough in energy to that of the excited electron state. In this case, the excited electron can alter its quantum spin so that it now mirrors that of the electron left in the unexcited ground state. This transformation is called intersystem crossing and results in the formation of a "forbidden" triplet state. The electron will eventually relax back down to the ground state and revert back to its original spin, but this process occurs at a rate order significantly slower than normal fluorescence (Figure 2.13). During this extended time period, the free electron is able to react with other entities in the system, leaving the original molecule from which the excited electron originated radically changed. In the case of chlorophyll, this radical change is the degradation of the chlorophyll. Because the chlorophyll remains in the triplet state for such a relatively long amount of time, chlorophyll becomes susceptible to reacting with external factors via reduction reactions, which inevitably result in the formation of radicalized species. These radicalized species, often singlet state oxygen because of its natural abundance (but potentially hydrogen as well), are incredibly reactive and can easily interfere with the chlorophyll and lead to rapid degradation of the chlorophyll molecule as a sensitizer. As such, it seems that chlorophyll would be too unstable to use as a sensitizer, especially over the extended periods of time that DSSCs would need to be operative in order to be practical for outside use (*78*).

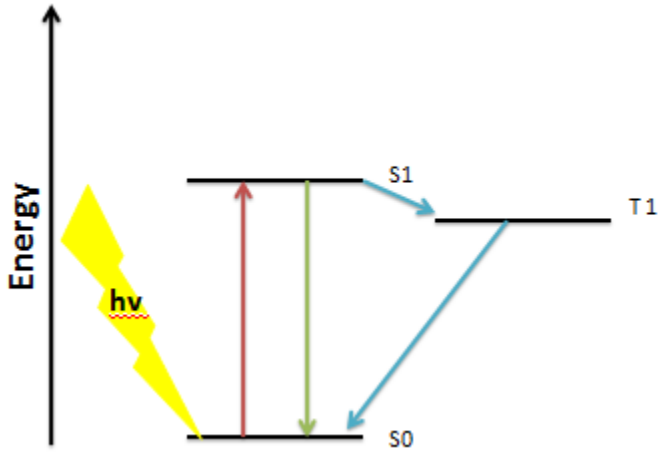

Figure 2.13. Energy diagram of the excitation of an electron form chlorophyll. When the light (hv) hits the ground state an electron is ejected (red arrow) to the next highest energy state S1. Here it can either fluoresce through relaxation (green arrow) or crossover to a triplet state and then fluoresce (blue arrow).

2.5.1.b. Artificial Dyes

Artificial dyes might at first glance seem much more promising for the efficiency of DSSCs than chlorophyll, but they too carry disadvantages. Ruthenium based dyes, such as N3 dye (Figure 2.14) are commonly used artificial pigments that absorb light wavelengths with peaks around 400 nm and 550 nm. Thus, N3 dye shows a higher absorbance than chlorophyll, and is able to cover a large amount of the non-linear solar irradiance (Figure 2.15). DSSCs incorporating N3 dye has a strong incident photon to current efficiency (ICPE), or the efficiency of the cell to convert photons into usable energy, of about 80%. However, despite its good binding properties with the TiO_2 semiconductor and a strong ICPE, N3 dye does not absorb well above 600 nm and thus leaves a lot of the photons from the natural sunlight in the 600-800 nm range unabsorbed. Further problems noted with Ruthenium based dyes are in the price and sustainability of the sensitizer. Ruthenium is a rare earth metal and as such is subject to higher market prices because of its limited supply.

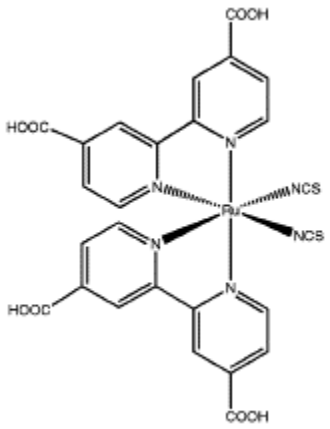

Figure 2.14. The molecular structure of (cis-bis(4,4-dicarboxy-2,2-bipyridine)dithiocyanato ruthenium(II) or N3 dye (*44*).

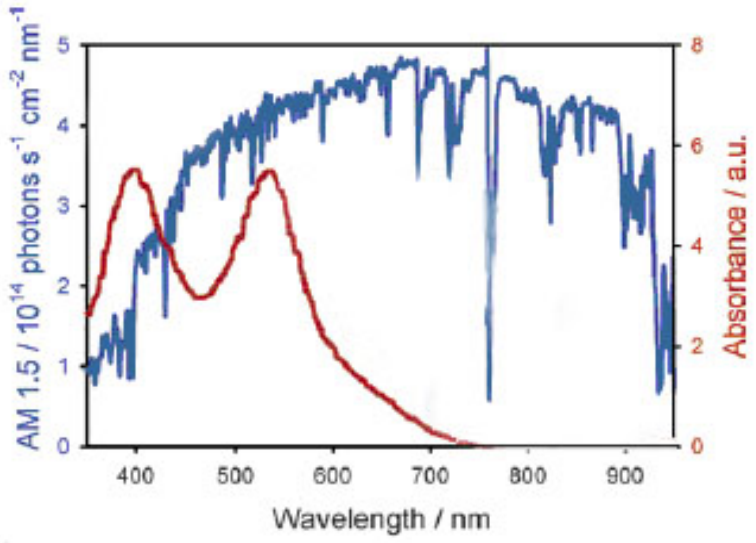

Figure 2.15. N3 dye absorbance (shown in red) compared with solar irradiance (overarching blue curve) (44).

Because N3 dyes do not absorb all wavelengths of visible light, pigments that absorb in the missing ranges have become the subject of many studies. One example is the recently developed synthetic Black Dye, which has a broad absorbance throughout the visible spectrum. Ru(4,40,400-tricarboxy-2,20:60,200-terpyridine)(NCS)3, also known as the Black Dye, is currently the most efficient dye for use in DSSCs. The Black Dye is a modification of the ruthenium polypyridyl complex N3 dye (Figure 2.16) (*44*).

Recent studies on the Black Dye show the dye to have a nearly quantitative absorbed photon to current efficiency (APCE), indicating this dye exhibits strong coupling to the semiconductor and minimal recombination (*44*). The Black Dye improves on the N3 dye by increasing the absorbance spectrum 100nm further in the infrared range (Figure 2.17). This expansion in the absorption increases the absorption of light, yields a higher V_{oc} and J_{sc}, and results in an increase to 15% efficiency without any modification to the cell (79).

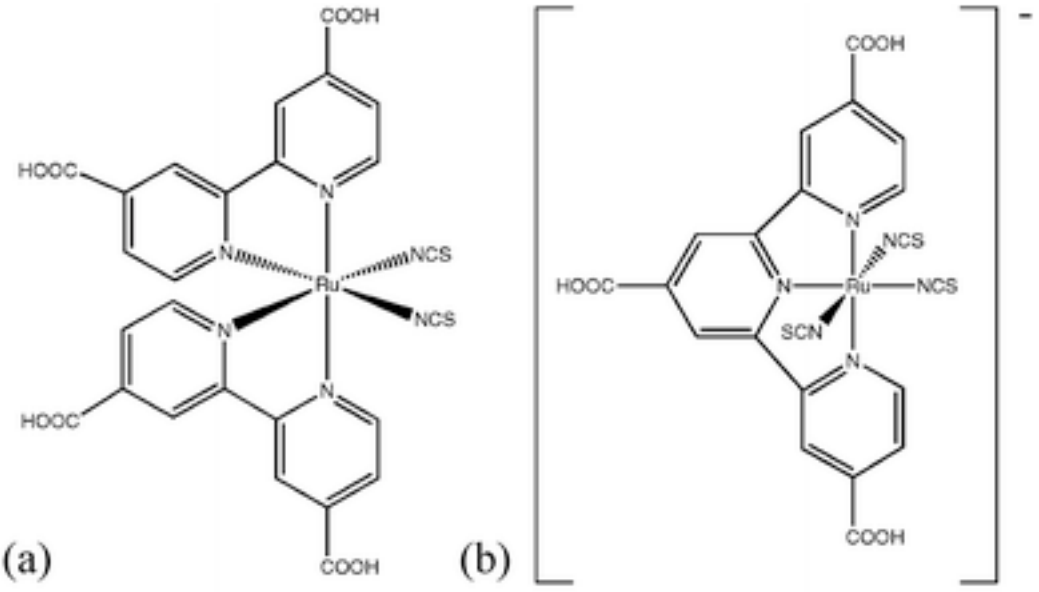

Figure 2.16. (a) Structure of Ruthineum Polypyridyl complex N3 dye. (b) Structure of the Black Dye (*44*).

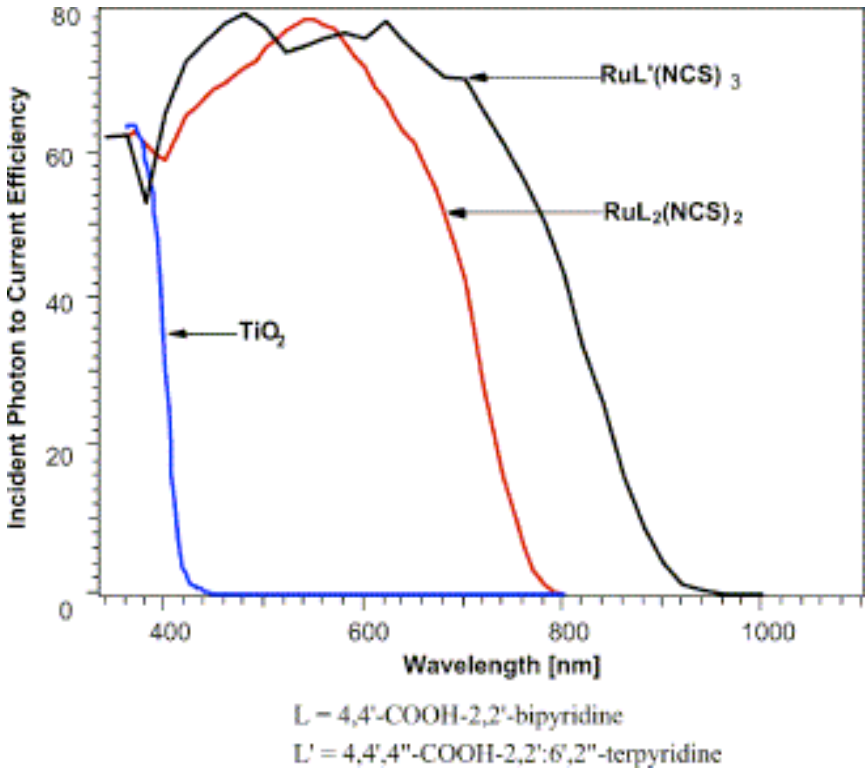

Figure 2.17. Graph of photocurrent action spectra of TiO2 (Blue), N3 (Red), and The Black Dye (Black) (79).

2.5.1c. Other Natural Photosynthetic Pigments – Carotenoids

Chlorophyll alone does not seem to be a very viable DSSC sensitizer, but other natural pigments exist that can replace the expensive, toxic, artificial pigments. Carotenoids, which often make up the majority of the accessory pigments in plants, make for an interesting study because they tend to absorb in the green range of the visible spectrum, where the sunlight intensity is the highest. Probably just as important as its added absorption to the overall solar cell, carotenoids possess the ability to act as a photoprotecting agent to shield chlorophyll from its own triplet state.

Carotenoids can act very effectively as agents for protecting photosystems against the harmful effects of the induced oxidation described above. They can quench the initial triplet state of the chlorophyll sensitizer by absorbing energy from it to return the

sensitizer to its original ground state singlet without the formation of harmful radicals. This process (outlined below) forms a triplet state carotenoid, but unlike the chlorophyll, triplet state carotenoids will dissipate their excess energy harmlessly as heat and not form radicals with existing O_2 molecules.

$Chl + \xrightarrow{h\nu} {}^1Chl^*$

${}^1Chl^* \rightarrow {}^3Chl^*$ (intersystem crossing into triplet state)

${}^3Chl^* + Car \rightarrow {}^3Car^* + Chl$ (triplet Chl returns to ground and Car excites to triplet state)

${}^3Car^* \rightarrow Car + Heat$ (degradation of triplet Car to singlet state)

Carotenoids also maintain the ability to react with the already formed radical and return them to their initial states, but the exact mechanism through which this processes occurs is still not well understood. The steps that are understood are outlined below (44):

$Chl + \xrightarrow{h\nu} Chl^*$ (singlet excited Chl)

$Chl^* \rightarrow {}^3chl^*$ (triplet excited Chl)

${}^3chl^* + O_2 \rightarrow Chl + {}^1\Delta_g O_2$ (Singlet oxygen)

${}^1\Delta_g O_2 + Car \rightarrow {}^3Car^* + O_2$ (transfer of energy to triplet Car)

${}^3Car^* \rightarrow Car + Heat$ (degradation of triplet Car to singlet state)

It must also be noted that various studies have found that the number of conjugated double bonds has a great impact on the efficiency of the carotenoid as a photoprotector. A study involving *M. luteus* showed that carotenoids with fewer than 9 conjugated double bonds are much less efficient in quenching singlet oxygen, since a mutant strain in which the carotenoid contained only eight conjugated bonds was three times less effective at protection. Studies have shown that carotenoids also have some effect acting like a sunscreen to protect various plants, algae and bacteria from degradation caused by "near UV" (UV-B and UV-A, of wavelengths between 280 nm and 400nm) (*44*).

2.5.1d. Carotenoids in DSSCs

With respect to the absorbance of carotenoids in DSSCs, two different studies examined the potential of using them as the sole sensitizing agent. De Padova et al. used beta-carotene (Figure 2.18), a completely nonpolar molecule, and achieved a voltage of 320 mV and a current output of 0.35 mA (*77*). This result is significant, because beta-carotene, being nonpolar, does not contain any moieties that would appear to allow it to bind with the TiO_2, but it still yielded an output statistically significant from blanks. In addition, beta-carotene is less expensive to purchase than chlorophyll or many other of the carotenoid pigments. If beta-carotene could prove as a viable substitution for artificial pigments, it would significantly lower the cost of constructing the DSSCs.

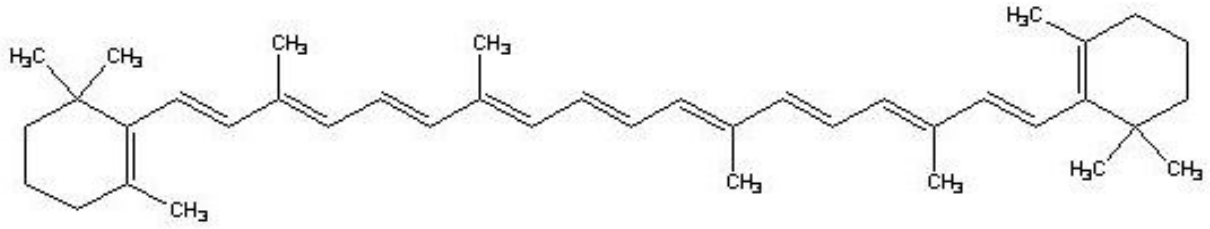

Figure 2.18. The molecular structure of β-carotene (44).

A second study involving carotenoids examined the use of two pigments, crocetin and crocin, as sensitizers. Both of these carotenoids are structurally similar to beta-carotene but contain two ester groupings on the end that allow it to bind better to the semiconducting layer. This improved binding allowed DSSCs sensitized with crocetin to achieve a voltage of 430 mV and a current of 2.84 mA, while DSSCs sensitized with crocin achieved a voltage 580 mV and a current 0.45 mA (80). Xanthophyll (Figure 2.19), a carotenoid similar to crocin and crocetin, is also promising and will be discussed later in this literature review.

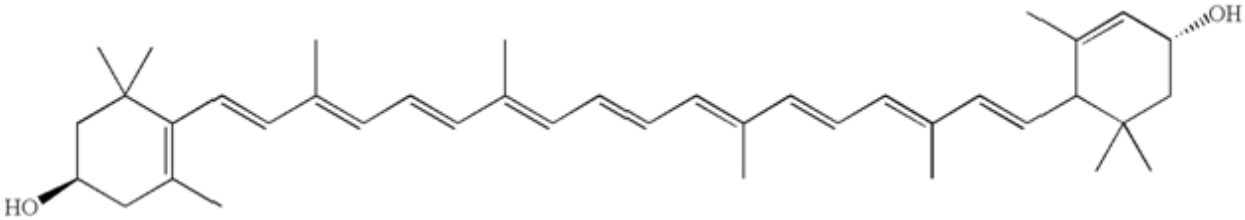

Figure 2.19. The molecular structure of xanthophylls (44).

2.5.1e. Anthocyanins

The search for natural pigments similar to N3 dyes in absorbance led researchers to turn to anthocyanins. Anthocyanins are glycosylated polyphenols that are water-soluble and produce a range of colors from red to purple in flowers, fruits and fall foliage. Grätzel and colleagues experimented with cyanin and achieved a V_{oc} of between 400 mV and 450 mV and a J_{sc} of between 1.5 mA and 2.2 mA for DSSCs sensitized with cyanin (*81*). In a comparable study, Tennakone et al. examined the use of cyanidin (an anthocyanin that is harder to isolate and less photostable then cyanin) from blood-red anthurium flowers. Tennakone et al. recorded a V_{oc} of 435 mV and a J_{sc} of 2.9 mA for DSSCs sensitized with cyanidin. However, they observed an immediate decay of the photocurrent from the cells when a potassium iodide (KI) electrolyte was utilized. They concluded, similar to Kay and Grätzel regarding the chlorophyll derivatives, that cyanidin was impractical as a sensitizer on its own because DSSCs sensitized with cyanidin achieved very low current and voltage outputs. Neither of these studies' results is near the 15%-17% efficiency required to make DSSCs commercially viable (*82*).

Many further studies have been conducted to explore the efficiency of using fruit juice extract containing anthocynanins to boost voltage and current outputs. Using just the juices extracted from a pomegranate containing the anthocyanin cyanidine-3-glucoside as a sensitizer, researchers were able to able to achieve voltages between 300

mV and 480 mV, and currents ranging from 0.18 mA to 0.86 mA depending on the electrolyte used in the cell. Like the studies before, these researchers observed a widening of the absorption spectra of the anthocyanin as it bound to the TiO_2 semiconducting layer and became stabilized (*83*). Many other such studies of anthocyanins as sensitizers have been preformed and their respective results are summarized in Table 2.1 below.

Anthocyanin Source Tested	Reported Photovoltage (mV)	Reported Photocurrent (mA)	Reported Max Power (mW/cm^2)	Reported Fill Factor (%)
Red Sicilian Orange (84)	340	3.84	0.66	0.50
Strawberry (84,85)	405	2.86	0.61	0.53
Blueberry (84,85)	360	4.29	0.52	0.34
Orange (84,5)	412	1.02	0.13	0.31
Red Cabbage (84,85)	525	4.70	1.51	0.61
Cochineal (84,85)	397	6.00	1.20	0.52
Skin of Jaboticaba (84,86)	660	2.60	1.10	0.62
California blackberry (84)	400	2.20	0.56	-
Skin of eggplant (84,86)	350	3.40	0.48	0.40
Black rice (84,87)	551	1.14	0.327	0.52
Rosa xanthina (87)	492	0.637	0.163	0.52
Betaxanthin (87)	220	2.00	-	0.51
Betanin (87)	270	0.51	-	0.47
Melanin (87)	230	0.75	-	0.35

Table 2.1. Different anthocyanins tested as sensitizers and their respective voltage and current outputs.

2.5.1f. Increased DSSC Performance with Combined Pigments

It has been shown that natural photosynthetic pigments can serve as an appropriate sensitizer in a DSSC. Individual plant pigments, such as chlorophyll, xanthophyll, carotenoids, and anthocyanins have appropriate light absorption characteristics when combined with TiO_2 to function sufficiently in DSSCs.

Some studies have shown that combinations of more than one plant pigment may increase energy output and solar energy conversion efficiency. Liu et al. tested cells sensitized with pure chlorophyll, pure xanthophyll, or a mixture of both pigments (*38*). The absorption spectra of each pigment at a presumed equal concentration and the mixed pigments indicated the absorbance of xanthophyll was greater than that of the mixture of the two pigments combined (Figure 2.20). The absorption of the mixed solution was the "linear superposition" of each of the pigments alone and lower absorbance values than each individual pigment because the mixture contained a reduced concentration of each pigment.

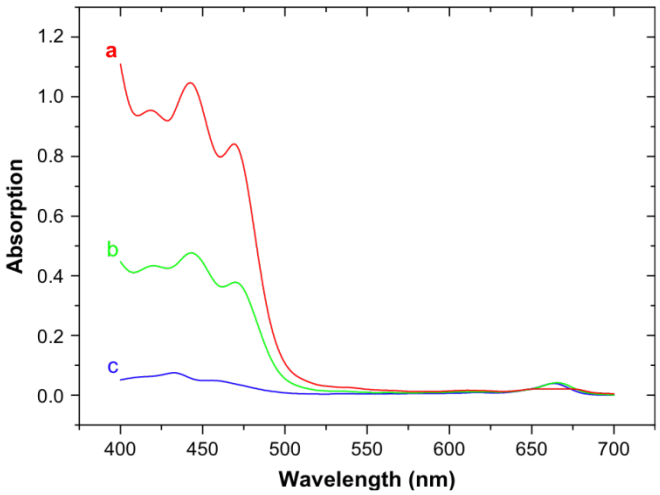

Figure 2.20. Shown are the absorption spectra for the same concentration of a. xanthophyll, b. chlorophyll and xanthophyll combined in a 1:1 ratio, and c. chlorophyll (38).

However, when the piments were bound to TiO_2, the absorption characteristics changed. The mixture had the greatest absorption spectrum in this study (Figure 2.21).

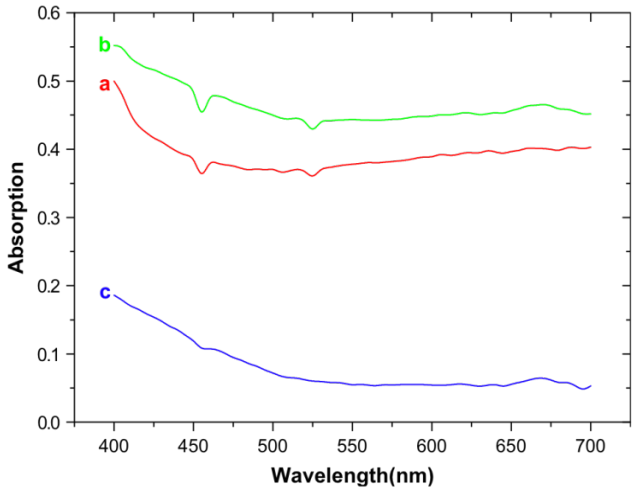

Figure 2.21. Shown are the absorption spectra for a TiO_2 electrode binded to a. xanthophyll, b. chlorophyll and xanthophyll combined in a 1:1 ratio, and c. chlorophyll (38).

Liu et al. suggested that the reason behind the increased performance of DSSCs created with the mixture of chlorophyll and xanthophyll was that the combination of chlorophyll and xanthophyll in DSSCs mimic the natural process of photosynthesis in plants and capture more incoming light (38). They further suggested that electrons excited in chlorophyll that were not injected into the TiO_2 band were captured by xanthophylls and that xanthophyll was therefore able to inject electrons from its own absorbance, as well as excess electrons originally excited in chlorophyll (*38*). Thus, according to Liu et al., the scheme of energy conversion between primary and secondary dyes in plants is recreated when chlorophyll and xanthophyll are used in DSSCs (*38*). They termed this higher output achieved through the use of a mixture a synergistic effect. While they provided no evidence of a real synergism, the phenomenon lends credibility

to the hypothesis that using naturally occurring ratios of plant pigments to sensitize DSSCs can lead to superior cells with the greatest energy output.

A study by Chang and Lo documented a similar trend with chlorophyll and anthocyanins (*88*). Chang and Lo extracted chlorophyll from pomegranate leaves and anthocyanins from mulberry fruit to sensitize DSSCs. Similar to the previous study, Chang and Lo showed the individual absorption spectra for chlorophyll and anthocyanins and compared it to the spectrum for the mixture of the two pigments. The overall effect was an increase in the total amount of light absorbed over all relevant light wavelengths.

Chang and Lo also provided a plot of Current Density versus Voltage for the cells treated with chlorophyll, the cells treated with anthocyanins, and the cells treated with a mixture. This revealing diagram showed that for any given value of voltage in the cells, there was approximately 1.5 times as much current in the cells treated with a mixture of the pigments as there was for either of the individual pigments. This means that the cells treated with a mixture of pigments were much more effective at creating an electrical current for the same applied light sources. Additionally, the value of photoelectric conversion efficiency for the mixture of pigments was approximately 1.2 times greater than that of either individual pigment. Clearly, the cells treated with a mixture of pigments exhibited a superior performance compared to those treated with either individual pigment, again displaying the synergistic effect.

In another study, Kumara et al. examined the effect between chlorophyll and shisonin, both extracted from shiso leaves (*39*). This study showed the electrical activity of the tested DSSCs with varying wavelengths of light. Similar to light absorption spectra, the electrical activity charts for cells treated with each pigment display peaks at

particular wavelengths of light, and as before, the chart for the mixture of the two pigments retained the peaks of individual pigments at slightly lower values. The overall effect discovered was that the cells treated with the combination of pigments exhibited a higher overall total electrical activity when summed over all wavelengths of light. Since electrical activity versus light energy is a critical characteristic of photovoltaic cells, the increase in overall electrical activity means that the DSSCs treated with combined pigments have superior performance to those treated with individual pigments.

Three distinct studies demonstrated the effect of using multiple natural plant pigments on the solar energy conversion of DSSCs. Not only did pigment combinations exhibit higher energy conversion and electrical activity than lone pigments, but combinations also mimicked some of the natural processes that occur during photosynthesis in plants. The synergistic effect of multiple plant pigments in DSSCs shows great promise for maximizing the output and solar energy conversion of these solar cells.

Despite the promise that seems to come from the synergistic effect, it is important to note that not all combinations of photosynthetic pigments have displayed this same synergistic effect when sensitizing a DSSC. Wongcharee et al. (2007) used rosella and blue pea extracts alone and in equal combination, but they found that the DSSC sensitized with rosella extract alone had the best sensitization (*89*). As an anthocyanin, it had the broadest absorption spectrum, and this spectrum was not improved by the combination (*89*).

Though their results did not support the previous results for the synergistic effect, they did display the complicated interactions of pigments in their sensitization of DSSCs.

The relationships between pigment spectra and ICPE (a measure of cell efficiency) are not simply additive. More research is required to fully understand mechanisms of pigment combinations and their binding affinities with TiO_2 in order to select optimal pigment combinations.

2.6. Conclusions of Literature Review

Based on our literature review, we have decided to focus our research on the dye of the DSSC. Instead of manipulating chemically produced dyes, we will use photosynthetic pigments. In order to further explore the effects of various pigment mixtures on DSSC output, we will use three photosynthetic pigments, alone and in combinations, that have been shown to produce at least some current. Plants display a wide range of synergistic effects in terms of the interactions between primary and accessory photosynthetic pigments. Therefore, we have designed our DSSCs so that they are similar to green plants in that we will use the three most common photosynthetic pigments in plants—chlorophyll, xanthophyll, and beta-carotene. The performances of DSSCs will be related to the absorbance spectra of the corresponding pigment solutions to determine if there is a correlation between cell performance and total pigment absorbance. We hypothesize that the larger absorption spectrum a cell's sensitizing pigment solution has, the larger the cell's output will be.

3. METHODS

3.1 Pigments

Stock solutions of beta-carotene, xanthophyll, and chlorophyll a were acquired from Sigma-Aldrich (Sigma-Aldrich Inc, St. Louis, MO, USA). Each pigment was diluted in ethanol to a final concentration of 1.119×10^{-4}M. The pigments were stored in the dark at -18°C.

3.1.1. Absorption Spectra

In order to measure absorption spectra of the pigments, pigment solutions were further diluted to a concentration of 1.119×10^{-5}M in ethanol. Absorption spectra were measured from 390-700 nm in 1nm increments using Shimadzu Model UV-2550 Dual Beam Spectrophotometer (Shimadzu Inc, Kyoto, Japan).

3.2. Electrodes and Counter Electrodes

Uncut transparent TiO_2-coated test cell TEC15 glass plates and Pt-coated test cell TEC15 glass plates were obtained from DyeSol (DyeSol, Queanbaven, NSW, Australia). TEC15 glass plates were chosen over TEC8 glass plates because TEC15 is a cheaper alternative to TEC8 glass and is the standard glass used in current DSSC research, as discussed previously in the Literature Review. The dimensions of the uncut glass plates were 161mm x 80mm. The plates were cut into 28 individual electrodes and counter electrodes measuring 20mm x 23mm ($460mm^2$) with an active area of 8mm x 11mm ($88mm^2$) coated with 18NR-T TiO_2.

The plates were cut using a Dremel grinder tool (Dremel, Racine, WI, USA) because a manual glasscutter was not sufficient. A score was first made at least half way through the glass while the temperature of the glass was kept low under a constant stream of cool water. After cutting a deep score, the section of the glass was snapped off by applying pressure to either side of the score. Sharp edges were then ground away with the grinder tool.

The electrodes and counter electrodes were heated on Fisher Scientific Isotemp Digital ceramic-top hot plate (Fisher Scientific, Pittsburgh, PA, USA) at 300°C for 45 minutes according to instructions from DyeSol. After the electrodes cooled to 90°C, the electrodes were placed in a vial containing 20mL of pigment solutions. The electrodes were soaked for 24 hours in the dark at room temperature. Three electrodes were soaked in each of the following pigment combinations:

	Pigment Combination
1	Blank
2	100% Chlorophyll
3	100% Chlorophyll
4	100% Beta-carotene
5	1:1 Chlorophyll: Beta-carotene
6	1:1 Chlorophyll: Xanthophyll
7	1:1 Xanthophyll: Beta-carotene
8	1:1:1 Chlorophyll: Xanthophyll: Beta-carotene
9	2:1:1 Chlorophyll: Xanthophyll: Beta-carotene
10	1:2:1 Chlorophyll: Xanthophyll: Beta-carotene
11	1:1:2 Chlorophyll: Xanthophyll: Beta-carotene

Table 3.1. Pigment solution used to sensitize electrodes.

Before assembling the solar cells, the counter electrodes were cooled to room temperature.

3.2.1. Cell Assembly

After the electrodes were soaked in the pigment solutions for 24 hours, they were carefully removed from the solutions with tweezers and allowed to air dry. The electrode was placed on top of the counter electrode in such a manner to maximize contact between the TiO_2 and platinum. Binder clips were placed along the edges of the cell to hold the glass plates together. Once the plates were secure, KI electrolyte solution was dropped onto the edge of the cell and spread between the glass plates through capillary action to cover the entire active area. Excess electrolyte was wiped off the solar cell.

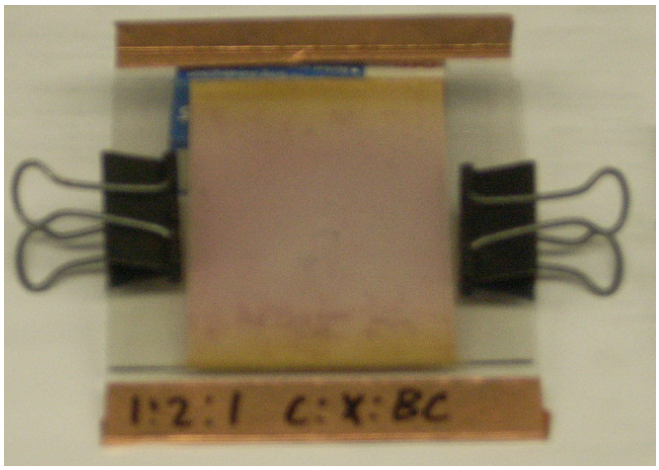

Figure 3.1. Photograph of cell placed electrode side up, displaying placement of copper tape and binder clips for the testing process.

As the last step of the construction process, copper tape was placed along the protrusions on the top and bottom of each cell (Figure 3.1). The copper tape served as a point of contact to which wires could be attached to complete circuits with the cells. The glass plates were specified to have a sheet resistance of 15 ohms, so the use of copper tape was designed to minimize any further increases in resistance associated with the electrode-wiring contact points.

3.3. Testing

The cells were placed in a Conviron Model BDW36 Growth Chamber (Conviron, Pembina, ND, USA). The chamber was equipped with 20 GE MVR400/HOR/MOG metal halide lamps (General Electric, Fairfield, CT, USA) filtered with a 1/8 inch Plexiglass type G barrier to remove most of the ultraviolet radiation from the chamber (Figure 3.2). The spectral irradiance inside the chamber is shown in Figure 3.3. The cells were evaluated at a temperature of 22°C and 15% relative humidity. Lights were turned on for the first 30 minutes, off for the next 30 minutes, then on again for the final 30 minutes. Three cells sensitized with the same pigment combination were attached to 21X Datalogger (Campbell Scientific, Logan, UT, USA). The Datalogger measured the voltage and current of each cell every second. The voltage and current values were averaged every 10 minutes. Data were recorded with PC200W Datalogger Starter Software (Campbell Scientific, Logan, UT, USA).

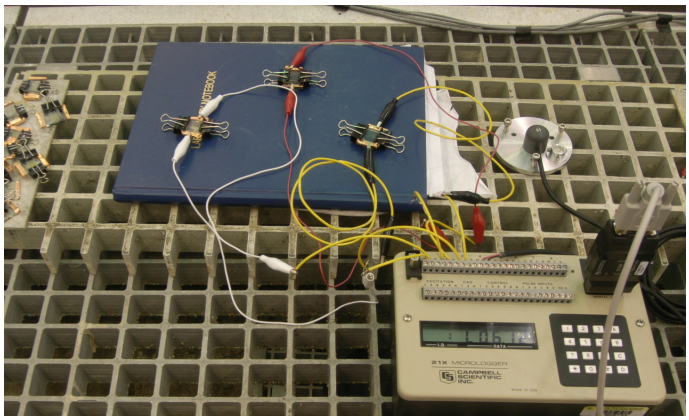

Figure 3.2. Photograph of three cells attached to data logger in growth chambers during testing process. The circular light sensor in the upper right quadrant of the photograph is a quantum used to verify the operation of the chamber lights.

3.4. Analysis

3.4.1. Absorption Spectra Analysis, Development of the A-value

In order to predict which pigment or pigment combination would be the most effective dye in terms of maximizing cell output, a variety of computations were conducted with the measured pigment absorbance spectra in order to produce an adjusted absorbance or "A" value for each pigment mixture. The simple absorption spectra of a pigment is not sufficient to compare the energy production results of the DSSCs since the total energy available to the DSSCs is determined by the combination of the pigments absorbance characteristics and the lamp output (energy available). Each lamp source has a unique spectral output so the effectiveness of a given pigment will vary depending the light source used to supply the energy to the cells. The output spectra for the specific lamp used in the growth chamber compared with normalized solar photon flux are shown on Figure 3.3 below.

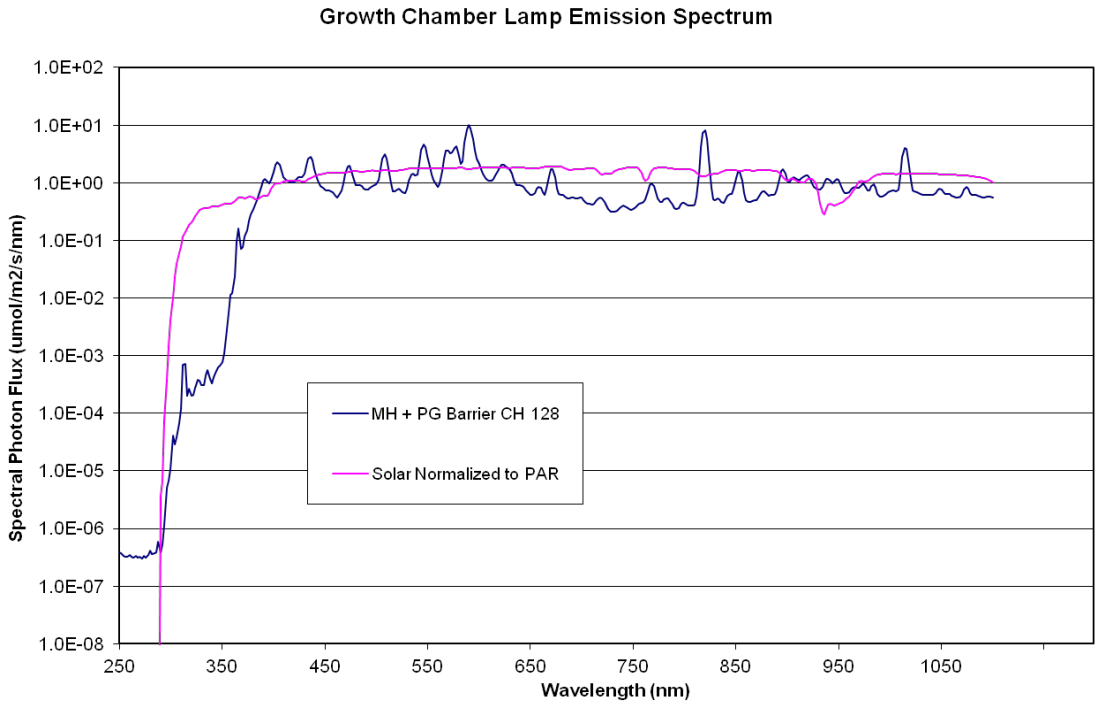

Figure 3.3. Emission spectrum from metal halide lamps (MH) filtered by a plexiglass barrier (PC) in a Conviron Model BD236 growth chambers (blue) compared to solar output normalized to PAR (pink), obtained with an Optronics Model 754 spectroradiometer (Optronics Inc. Orlando, FL, USA).

A number of mathematical computations were used to calculate an effective absorbance or "A" value for each pigment combination. First all spectra were normalized to unity at 710 nm in order to compare spectra. Second, these absorbance values were multiplied by the lamp output in moles at each nm to compute the adjusted absorbance for each pigment at each wavelength (Equations 3.1).

$$A_{adj} = A_{\lambda} \text{ X } PF_{\lambda}$$

Equation 3.1. Adjusted A-value at each wavelength.

where A_{adj} was the adjusted absorbance value for a given wavelength, A_{λ} was the measured absorbance at a given wavelength and PF_{λ} was the lamp emission at a given wavelength.

This process was completed for each collected absorption spectrum. An adjusted spectrum is shown below in Figure 3.4 for the solution of 100% chlorophyll in ethanol.

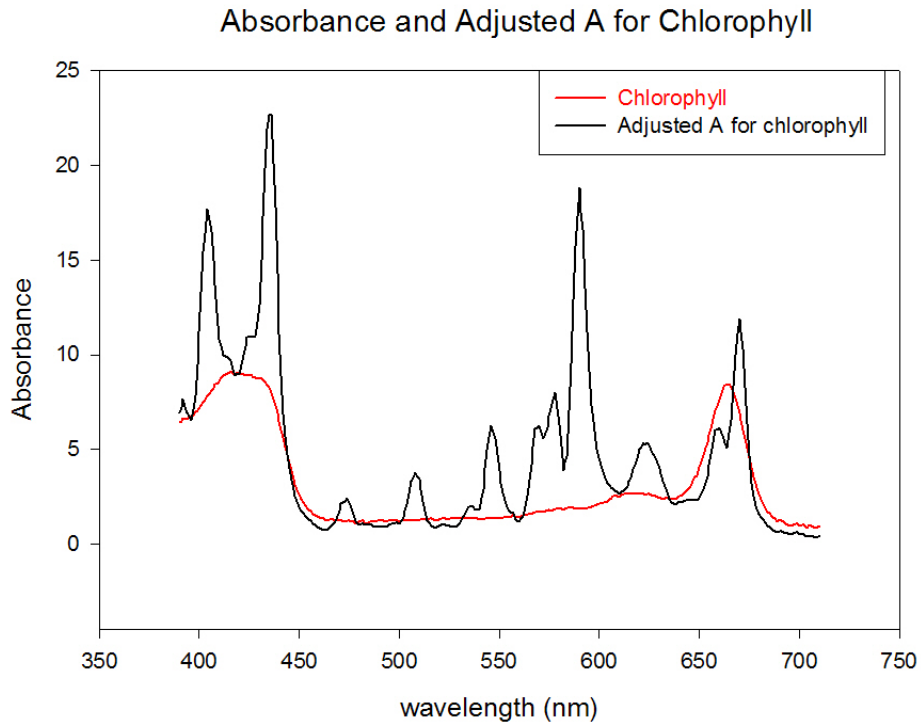

Figure 3.4. Adjusted absorption spectrum for 100% chlorophyll, obtained by multiplication of absorption values with scaled light output values.

The absorption spectrum for each tested pigment combination can be found in Appendix 2.1.

Finally the "A" value was obtained by determining the area under each adjusted absorbance cure. The process of calculating this value is summarized below in Equation 3.2. The areas under the adjusted absorption spectra were calculated using the method of trapezoidal Riemann sums according to the equation below.

$$Absorptive\ Area = A = \sum_{i=2}^{n} \frac{(a_i + a_{i-1})}{2} * (\lambda_i - \lambda_{i-1})$$

Equation 3.2. The area under absorption spectra curves termed the "A-value".

where *i* was the index of the absorption value, *n* was the total number of absorption values, a_i was the absorption value with the index indicated, and λ_i was the wavelength of the indicated index. The area under the adjusted absorption curve is now referred to as the A-value for a given pigment mixture.

The A-value then was calculated and assumed to represent the estimated total absorptive capability of a pigment mixture in that light source. Therefore, a pigment mixture with a higher "A-value" curve was theoretically better than a mixture with a lower "A-value" at absorbing the light from that source and producing cell power output. The ability of this value to predict cell output was tested by regression analysis using the cell output parameters described below.

3.4.2. Cell Output Data Analysis

To better understand the potential of the DSSCs to provide useable electricity, it was more prudent to examine output power rather than potential difference. The data logger stored data for both the current and potential difference of each tested cell. Using current and voltage information, power was calculated using the equation below,

$$P = IV$$

Equation 3.3. Equation for power.

where P was electrical power, I was the electrical current and V was the electrical potential difference.

Power was calculated for each cell at every time point by multiplying voltage and current, which yielded a power output curve versus time for each cell (three curves per pigment combination). The three curves were averaged together to produce an average power curve per pigment combination. While many photovoltaic measurements calculate the maximum power or P_{max} of the I-V curve, it was not calculated in this study because instead, power at each time point was calculated and averaged. This practice was suitable for the comparative purposes as all measurements used the same resistance based on the resistor in the data logger.

3.4.2a. Average Power Output

The average power output of each cell over the irradiation period was calculated in order to compare one pigment mixture to another based on DSSC output. This gave a single output value to compare overall electrical performance of each pigment combination.

The lights in the growth chamber were active for two 30-minute periods separated by a 30 minute dark period for each pigment mixture. This resulted in two distinct regions of electrical activity of the DSSCs. In many cases cell output was highly variable during the first irradiation period and was more stable during the second irradiation time period. For this reason, the cell outputs from only the second light interval were used to calculate the time average value. The sole exception to this general policy was the mixture of 2-1-1 beta-carotene to chlorophyll to xanthophyll. For this mixture, due to a timer malfunction, the second peak had values at only 2 separate points in time, which were not enough to calculate a reliable average (see Figure A2.2.9). This power output average over time for each pigment mixture was calculated and tabulated.

3.4.2b. Additional Cell Output Data

In addition to examining the time average power of DSSCs treated with each pigment combination, two other data analysis methods were performed. First the average of the maximum power values for each pigment combination were calculated by averaging the highest achieved power output for each cell, resulting in one maximum power value per pigment combination. These data were not further analyzed and are not shown here. The absolute maximum power output value was also recorded by taking the single highest achieved output value of any cell for that given pigment combination.

3.4.3. Statistical Evaluation of Results

The study was treated as a completely randomized design with 3 replicates of each cell pigment composition. Cell power output was compared with the A-value using the Mixed Model procedure of SAS (Statistical Analysis System, Cary, NC, USA). The Mixed Model was used to adjust for different replication number of cells. The model tested was average cell power vs. A-value. In order to compare output parameters for each cell pigment composition and determine whether there were differences between pigment mixtures, LSMEANS were computed and were separated using the LSD (Least Significant Differences) function of the SAS program.

4. RESULTS

4.1. Pigment Spectra

Pigment absorption capabilities were measured and analyzed for the development of a model to predict which pigments would be the best sensitizers for DSSCs. We measured the absorption spectra for the chosen pigments and pigment mixtures using a spectrophotometer. Shown in Figure 4.1 is the absorption spectrum for a solution of 100% chlorophyll diluted in ethanol. We measured the absorption for each single pigment as well as the absorption spectra for all of our tested pigment mixtures (see Table 3.1 for a list of all pigment combinations). The complete set of spectral data (i.e., the absorption spectra for every tested pigment and pigment combination) is compiled in Appendix 2.1.

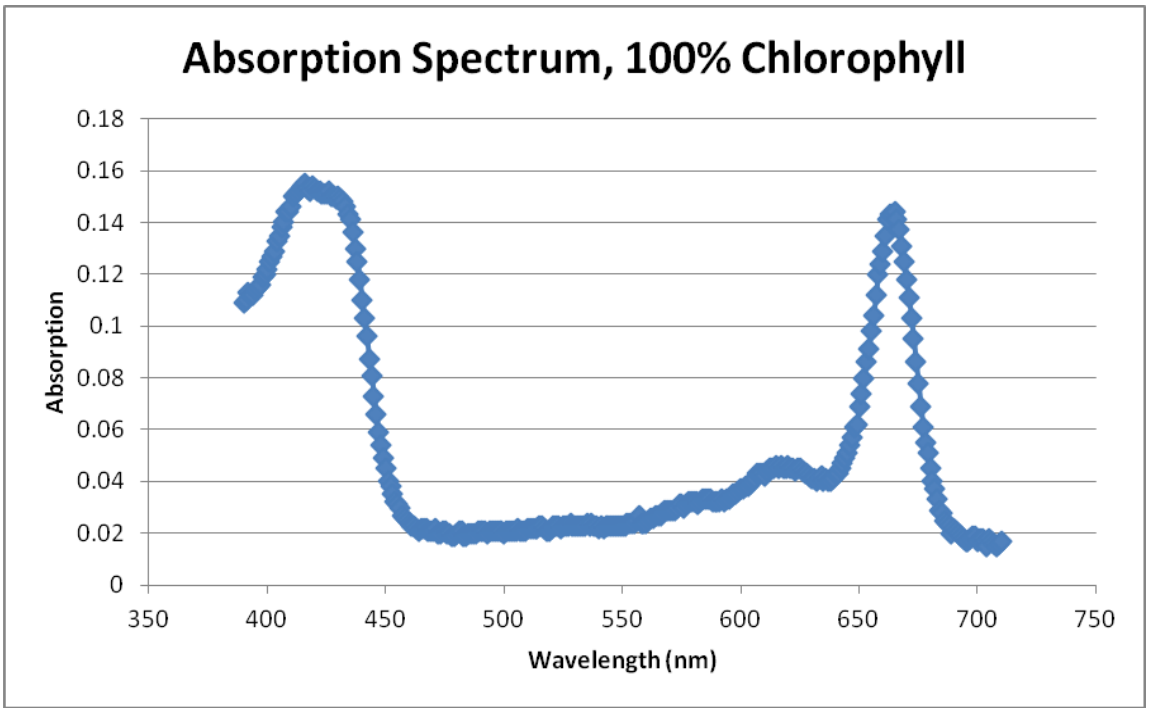

Figure 4.1. Absorption Spectrum for solution of 100% chlorophyll in ethanol.

The absorbance spectra of the pigment mixtures were also obtained in order to understand how absorptive capabilities change when pigments are combined. For example, Figure 4.2 shows the absorption spectra of a 1:1 ratio of chlorophyll to xanthophyll, a 5:1 ratio of chlorophyll to xanthophyll, and a 9:1 ratio of chlorophyll to xanthophyll. This graph illustrates the effect of increasing the percentage of chlorophyll in a mixture with xanthophyll.

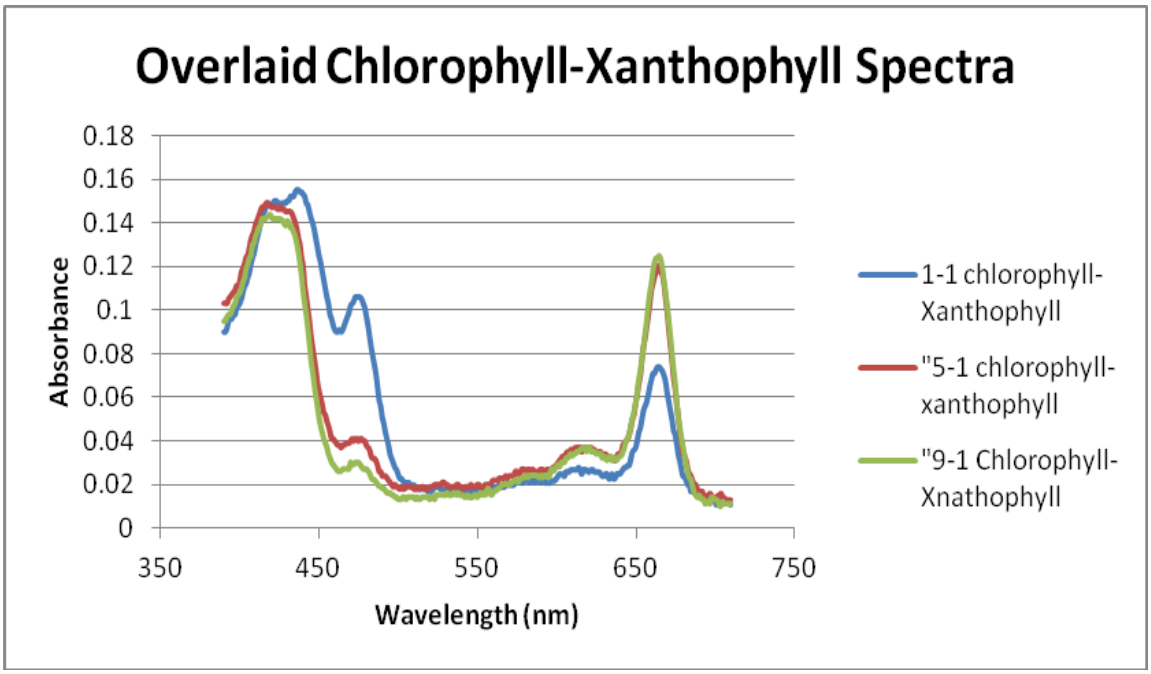

Figure 4.2. The overlay of 3 combinations of chlorophyll-xanthophyll with different composition ratios.

Figure 4.3 shows the overlaid absorption spectra of chlorophyll alone, a 1:1 ratio of chlorophyll and xanthophyll, and a 1:1:1 ratio of chlorophyll, xanthophyll, and beta-carotene. The combination of three pigments demonstrated a broadening of the absorbance peaks over a larger range of wavelengths compared to the pure solution.

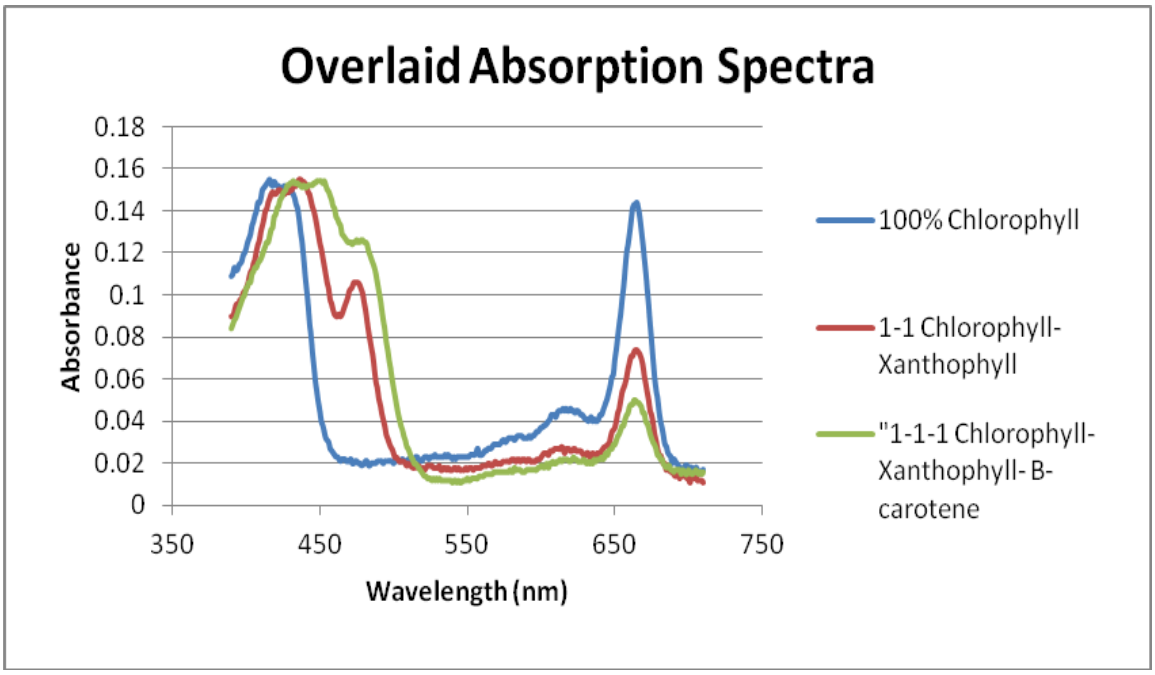

Figure 4.3. Shows the overlaid absorbance spectra for 100% chlorophyll, 1-1 chlorophyll-xanthophyll and 1-1-1 chlorophyll-xanthophyll-beta-carotene.

The complete set of absorption spectra were analyzed in order to determine a way to predict which pigments or combinations of pigments would best sensitize a DSSC. This analysis led us to the calculation of a parameter representative of the absorptive capabilities, and thus the sensitizing capabilities, of each pigment mixture. This "A-value," which was derived from our spectral data, will be discussed in the following section.

4.2 A-values

The A-value allowed us to numerically compare absorption spectra of each pigment combination with respect to the irradiance of the lamps in the growth chamber. The calculated A-values ranged from 686 to 1513 (see Table 4.1). Based on their high A-values, the pure chlorophyll and pure xanthophyll were predicted to be the best pigments

for sensitizing a DSSC. The next apparent grouping was the 1:1:1 mixture of all three tested pigments and all three of the 1:1 pigment mixtures. The combinations predicted to have the lowest cell outputs, in order of decreasing A-value, were 100% beta-carotene and the unequal mixtures (2:1:1). Since these values were calculated as a single value from three spectral scans of a single solution there were no statistical probabilities associate with the calculations.

Pigment Mixture	Adjusted Area, A-value
100% Chl	1513
100% Xan	1462
1:1:1 Chl: B-Car: Xan	1070
1:1 Chl: Xan	1052
1:1 B-Car: Xan	967
1:1 Chl: B-Car	952
2:1:1 Xan-: B-Car: Chl	820
2:1:1 Chl: B-Car: Xan	802
100% B-Car	772
2:1:1 B-Car: Chl: Xan	686

Table 4.1. Pigment mixtures and their adjusted areas, ranked highest to lowest.

4.2. DSSC Output

The data logger recorded the voltage and current output of the DSSCs. These data were stored in a tabular format for analysis. A sample of collected DSSC performance data for the pure chlorophyll solution demonstrates the two periods of irradiation separated by a dark period (Figure 4.4). The slope of the curve during the first irradiation period may be attributed to the growth chamber lamps warming up or to the "break-in" period of the solar cell.

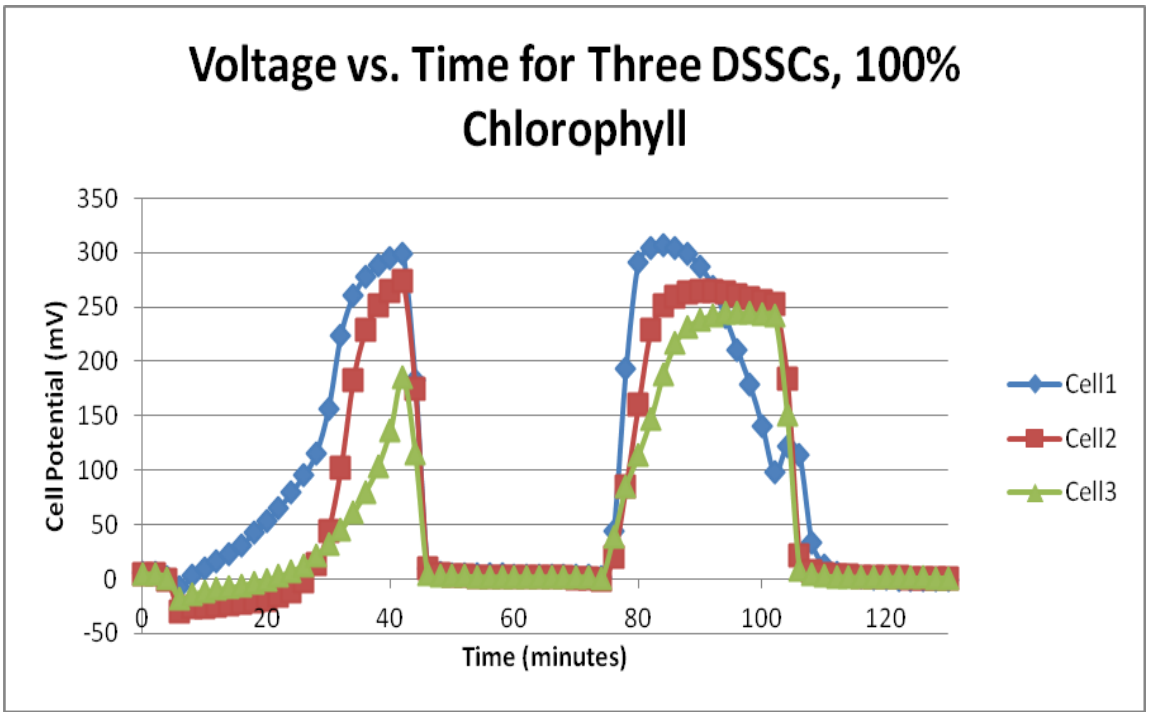

Figure 4.4. DSSC cell potential difference (voltage) plotted against time for 3 DSSC cells coated with chlorophyll and measured in a growth chamber with alternating 30-minute periods of light and dark cycles. Note the increased stability during the second light period.

To better understand the electrical potential of our DSSCs we calculated power output, as described in Section 3.4.2, by multiplying voltage and current values for each cell at each time. This produced a curve of output power versus time for each cell. The three power curves from each cell were averaged together to produce an average power curve for that pigment combination. A sample average power curve for 100% chlorophyll can be seen below (Figure 4.5). All data are shown in the appendix.

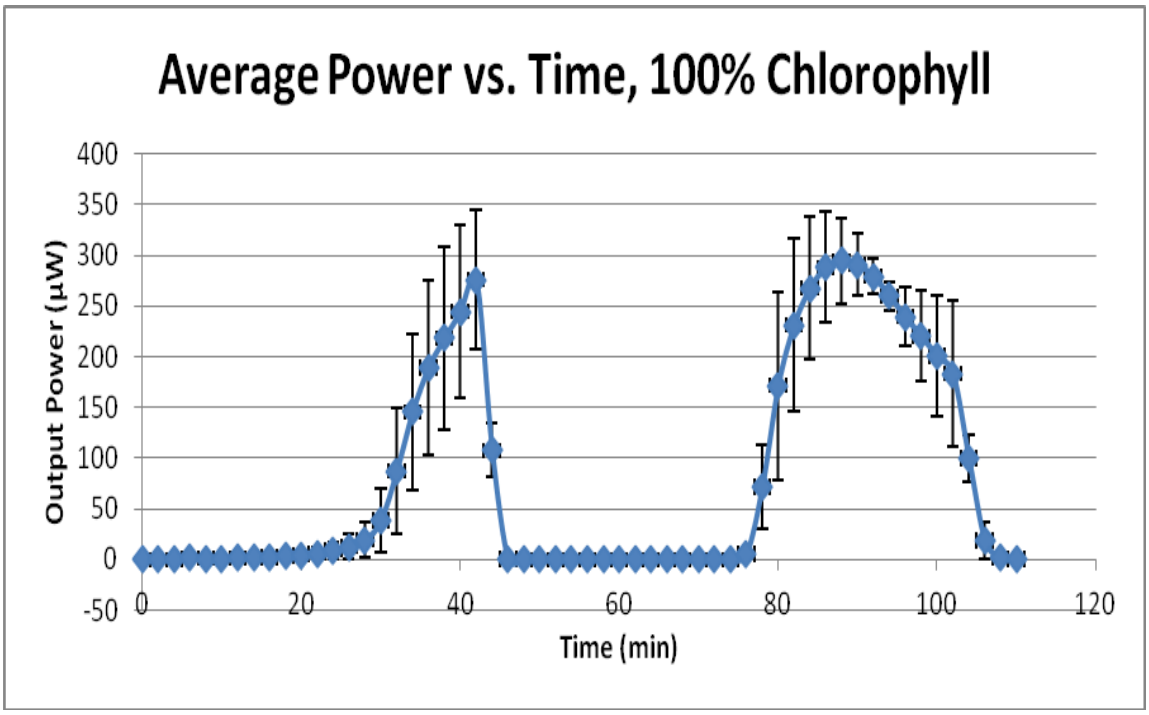

Figure 4.5. Average power-output for 3 DSSCs coated with 100% chlorophyll over a 2-hour period of alternating light and dark cycle. Error bars represent + 1 standard error of the mean.

To compare the cell power output of all cells, cell power output over the second irradiation period was averaged as described in section 3.4.2. This provided a single number representing the overall cell performance of each pigment combination (Table 4.2 and Figure 4.6). All outputs were statistically different from the blank according to Least Square Means ($p < 0.05$). The blank had a slight power output as expected from our literature review (*79*). The cells soaked in pure chlorophyll had the highest average power output and this was significantly different from all other pigment combinations except for the 1:1:1 mixture of all three pigments (Table 4.2). The other pigments exhibited lower power output and fell into three (3) general groupings with the 2:1:1 xanthophyll: beta-carotene: chlorophyll-treated cells having significantly lower output than all other combinations except the blank.

Pigment Mixture	Average Power
100% Chl	206.93 ± 20.5 a
1:1:1 Chl: B-Car: Xan	172.0 ± 25.2 ab
100% Xan	131.1 ± 25.2 bc
100% B-car	130.9± 25.2 bc
1:1 B-Car: Xan	123.1 ± 25.2 bc
1:1 Chl: B-Car	106.07 ± 35.6 bcd
2:1:1 Chl: B-Car: Xan	105.8 ± 20.5 cd
2:1:1 B-Car: Chl: Xan	86.1 ± 20.5cd
1:1 Chl: Xan	79.2 ± 25.2cd
2:1:1- Xan: B-Car: Chl	70.2.5 ± 20.5d
Blank	0.6 ± .1e

Table 4.2. Average power values for DSSCs coated with various pigment combinations and measured over a 30 minute irradiation period in a growth chamber. Pigment combinations followed by the same letter are not statistically different according to LSD.

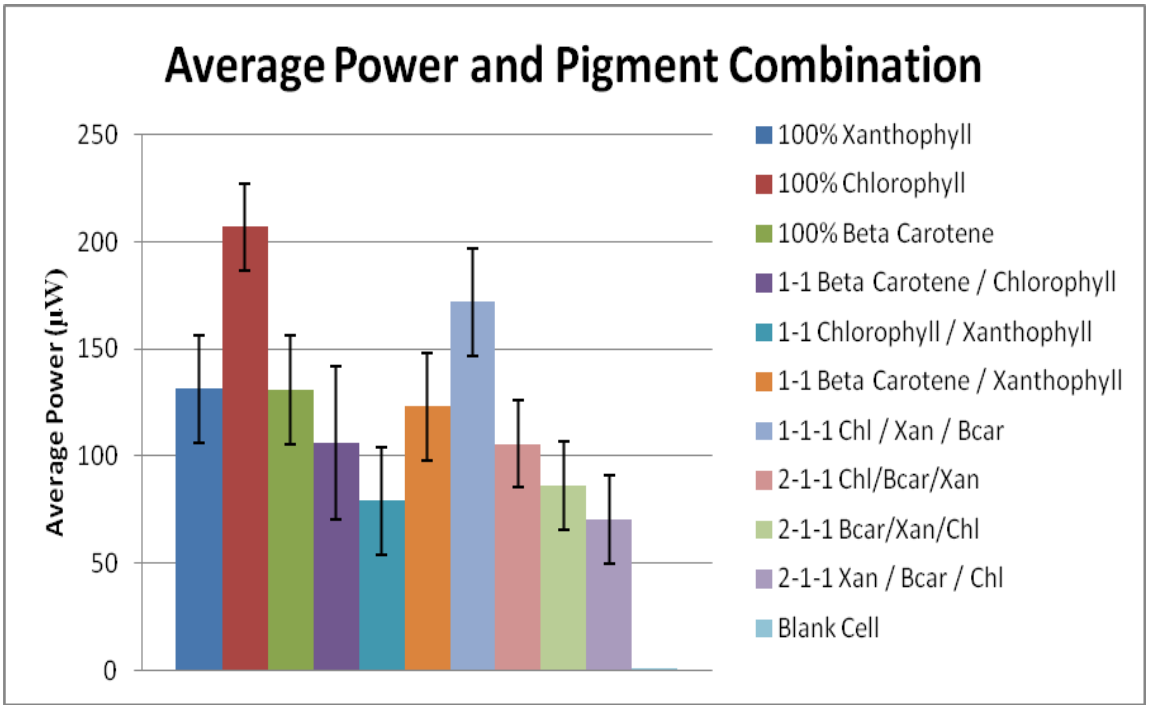

Figure 4.6. Graphical representation of average power output of DSSCs from Table 4.2. Each bar is the mean of three cells and vertical bars are the standard error of the mean.

4.3. Correlation between A-value and Average Power Output

To determine the relationship between the A-value and average power output, the average power values over the second irradiance period were plotted against the A-value for each pigment mixture. The second irradiance period was used because it was more consistent and, unlike the first irradiance period, did not include the "break-in" period of the cells or the warming of the lamps. There was a positive relationship between cell output (dependent variable) and the A-value (independent variable) with an R^2 of 0.44 (Figure 4.7).

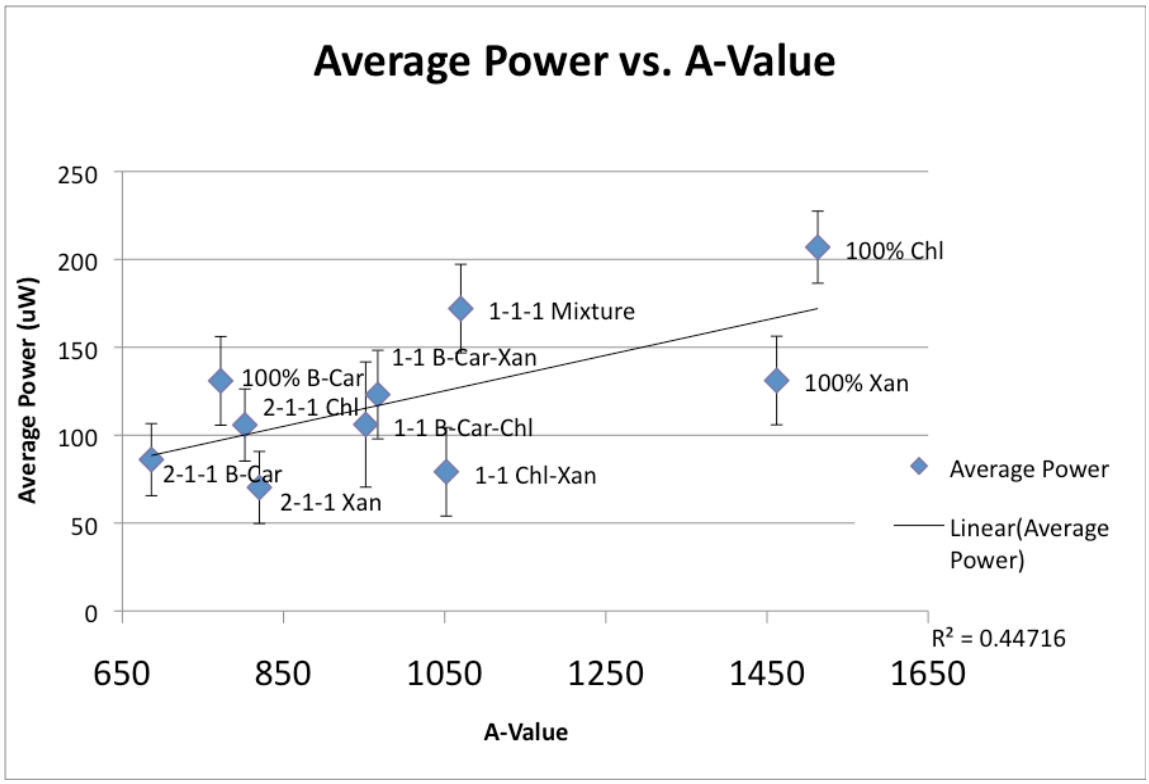

Figure 4.7. Average power for each DSSC pigment combination plotted against its corresponding A-value. The calculated linear regression line is also shown.

Including every pigment combination's average power versus the A-value in the regression gives an overall perspective of the predictive value of the A-value parameter. However for closer analysis removing some data from the regression may provide more

insight into the relationship between average power and A-value in terms of each pigment. For example, since pure chlorophyll was the best sensitizer for the DSSCs a regression was constructed with those mixtures that contained chlorophyll (Figure 4.8). The R^2 value for this relationship was 0.68, indicating that the A-value may be a better predictor of cell output for chlorophyll then for other molecules. However, there was no obvious linear response for chlorophyll concentration. If that has been the case then we would have expected the A-value and cell output from the 1:1:1 mixture (e.g. 33% chlorophyll) to fall below that of the 1:1 or 2:1:1 chlorophyll rations (e.g. 50% chlorophyll).

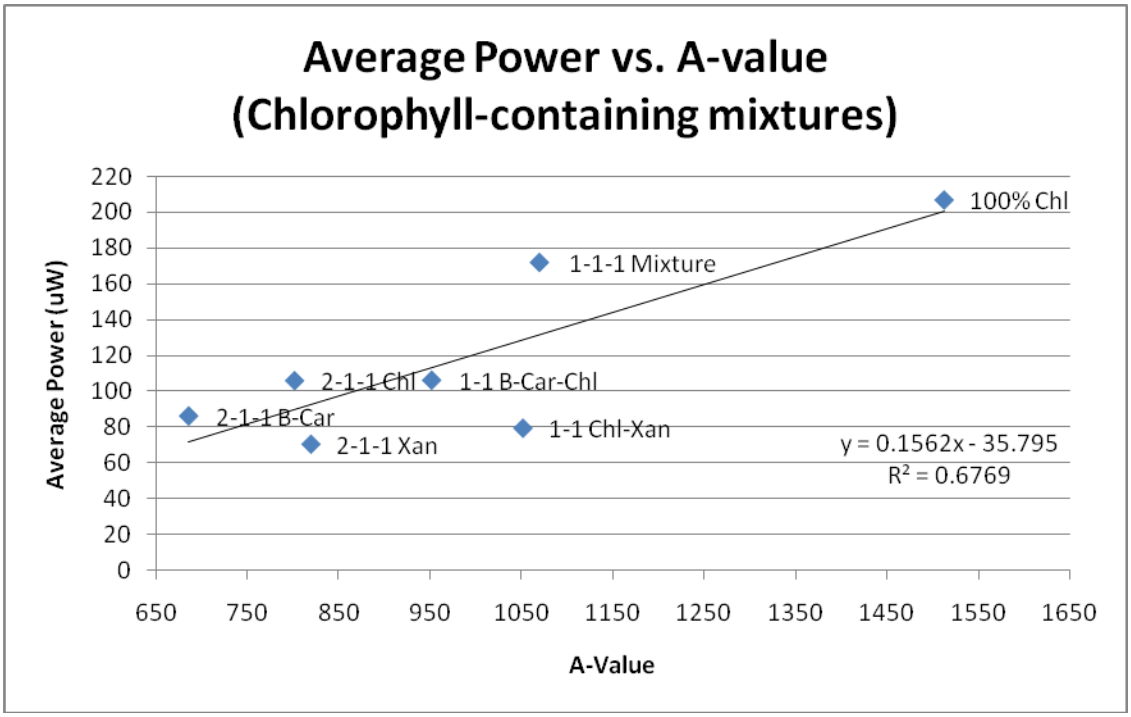

Figure 4.8. Average power for only the DSSC pigment solutions that contain chlorophyll plotted against its corresponding A-value. The calculated linear regression line is also shown.

Constructing separate regression analyses for mixtures containing either beta-carotene or xanthophyll failed to increase the coefficient of determination (Figures 4.9 and 4.10). The R^2 value for beta-carotene mixtures was 0.47 or essentially the same as

that for the entire suite of mixtures evaluated and the R^2 value for xanthophyll mixtures was 0.26, which was lowest of all the regressions. This suggests that the A-value did not have as much predictive power for xanthophyll solutions as the other molecules. In fact, if xanthophyll when present as the dominant or co-dominant pigment in any combinations is removed from the predictive model, the R^2 increases to 0.82 (Figure 4.11).

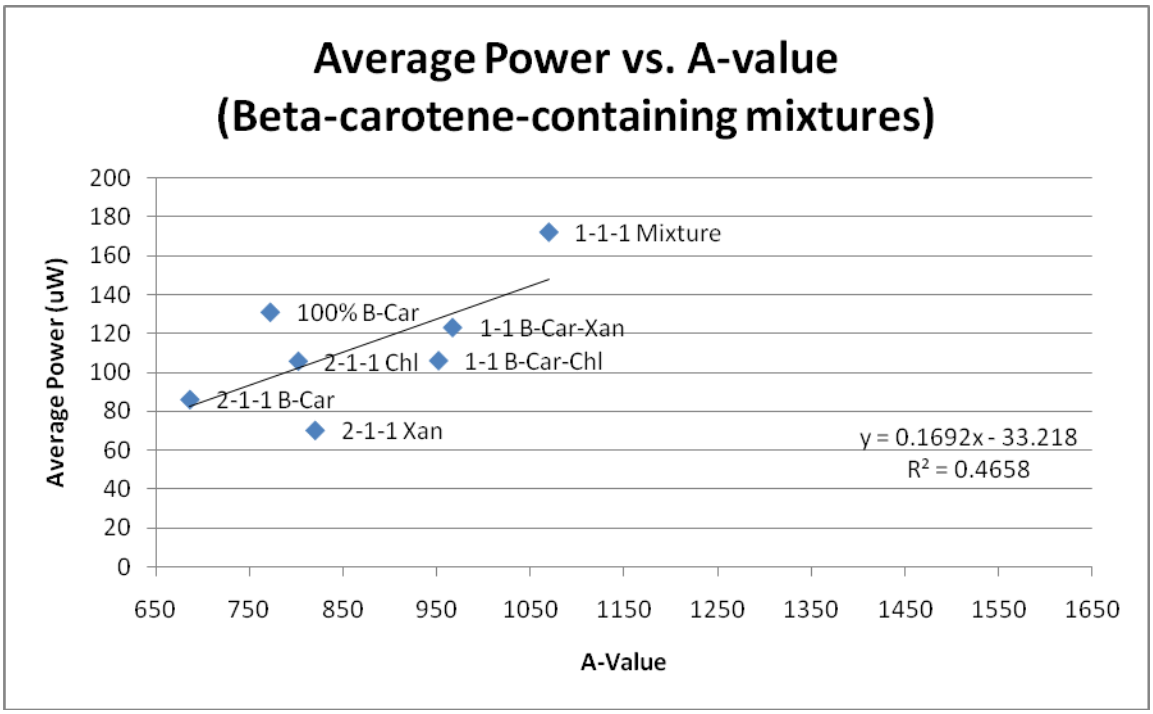

Figure 4.9. Average power for only the DSSC pigment solutions that contain beta-carotene plotted against its corresponding A-value. The calculated linear regression line is also shown.

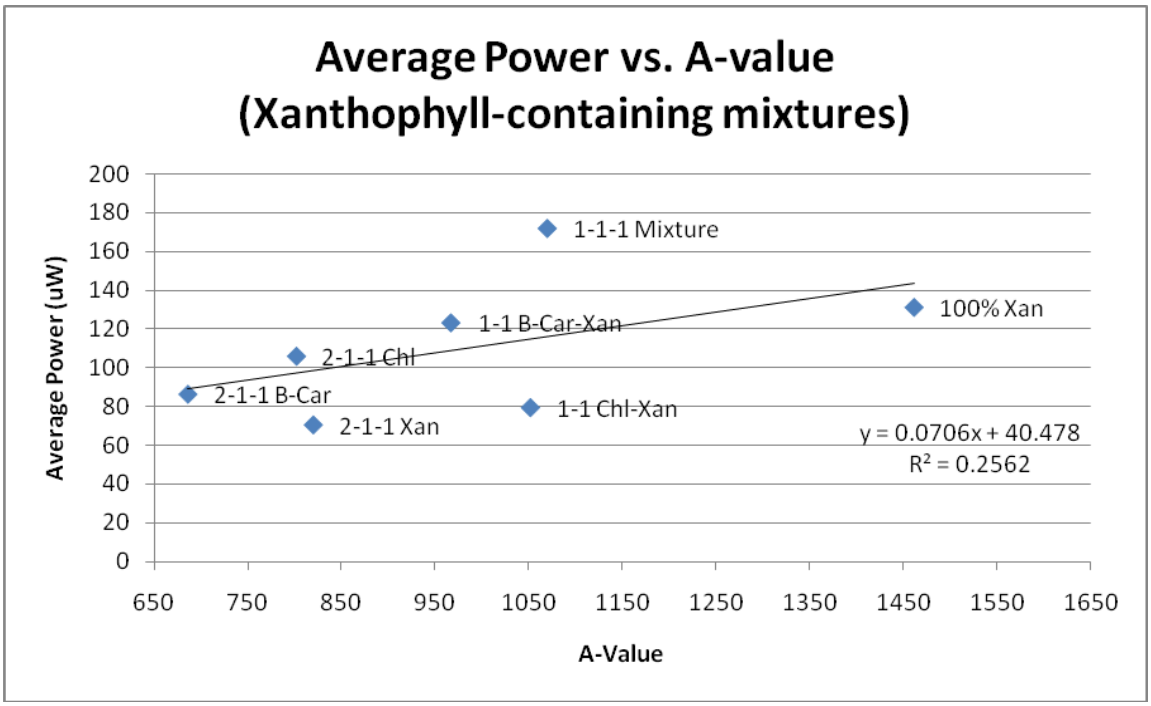

Figure 4.10. Average power for only the DSSC pigment solutions that contain xanthophyll plotted against its corresponding A-value. The calculated linear regression line is also shown.

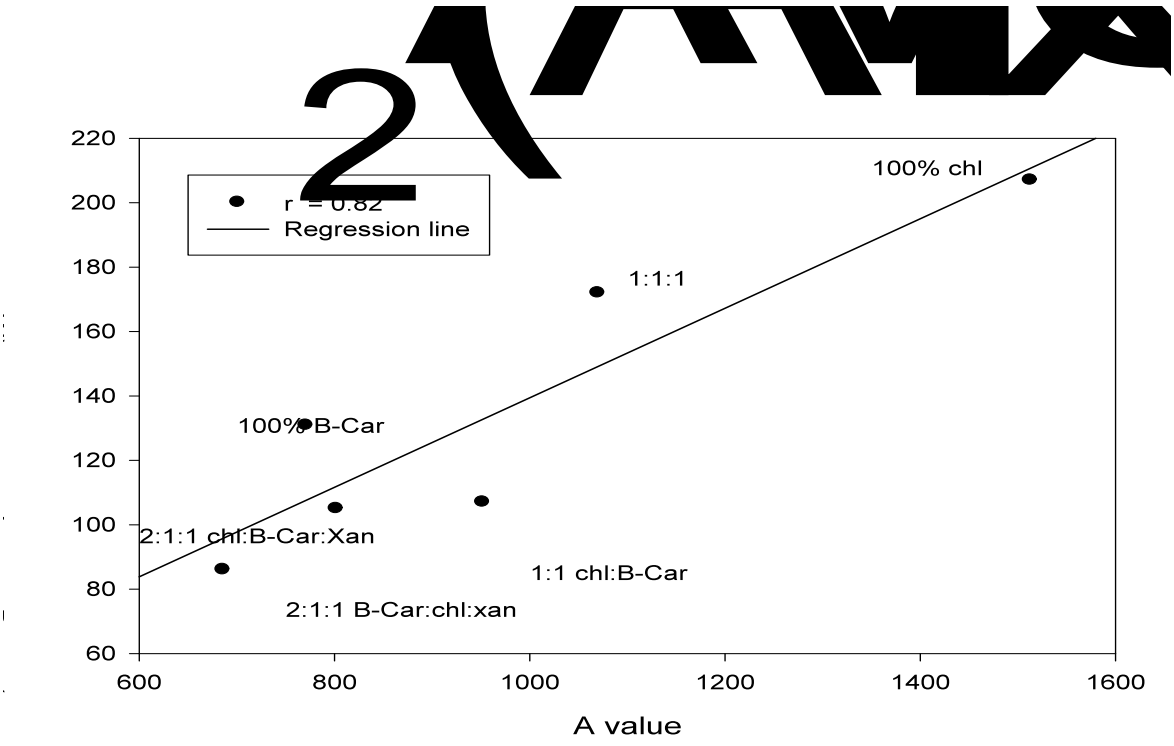

Figure 4.11 Average power for only the DSSC pigment solutions that contain xanthophyll plotted against its corresponding A-value. The calculated linear regression line is also shown.

4.4 Maximum Power

We also recorded the absolute maximum power output achieved by cells in each pigment combination. This value, which we termed highest achieved power, was simply the maximum calculated power for each pigment combination. Maximum power was assessed to compare our cell output with literature values since maximum power was commonly reported in other studies. This output may be an indication of the potential capacity of a given pigment mixture. There was no statistical probability associated with this value however, since it was obtained as the highest single 10-minute average cell output. However, observationally, the cells coated with pure chlorophyll had the highest achieved power, corresponding with the highest average power (Table 4.3, Figure 4.8). Similarly, the 2:1:1 xanthophyll: chlorophyll: beta-carotene cells had the lowest output in terms of average power and the second from the lowest output of highest achieved power. There was weak positive correlation between A-value and highest achieved power (R^2 = 0.28, data not shown).

Pigment Mixture	Highest Achieved Power
100% Chl	392.1
100% B-Car	309.7
1:1 Chl: B-Car	240.5
1:1 Chl: Xan	231.4
1:1 B-Car: Xan	192.7
100% Xan	178.3
1:1:1 Chl: B-Car: Xan	162.7
2:1:1 Chl: B: Car: Xan	140.5
2:1:1 Xan-B: Car: Chl	140.5
2:1:1 B-Car: Chl: Xan	117.3
Blank	2.6

Table 4.3. Highest achieved power for tested pigment mixtures.

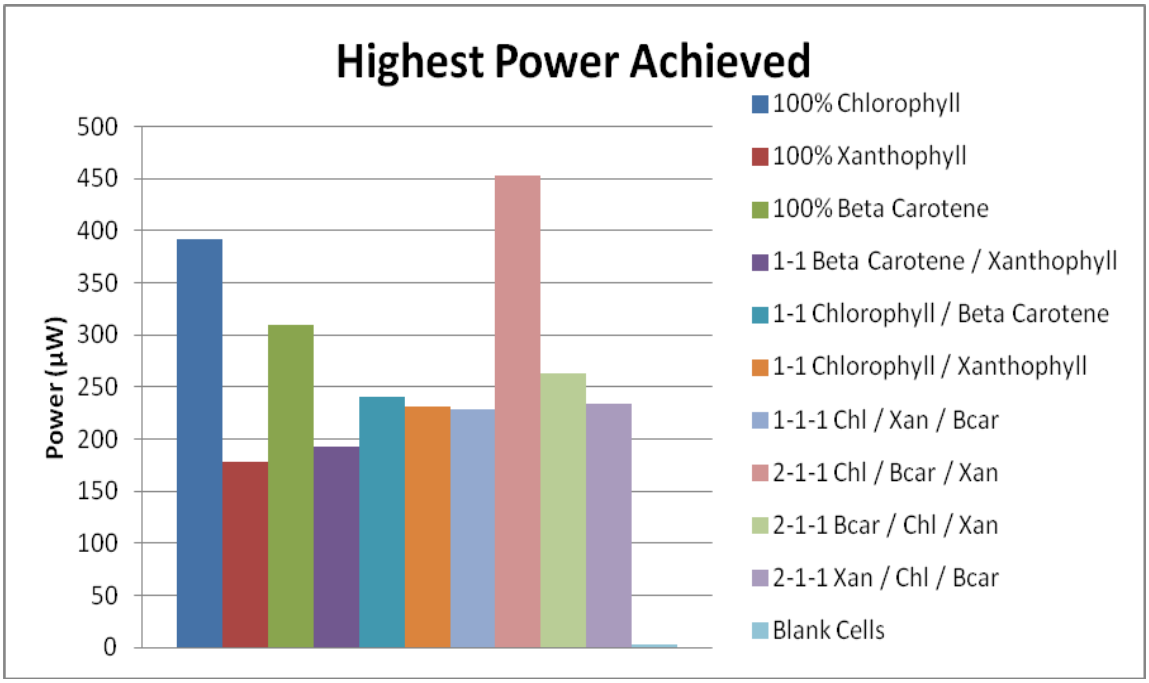

Figure 4.11. Highest achieved power values for tested pigment combinations.

5: DISCUSSION

5.1. Restatement of Question and Our Answer

We explored the utility of using natural pigment solutions as sensitizers for Dye Sensitized Solar Cells (DSSCs). Our goals were to determine whether there were differences in power output of the DSSCs due to the use of different pigments and whether the use of pigment mixtures could improve the efficiencies of the cells through synergistic interactions between the pigments. In addition, our research aimed to determine a relationship between the absorption spectra of the various combinations of pigments and the resulting electrical output when incorporated into DSSCs.

We found differences in pigments tested and disproved our null hypothesis that there would be no differences in cell output due to changes in plant pigments. Chlorophyll was the best sensitizer, as DSSCs sensitized with 100% chlorophyll achieved the highest average power and the highest maximum achieved power. The calculated A-value proved to be a reasonable predictor of DSSC electrical output by relating DSSC output to pigment optical properties. We are not aware of any other studies that have attempted to establish this relationship. However, the high degree of variability of cell output and unexplained variation in the relationship suggests that more research is needed in order to understand the interactions between the pigments and to improve efficiency of DSSCs.

5.2. Plant Pigments as DSSC sensitizers

Our spectral analysis documented the differences in absorbance of the single pigments and their combinations as expected from Beer's law. In many cases the

pigment combinations expanded the absorbing area compared to that of the respective single pigments. For example, as seen in Figure 4.3, the absorbance band of the 1:1:1 chlorophyll: xanthophyll: beta-carotene (blue) exhibited a broader absorbance than Chlorophyll alone in the 440-525 nm range. However, the increase in absorbance at those wavelengths attributable to the addition of xanthophyll and beta-carotene was offset by the loss of absorbance at the longer (red) wavelengths (650-700 nm range) due to the dilution of chlorophyll. This led to a reduction in both the cell output and the calculated A-value for that mixture. According to our hypothesis, a change in total absorbance would be expected to result in a change in DSSC output and this was the case.

There was a substantial difference in DSSC electrical output when different photosynthetic pigments were used to sensitize the photovoltaic cells. For example, the mixture of 1:1:1 chlorophyll: xanthophyll: beta-carotene produced an average power of 172.0 ± 25.2 μW, while the mixture of 2:1:1 beta-carotene: chlorophyll: xanthophyll produced an average power of 86.1 ± 20.5 μW. Different pigment combinations reacted differently with the incoming light to produce different electrical outputs. This disproves our null hypothesis, which stated that there would be no difference in DSSC performance with changes in sensitizing pigments.

5.2.1. Previous studies

The use and the manipulation of photosynthetic pigments to sensitize DSSCs in the literature have been limited to a few similar studies. Liu et al. used xanthophyll and chlorophyll, Kumara et al. used chlorophyll and shisonin, and Wongcharee used rosella and blue-pea extract (both abundant in anthocyanins). All three studies made DSSCs

sensitized with either 100% of the first pigment, 100% of the second pigment, or a 1:1 ratio (50% and 50%) of both pigments (*38, 39, 89*). Liu et al. and Kumara et al. both reported an increased DSSC output when sensitized with mixtures compared to pure or at least presumed "single" compounds and termed this a "synergistic effect." Neither of these two studies could explain the molecular mechanism of the presumed synergistic effect, though they believed that it could potentially mimic the interaction between multiple photosynthetic pigments in plants. Plants consist of both primary (e.g. chlorophyll) and secondary (e.g. xanthophyll) pigments. These primary and secondary pigments work together to increase the light capturing capabilities of the plants and aid the plants in other methods such as quenching chlorophyll fluorescence and providing protection to the plant (69*, 71*). It should also be noted that neither of the above studies report any replication or statistical analysis of their results. Therefore, it cannot be validated that any one pigment or combination actually improved DSSC electrical output.

Although Liu et al. and Kumara et al. suggested the synergistic effect, the results of Wongcharee et al. did not (*38, 39, 89*). Wongcharee et al. used DSSCs sensitized with 100% rosella extract, blue pea extract, and a 1:1 pigment solution of rosella extract and blue-pea extract. They also evaluated differing extraction temperatures and pHs and thus shifted the absorbance of the anthocyanins, which they determined were a major part of the extract. In this case, they reported that the rosella extract had the largest absorption spectrum and achieved the highest power output. Other than indicating some putative primary compounds in the extracts no further chemical identification or quantification was attempted in that study. Therefore there is no evidence in this study that synergism exists with regard to DSSC output.

Overall these studies, as compared to our study, integrated only two different types of pigments or the pigments were largely unknown and simply whole leaf extracts. Also, the precise concentrations used were either not specified at all or it was stated that they were "equal." These factors plus the lack of statistical analysis in any of the three studies above make it difficult at best to interpret the results of these studies in terms of whether there was any synergism of pigment combinations as asserted by those authors.

The results of our study indicate that DSSC output varies among pigments and mixing ratios, and some of our results indicate that a possible synergistic or at least additive effect may exist. For example, with the triplet combination groupings, the 1:1:1 cells displayed a materially higher energy output than any of the 2:1:1 cells. This indicates that a cell coated with a combination of 33% of each pigment outperforms one where a single pigment of the three comprises 50% of the coating. To point, even though the pure chlorophyll coating was the clear forerunner of the single pigment cells, in the case of 2:1:1 chlorophyll: xanthophyll: beta-carotene, increasing the chlorophyll percent composition did not lead to higher outputs. This result suggests that a non-additive synergistic response may exist wherein combinations of pigments may be stronger than the sum of their parts.

On the other hand, it is clear that all pigments combinations do not exhibit synergistic or even additive effects. For example, we found no indication of synergism and in fact a reduction of output from the pure pigment cells to the 1:1 mixtures. There was a drop in power output when comparing the output of the 100% chlorophyll and 100% beta-carotene cells and the 1:1 combination of the two. The reduction of output does not support synergism, because at the very least one would expect that the

combination of chlorophyll and beta-carotene would be no lower then the beta-carotene dye as a lone sensitizer. Overall the three single pigments and the 1:1:1 ratio of them produced the highest average DSSC power. This does not seem to support a synergistic effect among pigments when sensitizing DSSCs.

5.2.2. Variation in cell output

Cell output was extremely variable and so more replication would have certainly assisted in the interpretive power of the results. Further discussion will follow in later sections on some of the technological considerations that may have contributed to this variation. However a consideration of the chemistry and structural organization of the pigments may also explain some of the variation and unexpected cells responses. Also, the underlying mechanism of the synergistic effect may not necessarily depend on pigments' combined absorption but may be understood based on analysis of the binding properties of pigments to TiO_2.

We used beta-carotene as a sensitizer because of its prominence in plants as an accessory photosynthetic pigment and also because of its relatively low cost. The potential problem with beta-carotene is that its structure suggests that it will not bind well to TiO_2. However, De Padova et al. showed that a cell sensitized with beta-carotene did produce a current and voltage (*77*). We found that DSSCs sensitized with 100% beta-carotene achieved the lowest average output compared with the other pure solutions and that combining beta-carotene with both chlorophyll and xanthophyll (in 1:1:1) improved the DSSC performance compared to DSSCs sensitized with beta-carotene alone. Thus, our results provide novel insight into beta-carotene integration by combining it with both xanthophyll and chlorophyll.

5.2.3. TiO2 pigment binding characteristics

The above discussion on beta-carotene brings up the important question of whether the optical properties that we measured in ethanol solutions is equivalent to those when the pigments were bound to the TiO_2 molecules on the DSSC electrodes. In order to be effective as dyes each pigment must be bound to the TiO_2 nanoparticles in order to transfer electrons. If binding is not equal for all the pigments then DSSC output will not be simply a function of pigment optical properties but will also be scaled by binding affinity. Liu et al. and Kumara et al. reported optical properties of pigments bound to TiO_2 and this is the condition in which they reported expanded absorbance ranges and where they reported apparent enhanced DSSC output in mixtures (*38, 39*). Unfortunately we were not able to measure pigment optical properties while bound to the DSSC electrodes so we are not able to partition the variation in DSSC output between pigment optical properties and pigment binding properties to TiO_2.

5.2.4. Structural orientation of the pigments.

Another factor that may have contributed to variation in DSSC output differences between pigments is the structural arrangement of the pigment molecules on the electrodes. In plants, there is a very structured organization of pigments. Typically the chlorophyll molecules are located in the center of the light harvesting complex of the plant's photosystem, and are surrounded by accessory pigments, such as xanthophyll and beta-carotene (Figure 5.1). The energy in the photons captured by xanthophyll is then transferred into a series of chlorophyll molecules, ultimately reaching the reaction center.

The chlorophylls utilize this transferred energy to facilitate excitation and energy transfer of their own electrons.

In our cells, however, the pigments were mixed together and the cells were soaked in a non-structured matrix. Unlike in plants, our cells contained a random distribution of the pigments in each mixture (Figure 5.1). Due to the lack of defined structure, the cooperative properties between pigments, as seen in plants, might not have existed in our cells.

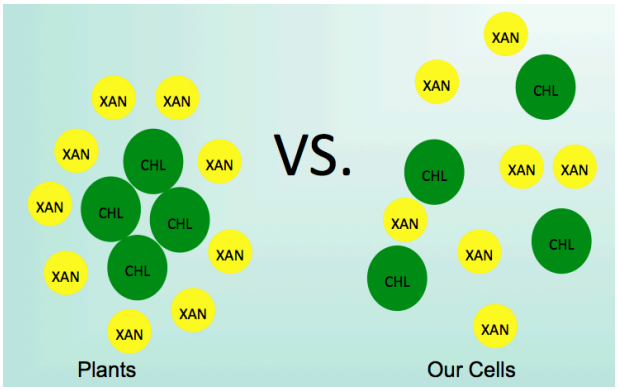

Figure 5.1 A rough pictorial representation of the structural differences in pigment layout between plants and our cells.

Absorbance, binding, and structural differences may not have been the only reason that pigments were not equally suited as DSSC dyes. In addition to expanding the effective absorbing range of light in plants, the accessory pigments such as xanthophyll and beta-carotene have the special ability to act as antioxidants and to absorb excess energy to protect the chlorophylls from being over-stimulated. In short they may "scrub" excess electron and use this excess reducing power to change the oxidation state of xanthophylls in what is called the zeazanthin cycle (71). This essential "recycling" of electrons and excess energy plays a major role in protecting plants from photoinhibition in high light environments. If xanthophyll molecules were in facts "scrubbing" electrons

in the DSSC cells then this could have reduced the power output of the cells that included xanthophylls. The possible premature electron quenching, may have hindered the development of charge differential between the plates of the cell, materially reducing photon conversion efficiency and power output.

5.2.5. Conclusions

Chlorophyll was the best pigment for use in DSSCs in terms of electrical power. Since the chlorophylls are the primary photosynthetic pigments this is not surprising. However, the photo stability of the molecule poses series problems that must be addressed before DSSCs sensitized with chlorophyll could be used for long-term DSSC electricity production. Adding in accessory pigments to DSSC electrodes similar to what might be found in a chloroplast in order to stabilize chlorophyll and enhance electron output did not yield a great electrical power in this study.

5.3. Correlation between Average Power Output and the A-value

This is the first study that we have found that has attempted to explain DSSC output by a spectral analysis of the pigments. Several previous studies have used either chlorophyll or simple chemical derivatives of it. Others have used mixtures of 2 pigments that seem to have been either randomly chosen or simply because the plants they were extracting pigments form contained those pigments. One of our goals was to explain DSSC output based on the optical absorbance properties of the pigments we used.

We found a significant correlation (e.g. Figure 4.7), between the A-value and the realized power output that explained a little less than half of the variation in cell output

($R^2 = 0.45$). These novel data provide insight into the absorption and output relationship of triple, double, and single combinations

5.3.1. Trends in the A-value and DSSC output

The high variation in DSSC output and low repetition or overall unexplained experimental error certainly contributed greatly to the unexplained variation in DSSC output. However there were also some interesting trends in the analysis that are of importance to note. For example the positive relationship between the output of the triplet-combinations and the dyes' A-value suggested that there are mixtures that are more effective than others in terms of DSSC output.

Using only pigments that contained chlorophyll strengthened the correlation and coefficient of determination (i.e. increasing R^2 from 0.44 to 0.68). This again confirms the importance of chlorophyll as the most effective of the pigments tested in terms of DSSC power. However, a linear relationship between chlorophyll concentration and DSSC output was not found (Figure 4.8). This suggests that the contribution of other pigments may not be purely additive. For instance, the 1:1:1 chlorophyll: xanthophyll: beta-carotene (reduction in chlorophyll concentration by about 66%) had both one of the highest power outputs (172.0 ± 25.2 μW) as well as the third highest A-value. A theoretical consideration of the binding properties to the TiO_2 and the in-situ chemical functions of the pigments in a plant may help to explain the relationship between out calculated A-value and DSSC output.

5.3.2. Increasing the coefficient of determination (R^2)

While the A-value provides an explanation for about half the experimental variance, other potential variables can be used to explain the additional variance. These consist of two main categories: those that affect the calculation of the A-value and those that affect the power output.

Since incident photon flux on the DSSCs was a used in the calculation of the A value the A-value would change if the spectral qualities of the light source changed in either a quantitative or qualitative manner. Our initial attempts to generate a predictor value for cell output was called the S-value and was computed as the summation of the intensity of sunlight as a function of wavelength multiplied by the measured absorbance corresponding to each wavelength, over the visible range of light (400-700 nm). This is shown in equation 5.1 below.

$$S = \sum_{\lambda=400}^{700} (Intesnity\ of\ sunlight\ at\ \lambda)(Absorption\ of\ pigment\ mixture\ at\ \lambda)$$

Equation 5.1. S-value calculation equation.

However, we modified the value by calculating it in the same manner except that the actual irradiance of the lamps in the growth chamber were substituted for sunlight> It was presumed that the A-value would be more appropriate as an indicator of cell output since actual photon fluxes were used. However, the lamp output was fairly similar to sunlight in spectral distribution (see Figure 3.3) so using sunlight instead of the lamp spectra would likely have only changed the magnitude of the A-value (higher photon

flux) but not the relationship between the calculated values. There were however, some key assumptions inherent in the process that should be evaluated.

In modeling the A-value, we made two major simplifying assumptions. The first was that the photon conversion efficiency (IPCE) of every dye was 100%. This assumption is not accurate in reality, as no dye has 100% conversion efficiency and as Kumara et al. demonstrated, pigments do not necessarily have the same IPCE (39). We were not able to measure IPCE but the assumption that it was equal for all pigments instead of weighting each for its own IPCE could well have affected the relationship between the A-value and power output.

The second assumption was that every molecule bound to the TiO2 perfectly, and thus there was seamless transfer of the electron from the sensitizer to the semiconductor. As previously discussed, each pigment's specific absorption spectrum does not take into account the absorptive capabilities of the pigment when combined with the TiO_2. Liu et al. (2008) showed that binding with TiO_2 modified the absorption spectra of chlorophyll, xanthophyll, and a 1:1 ratio of the two (Figure 2.21) (*38*). They found that the area under these absorption spectra was much higher when bound to TiO_2 than the absorption spectra of chlorophyll, xanthophyll, and the 1:1 ratio alone (Figure 2.20) (*38*). The binding of the pigment to TiO_2 could stabilize the dyes and thus decreases the HOMO-LUMO gap between the semiconductor and the sensitizer allowing excitation at different wavelengths and lead to both a broadening of the absorbance peak and red-shift expanding the actual absorbance. However, our study did not take into account the absorption spectra of the pigments bonded with TiO_2 because we were interested in analyzing output based on absorptive capabilities of pigments alone. Corrections to the

A-value based on pigment absorbance when bound to the electrode substrate could improve the algorithm to determine which pigments or pigment combinations would lead to the highest output of a DSSC.

We propose that a modification of the A-value computation could address the potential issues resulting from these simplifications. The new A-value would include additional parameters of the absorbance of a dye combination bound to the TiO2 at a given wavelength, the IPCE of each pigment in the sensitizing solution and the percent composition of each pigment in the solution. The new A-value would be the summation of the products of these parameters as shown below in Equation 5.2.

$$\sum_{\lambda=400}^{700} (\text{intensity of sunlight at } \lambda)(\text{Absorption of pigment mixture at } \lambda)\,(IPCE_X(\lambda))(\%X)(IPCE_Y(\lambda))(\%Y)$$

Equation 5.2. Modified A-value equation.

This equation could be modified for the inclusion of additional pigments in the solution, by simply expanding the last two elements of the product to include the metrics for each new pigment. This modified A-value would take into account the different IPCEs of the pigments involved as well as any red-shifting, and should serve as a better model for further exploration.

In addition to the optical properties of the pigments and their conversion of incoming light to electron flow there are biological aspects of these pigments that may contribute to the results of this study. As alluded to previously, of the three pigments used, chlorophyll appeared to be the primary pigment driving power generation from the DSSCs. The variation in DSSC signal that was explained by chlorophyll content was 66% when only those mixtures containing chlorophyll were included. On the other hand, while xanthophyll alone was useful as a dye, the relationship between xanthophyll

content and DSSC power output was poor (Figure 4.10) and cells that had xanthophyll in the dyes appeared to consistently fall under the predicted regression line. In fact removing xanthophyll from the analysis when it had equal or greater concentrations then either or both of the other pigments substantially increased the predictive power of the regression. In the case the R2 increases to 0.82, albeit with only 6 solutions left in the analysis. The structural considerations presented above and the biochemical role of xanthophyll in plants as an electron scavenger, call into question its value as a dye component. However, more research is required on this topic and it is possible that a benefit of xanthophyll, just as in a plant, could be as a chlorophyll stabilizer by protecting chlorophyll from excess excitation energy.

5.4. Study Limitations and Uncertainty

Throughout our study, we strove to be precise and accurate with our methodology and testing. However, as with all experimental studies, there were limiting factors and random errors associated with the data that adds uncertainty to the results. These and the photochemical and biological considerations discussed above contributed to the variations observed in DSSC output. Some of these are briefly discussed below in an effort to assist other groups that might continue these studies.

Due to budgetary constraints we were limited to testing three cells per dye combination. This sample size is at the minimum number for most statistical tests to have validity and with only three trials available, the elimination of any apparent anomalies or outlier would have had a material affect on the DSSC output and a secondary affect on the regressions.

Our initial plans were to test the cells for 24 hour time periods and at 5 different light levels. However, our limited budget also prevented us from purchasing sealants for the cells and our tests with various forms of hot glue and other adhesives proved to be ineffective and may have interfered with cell operation, because the glue reacted with the KI electrolyte. Without proper sealant, our cells were only active for about 2 hours, after which the KI evaporated. Additionally, opening up the cells to oxygen could have led to the increased degradation of some of the pigments leading to a reduction in output over time. A key missing component in the assessment of the cells was a light response curve for each pigment combination. This would have given us a measure of the quantum efficiency and saturation level of each pigment and would have greatly strengthened the interpretive power of our results.

Also, some of the variability and apparent instability in cell output may have been due to faulty electrical connections within the data logger or "noise" due to variations in resistance through the connections or alligator clips. Electronic "noise" is always present in such connections but in this case, with very low DSSC electrical output, the signal to noise ratio may have been so low that the noise contributed significantly to apparent DSSC output. However, the DSSC coated with pigments had about a ten-fold grater output than the uncoated blanks so we were still able to detect differences between the pigments.

Further, there was an apparent general discrepancy in the shapes of the output voltages between the two irradiation periods. The first time the light was turned on, the cells exhibited a sort of charging up effect similar to electrical capacitance. However, the second time the lights were turned on, the cells tended to reach maximum capacity at a

more rapid rate. The lamps in the chambers require several minutes to warm up and achieve a stable temperature and output, especially in the shorter, more energetic, wavelengths so it is possible that the more rapid response during the second irradiation period was due to the lamps having already warmed up. In retrospect, we could have eliminated this problem by warming up the lights to a stable temperature prior to placing the DSSCs beneath them and then covering the DSSCs for the dark period rather than turning off the lights.

Finally, we measured the performance of our DSSCs in a growth chamber to control for light and humidity. However, the spectrum of the light inside the growth chamber does not match that of natural sunlight. Although this did not directly affect our findings, as we sought only to make comparisons between cells, it should be noted that our results should not be extrapolated to DSSC performance in natural sunlight.

5.5. Future Directions

5.5.1. Additional Pigment Combinations

Due to time constraints, we were only able to test 10 different pigment combinations. While we focused on only three pigments, previous studies have examined the potential use of anthocyanins as sensitizers (*80-82*). DSSCs sensitized with various anthocyanins achieved voltages up to 480 mV and currents up to 2.9 mA (*82, 83*). There are hundreds of different pigments and other photosynthetic dyes that exist in nature, and each has its own unique absorption spectrum and other physical characteristics. Future studies could explore the use of these additional natural

photosynthetic compounds as well as additional ratios beyond the scope of our experiment.

However, screening hundreds of compounds to incorporate into DSSCs as sensitizers is not practical or feasible. Therefore, a means to determine the most viable options will be required. The algorithm we developed needs further development and additional consideration of the electron configuration of putative pigments may assist in the selection of the pigments that are most likely to be good choices for electrode sensitizers.

Every pigment molecule contains a highest occupied molecular orbital (HOMO) and a lowest unoccupied molecular orbital (LUMO) which is its lowest excited electron state. The energy gap associated with the jump between HOMO and LUMO energy states is referred to as ΔE_g. The lower the ΔE_g (i.e. the closer the HOMO and LUMO are to one another), the less energy that is required to eject an electron from the HOMO band to the LUMO band and therefore the more likely it will be that an incident photon will create free charge. Additionally, a smaller ΔE_g leads to increased pigment spectral area towards longer wavelengths with lower energy. However, there is a limiting factor in how close the HOMO and LUMO can be. In order for the DSSC to work, the conducting band of the semiconducting band must be of lower energy than the LUMO. This allows the semiconductor to capture the excited electron as it relaxes back down to the ground HOMO state and prevents the cell from a short-circuit or the energy will simply be lost as heat (90). Further research could determine the suitability of pigments as sensitizers based on their reduction potential to comprise a list of possible candidates.

In addition to the restriction put on the system by the ΔE_1 requirements, there is an additional requirement that must be met to make an efficient DSSC. The energy level between the electrolyte and the HOMO is called ΔE_2. The electrolyte must be at a sufficiently higher energy level than the HOMO so that it can easily transfer the electrons to fill in the electron hole resulting from the loss of electron due to excitation. This complicated system can be seen below in Figure 5.2. (90).

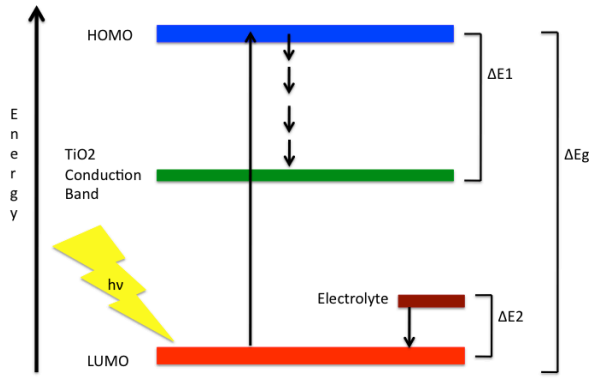

Figure 5.2. The energy changes associated with electron transfer between the dye and the semiconductor in DSSCs. The excited electron from the LUMO relaxes from the HOMO to the TiO_2 conductive band. (90)

5.5.2. Adding concentration to the Algorithm

The relationship between the concentration of a pigment and its ability to act as a sensitizer is unknown since we only tested using single pigment concentrations. If the relationship between concentration and DSSC output is linear, then adding additional pigment to the cell will be continuously beneficial and lead to a higher output. However, if or when the DSSC saturates then the relationship becomes asymptotic in nature. At that point, there would be a diminishing marginal return on power output. Increasing the concentration of a pigment beyond this point would yield diminishing increases in power, limiting the benefit of the increasing concentration. Further investigation using a range

of pigment concentrations could be carried out to model the nonlinear change in power as a function of pigment concentration. Knowledge of the diminishing returns of additional pigment concentration could be combined with the A-value computation to predict ideal pigment concentrations.

5.5.3. Durability

Our research focused primarily on improving the efficiency of the DSSC, but did not determine the stability of the performance over an extended period of use. Although DSSCs sensitized with 100% chlorophyll achieved the highest average power output and the highest maximum power achieved, it is unknown how long this performance will last. The durability of the DSSCs must be determined in order to analyze the potential use of DSSCs commercially.

5.5.4. Natural Sunlight

While the growth chamber is a decent model for natural sunlight, light used in the growth chamber was only about 500 μmol, or just a quarter of the light from the sun. In addition, solar intensity and duration varies on a latitudinal, seasonal and diurnal basis. The light that strikes Canada on a winter day is different in intensity than the light that strikes the tropics at the same time. Plants have adapted in part to varying levels of sunlight by developing photosynthetic light harvesting complexes that vary quantitatively and qualitatively. Additional experiments should examine whether the performance of the DSSCs changes in natural sunlight and if the composition of the cell can be changed to maximize the efficiency based on geographical location.

5.6. Summary

DSSCs are a promising solar energy technology that can help alleviate our current dependence on fossil fuels. However, their current widespread use is limited by their high cost and low efficiency. In a step towards improving the efficiency of DSSCs, we have tested the potential use of several natural plant photosynthetic pigments as sensitizing pigments. We used various combinations of chlorophyll, xanthophyll, and beta-carotene, as well as novel combinations incorporating all three pigments to sensitize DSSCs. We found a difference in DSSC output among the pigments tested, with chlorophyll being the pigment that resulted in the highest DSSC power output. In order to explore why the pigments varied in their utility as DSSC sensitizers dyes and to predict the response of other pigments, we also developed an algorithm to calculate an A-value for each pigment. This value was correlated ($R = 0.66$) with cell output and the regression explained just under 50% ($R^2 = 0.45$) of the variability of cell DSSC output. This study is the first attempt to use a natural plant product's optical properties to determine its likely use in DSSCs. However, further research is needed in order to successfully implement DSSCs sensitized with plant pigments into practice.

APPENDIX 1: METHOD DEVELOPMENT

A1.1 Pigments

A1.1.1Column Chromatography Extraction

Our first method of acquiring pigments involved a plan that we thought would be the cheapest: extracting pigments from plants ourselves. We chose to work with spinach, since it contains a high level of chlorophyll as well as other pigments. Beta-carotene and chlorophylls a and b were separated using column chromatography. The two chlorophyll pigments are highly polar while beta-carotene is a hydrocarbon and therefore nonpolar. Separation was achieved by changing the solvents run in the column.

First, fresh spinach leaves were ground with a mortal and pestle in a hexane solution after the stems and central veins of the leaves were removed. For every 1.0 g of dry spinach leaves, 2.0 g of sand were added and then ground into the leaves until a green powder consistency was achieved. The product was suspended in acetone, and a Rotovap apparatus was used to evaporate out all the liquid. Following evaporation, the extract was re-suspended in 10 mL of hexane.

For the column chromatography, the column was packed with silica gel. For the mobile phase, we used a solution of 7 % hexane and 30% ethyl alcohol. A less polar mobile solution was run through the column to elute the beta-carotene from the spinach extract. After the beta-carotene was collected, a more polar solution was run through the column to elute the chlorophyll pigments. As each mobile phase was run through the column, the spinach extract separated into different colored bands, each of which corresponded to different pigments.

After collecting the samples, the purity of the pigments was tested using thin layer chromatography (TLC). A horizontal line was drawn onto a TLC plate 1 cm from the bottom, and a drop of each solution was placed on this baseline using a glass pipette. About 10 mL of 70%-hexane-30% acetone solution was added to a chromatography jar. The filter paper was then placed into the jar with the end closest to the baseline in the solvent. The jar was capped and the solvent moved up the plate by capillary action. The plate was removed from the jar when the solvent front reached about 1 cm from the top. A line was drawn on the paper to mark the solvent front and the spot of each pigment was circled. The retention fractions for each pigment were calculated by dividing the distance the pigment traveled from the baseline by the distance the solvent traveled.

The absorbance spectrum of each pigment was also found to further verify the purity of the pigments. Using a Shimadzu Model UV-2550 Dual Beam Spectrophotometer (Shimadzu Inc, Kyoto, Japan), the absorbance spectrum of a 1 mL sample of each pigment was measured for the entire visible light spectrum (390 - 700 nm). These spectra were then compared with spectra recorded in the literature to determine purity.

Unfortunately, spectral readings of the different colored solutions we obtained from the column chromatography proved too contaminated to determinately conclude the identity of each pigment. We were thus reluctant to use them in an analysis to determine the effects of varying pigment combinations on solar cell efficiency.

A.1.1.2. Extraction of Chlorophyll and Xanthophyll

In an attempt to improve the purity of the pigment solutions, we decided to follow the extraction methods of chlorophyll from Chinar and xanthophyll from chrysanthemum

as shown previously in Liu et al (*38*). Instead of Chinar, we used spinach leaves to extract chlorophyll due to their high concentration of chlorophyll, as stated previously. Approximately 5 g of leaves were dried in air and then ground with a mortar and pestle using petroleum ether. The liquid was separated out and the ground leaves air-dried. Afterwards, 20 mL of acetone was mixed with the leaves. Since chlorophyll and acetone are both polar, the chlorophyll separated into the acetone. The acetone solution was collected and stored at -18C.

Xanthophyll was extracted from chrysanthemum flowers. Approximately 5 g of yellow chrysanthemum leaves were ground with a mortar and pestle using a solution of 60% ethanol and 40% petroleum ether. The liquid, which contained xanthophyll, was filtered and diluted to 20mL with a 60% ethanol-40% petroleum ether solution. The pigment solution was stored at -18°C. The purity of the pigments was verified by obtaining their absorption spectra as described previously. Although this extraction provided much better results than the previous method, the purity of each solution could not be established conclusively.

A1.1.3. Final Plan:

When enough funding was obtained, stock solutions of beta-carotene, xanthophyll, and chlorophyll a were acquired from Sigma-Aldrich (Sigma-Aldrich Inc, St. Louis, MO, USA). Each pigment was diluted in ethanol to a final concentration of 1.119×10^{-4}M. The pigments were stored in the dark at -18°C.

A1.2. Absorption Spectral Analysis

Absorption spectra of the beta-carotene, xanthophyll, and chlorophyll a pigment solutions were measured from 390-700 nm using a Shimadzu Model UV-2550 Dual Beam Spectrophotometer (Shimadzu Inc, Kyoto, Japan). After the spectra were collected, a value we deemed the S-value was computed for each pigment combination. The S-value was calculated by multiplying the intensity of sunlight at 100mW/cm^2 for air mass (AM) 1.5 at every wavelength in the visible spectrum by the recorded absorption of the specific pigment combination at the corresponding wavelengths. The S-value of the sensitizing pigment combination was used to predict the output of a particular pigment combination relative to a different pigment solution. Mathematically this can be shown as:

$$S = \sum_{\lambda=400}^{700} (intesnity\ of\ sunlight\ at\ \lambda)(Absorption\ of\ pigment\ mixture\ at\ \lambda)$$

Equation A1.1. Original S-value equation.

Combinations	Chl	Xan	Car	Chl-Xan	Chl-Car	Xan-Chl	Xan-Car	Car-Chl	Car-Xan	Chl-Xan-Car
Combination ratios										
100%	21.84	30.47	39.63							
9:1				18.91	16.36	28.00	26.77	38.64	39.48	
8:1				23.01	17.26	26.82	20.75	39.14	40.38	
7:1				23.34	19.24	26.21	23.40	39.25	38.51	
6:1				19.53	19.75	21.13	24.98	39.40	42.96	
5:1				20.74	26.30	23.35	22.68	39.12	45.13	
4:1				21.86	22.05	21.28	27.63	39.72	40.20	
3:1				19.14	26.19	21.78	28.20	38.84	39.04	
2:1				21.92	28.15	21.78	30.72	36.26	37.99	
1:1				22.77	37.11	22.77	34.07	37.11	34.07	
1:1:1										93.66
2:1:1										59.22
1:2:1										54.27
1:1:2										82.95

Table A1.1. Table of the computed S-values from every pigment combination's absorbance spectrum.

A1.3. TiO_2 Paste

Though our final methodology involved electrodes and counter electrodes pre-spread with TiO_2 and platinum, respectively, we initially made and spread those pastes ourselves.

A1.3.1. Initial Trials

The TiO_2 paste was made by adding step-wise 10 g of AEROXIDE® TiO_2 P 25 powder (Evonik Degussa) and 20 mL of 0.1 M nitric acid. We used a mortar and pestle to vigorously grind the mixture together for 20 minutes. Finally, 50 drops of Triton X 100 surfactant were added. Although the source for this recipe, Wongcharee et al. 2007 called for polyethylene glycol, Dr. Michael Grätzel, when he visited us in November 2010, warned us against its use because it plays the same surfactant role as the Triton X 100 (89). Using both the polyethylene glycol and Triton X 100 would have added too much surfactant to the mixture.

A1.3.2. Hand Mixer:

Our initial method for mixing the paste was time consuming and not consistent between team members and trials. Aiming for uniformity, we ultimately agreed to use an electric Hamilton Beach hand mixer commonly used in the kitchen. As the TiO_2 powder and 20 mL of 0.1M nitric acid were added step-wise, the mixture was blended with the hand mixer. The mixture was then further ground with a mortar and pestle for 20

minutes. Finally, 50 drops of Triton X-100 surfactant were added to the paste. The TiO_2 paste was stored in plastic vials at room temperature.

After coating and testing cells of size 10cm x 10cm with this TiO_2 paste, correspondents at DyeSol informed us that mixing the TiO_2 with an electric blender actually destroyed the mesoporous nature of the TiO_2. Consequently, the TiO_2 could not adequately absorb the dye and sensitize the cell. Because the TiO_2 was essentially ruined, the results from this trial were worthless.

A1.3.3. Spreading

A1.3.3.1. Thickness Tests of TiO_2

In the preliminary trials of testing our cells, the TiO_2 layer of the electrode was prone to flaking off either while baking, while being soaked in the pigment solution, or after cell assembly. To solve this problem, we did a few rudimentary tests to find out what was causing the flaking. First, we manipulated the components of the paste: increasing and decreasing relative acid levels, thinking that a more or less watery paste might behave differently. We found that no matter the ratio of acid to powder, the paste still flaked off the electrode.

Next, we varied the thickness of the paste. We baked several electrodes simultaneously with the same batch of TiO_2 paste, but with different thicknesses of paste spread on each. The only electrode that maintained a smooth, non-flaking layer of TiO_2 was the thinnest layer. Additionally, inconsistencies in spreading created variability in the TiO_2 thickness on each electrode. The thicker regions on each electrode always flaked off.

We concluded that at very high temperatures, the TiO_2 molecules preferred to bind to each other, rather than to the glass. Since the TiO_2 paste did not adhere to the plate when it was spread in thicker layers, it peeled away from the glass when soaked or handled. We thus determined that the thinnest layer possible of TiO_2 was necessary to obtain accurate measurements of each cell's efficiency. As discussed in the literature review, many different methods of sputtering and spraying TiO_2 are used in the industry, but we sought to develop a similarly consistent method for our less industrial lab.

A1.3.3.2. Metal Spreader

We first developed a hand-held metal spreader that was angled and sharpened to produce an even, sharp edge. This spreader was used to spread TiO_2 on the 2.54 cm x 2.54 cm glass plates. Prior to spreading the TiO_2, clear tape was placed on three sides of the conductive glass plate to approximately cover 3 millimeters on each side. TiO_2 was then placed on the surface of the glass plate with a metal spatula and distributed as evenly as possible with the metal spreader. A designated person spread the TiO_2 on all cells using this method to reduce variability in spreading thickness and distribution.

A1.3.3.3. Automated Spreading Technique

Following preliminary trials involving different spreading techniques, we decided to develop an automated spreader that would eliminate spreading inconsistencies Since an automated process for spreading the paste would produce uniformity in coating thickness and consistency, it was advantageous over our previous methods that could not remove human error. An automated spreader was built on an aluminum u-channel base to provide mechanical rigidity (see Figure A1.1). The aluminum base measured

approximately 21.25 inches in length. A geared electric motor was attached to one end of the base. The motor was powered by an alternating current wall source through an adaptor and produced an estimated linear speed of one-quarter inch per second. The motor was coupled to a threaded rod by a flexible shaft collar. When the motor was turned on, it caused the threaded rod to spin and push or pull a white Delrin block linearly along the aluminum base. Another piece of white Delrin was cut to precisely hold a 10 cm x 10 cm glass plate. This removable plate mount fit over the Delrin sliding block.

Figure A1.1. Finished model of the automated spreader.

The spreading blade was also cut from white Delrin and sharpened to create a defined edge. The blade was mounted on a rigid steel triangular frame with a steel cross bar to maintain precision. The height and tilt of the blade was adjusted with two different micrometer heads. Two couples that rotated freely in the spreading blade connected the micrometer heads to the blade.

In order to spread the TiO_2 on the plate, TiO_2 was placed on one edge of the conductive side of a glass plate. The TiO_2 was distributed with a metal spatula along the side to facilitate even spreading. The glass plate was then placed on the plate mount with the side covered with TiO_2 closest to the plate. The motor was then turned on causing the

plate to move towards the spreading blade with constant velocity. As the glass plate moved under the blade, the blade spread the TiO_2 over the conductive surface.

A1.3.3.4. Glass Pipette

Because the automated spreader produced significant variation in the TiO_2 that could not be prevented, we decided to employ a simpler technique using a glass pipette to push the TiO_2 paste over the surface. Although this process was not automated, it produced less variability in the thickness and distribution of the paste. As with the automated coating process, clear tape was placed along three edges of the conductive side of a glass plate. TiO_2 was placed on one edge and spread across the glass surface by sliding the length of a glass pipette over the surface towards the edge not covered with tape. The thickness of the coating was approximated to the thickness of the tape, or about 1 mm.

A1.3.3.5. Final Method Choice for TiO_2 and Spreading – TiO_2-coated Test Cell Glass Plates

While the glass pipette method provided uniform coating, the thickness of the coat was limited by the thickness of the tape. During our meeting with Dr. Grätzel in November 2010, we were informed that the TiO_2 paste should appear clear when applied to the glass plates. Because any spreading method available to us could not produce a thin enough layer and after suffering those devastating results, we discovered the availability of TEC15 transparent TiO_2-coated test cell FTO glass plates from DyeSol (DyeSol, Queanbaven, NSW, Australia). The dimensions of the electrodes were 20 mm x 23 mm (460 mm^2) with an active area of 8 mm x 11 mm (88 mm^2) and a thickness of

3.2 mm each. The electrodes were purchased as a plate of size 161 mm x 80 mm, and the uncut plates were then cut into 28 individual, pre-coated electrodes. Since the TiO_2 was already made, spread, and baked onto these plates, the most time-consuming part of our methodology was eliminated.

A1.4. Electrode

After the TiO_2 paste was evenly spread onto the electrodes, the electrodes were baked to adhere the paste to the glass and to expel any moisture from the TiO_2, so that the pigment could bind. Our preliminary baking of the electrodes focused on heating the electrode on a hotplate on the highest setting until we saw a color change in the TiO_2 paste from white to brown all the way back to white. The hotplate was then turned off and the electrode cooled until it could be moved without cracking.

However, in some of the glass plates, this method produced cracks in the glass due to uneven heating of the plates. Our subsequent electrodes were baked according to a firing profile protocol provided by DyeSol on a Fisher Scientific Isotemp Digital ceramic-top hotplate (Fisher Scientific, Pittsburgh, PA, USA). The glass plates were placed in the center of the hotplate to avoid uneven heating.

	Time minutes	WE set T°C	WE set T°F
0	0	25	77
10	10	325	617
5	15	325	617
5	20	375	707
5	25	375	707
5	30	450	842
15	45	450	842
5	50	500	932
15	65	500	932
60	125	25	77

Table A1.2. Firing Profile for Working Electrode from DyeSol.

After the electrodes cooled to 90°C, they were placed in Petri dishes containing a 35 mL solution of different combinations of xanthophyll, beta-carotene, and chlorophyll. The Petri dishes were sealed with Parafilm and placed in the dark for 24 hours at room temperature. Three electrodes were soaked in each of the following 17 combinations:

	Pigment Combination
1	Blank
2	100% Chlorophyll
3	100% Chlorophyll
4	100% Beta-carotene

5	1:1 Chlorophyll: Beta-carotene
6	1:1 Chlorophyll: Xanthophyll
7	1:1 Xanthophyll: Beta-carotene
8	1:2 Chlorophyll: Xanthophyll
9	1:2 Chlorophyll: Beta-carotene
10	1:2 Xanthophyll: Chlorophyll
11	1:2 Xanthophyll: Beta-carotene
12	1:2 Beta-carotene: Chlorophyll
13	1:2 Beta-carotene: Xanthophyll
14	1:1:1 Chlorophyll: Xanthophyll: Beta-carotene
15	2:1:1 Chlorophyll: Xanthophyll: Beta-carotene
16	1:2:1 Chlorophyll: Xanthophyll: Beta-carotene
17	1:1:2 Chlorophyll: Xanthophyll: Beta-carotene

Table A1.3. Pigment combinations used to sensitize electrodes.

A1.4.1. Final Method for Electrode

When using the pre-spread plates from DyeSol, we heated the cells to 80-90^{o}C to get rid of any moisture, and then placed them in triplicates in each combination of pigments. The same concentrations and combinations were used as listed in Table A1.3 above.

A1.5. Counter electrode

A1.5.1. Carbon Catalyst

We initially coated the conductive side of the counter electrode with a carbon catalyst produced by holding a flame to the glass plate and rapidly moving the flame over the plate to produce an even coating without burning the cell. However, despite our efforts to produce an even carbon layer, this method did not provide consistent results.

Further, although the flame coated the 2.54 cm x 2.54 cm cells adequately, it was not a reasonable option for the much larger 10 cm x 10 cm cells.

A1.5.2. Platinum Catalyst:

We decided to use Platinum Paste PT1 to prevent additional inconsistencies (DyeSol, Queanbaven, NSW, Australia). As previously mentioned in the literature review, platinum catalysts are commonly incorporated in solar cells. Although platinum catalysts are more expensive than carbon catalysts, methods for coating the counter-electrode with carbon are not automated and are thus subject to human errors (57).

Clear tape was placed along three edges of the conductive side of the 10 cm x 10 cm counter-electrode to cover 1 cm on each side covered by tape. Platinum paste was placed on one edge of the glass plate and spread with a glass pipette using the same method used to spread the TiO_2 paste. The thickness of the platinum paste was about as thick as the thickness of the tape. After the tape was carefully removed, the counter-electrode was baked on a hot plate according to a baking protocol provided by DyeSol.

	Time minutes	WE set T°C	WE set T°F
0	0	25	77
10	10	235	455
5	15	235	455
5	20	285	545

5	25	285	545
5	30	360	680
5	35	360	680
5	40	410	770
15	55	410	770
60	115	25	77

Table A1.4. Firing profile for the counter electrode (CE) from DyeSol.

A1.5.4.3. Pre-coated counter-electrodes:

After deciding to order pre-treated TiO_2 electrodes from DyeSol, we also ordered the matching Pt-coated test cell TEC15 glass plates.

A1.6. Cell Assembly

After the electrodes soaked in the pigment solutions for 24 hours, they were carefully removed form the solutions with tweezers and allowed to air dry. The electrode was placed on top of the counter electrode in such a manner to maximize contact between the TiO_2 and platinum. Binder clips were placed along the edges of the cell to hold the glass plates together. Once the plates were secure, KI electrolyte solution was dropped onto the edge of the cell and spread between the glass plates through capillary action to cover the entire active area. Excess electrolyte was wiped off the solar cell. As previously discussed in the literature review chapter, KI is an affordable and common electrolyte, even though it is not the optimal choice.

As the last step of the construction process, copper tape was placed along the protrusions on the top and bottom of each cell. The copper tape served as a point of contact to which wires could be attached to complete circuits with the cells with minimal resistance. The glass plates we bought carried a sheet resistance of 15 ohms, but a point contact with any wires could raise the resistance due to the glass significantly. Placing copper tape along the edges allowed for any electrons created by the cells to travel more freely and with the written resistivity.

A1.7. Testing

Three cells of each pigment combination were tested concurrently in a Conviron Model BDW36 Growth Chamber (Conviron, Pembina, ND, USA). The chamber was equipped with 20 GE MVR400/HOR/MOG metal halide lamps (General Electric, Fairfield, CT, USA) filtered with a 1/8 inch Plexiglass type G barrier to remove most of the ultraviolet radiation from the chamber. The spectral irradiance inside the chamber is shown in Figure 3.1. The cells were evaluated at a temperature of 22^{o}C and 15% relative humidity. Lights were turned on for the first 30 minutes, off for the next 30 minutes, then on again for the final 30 minutes. The average voltage and current of each cell were measured every 10 minutes using a 21X Datalogger (Campbell Scientific). Data were recorded with PC200W Datalogger Starter Software (Campbell Scientific).

APPENDIX 2: RESULTS

A2.1. Spectral Data

The following graphs are absorption spectra for the pigment combinations used on the DSSCs. All absorption spectra were normalized with a blank of ethanol and are displayed as the average of three readings by the Shimadzu Model UV-2550 Dual Beam Spectrophotometer (Shimadzu Inc, Kyoto, Japan).

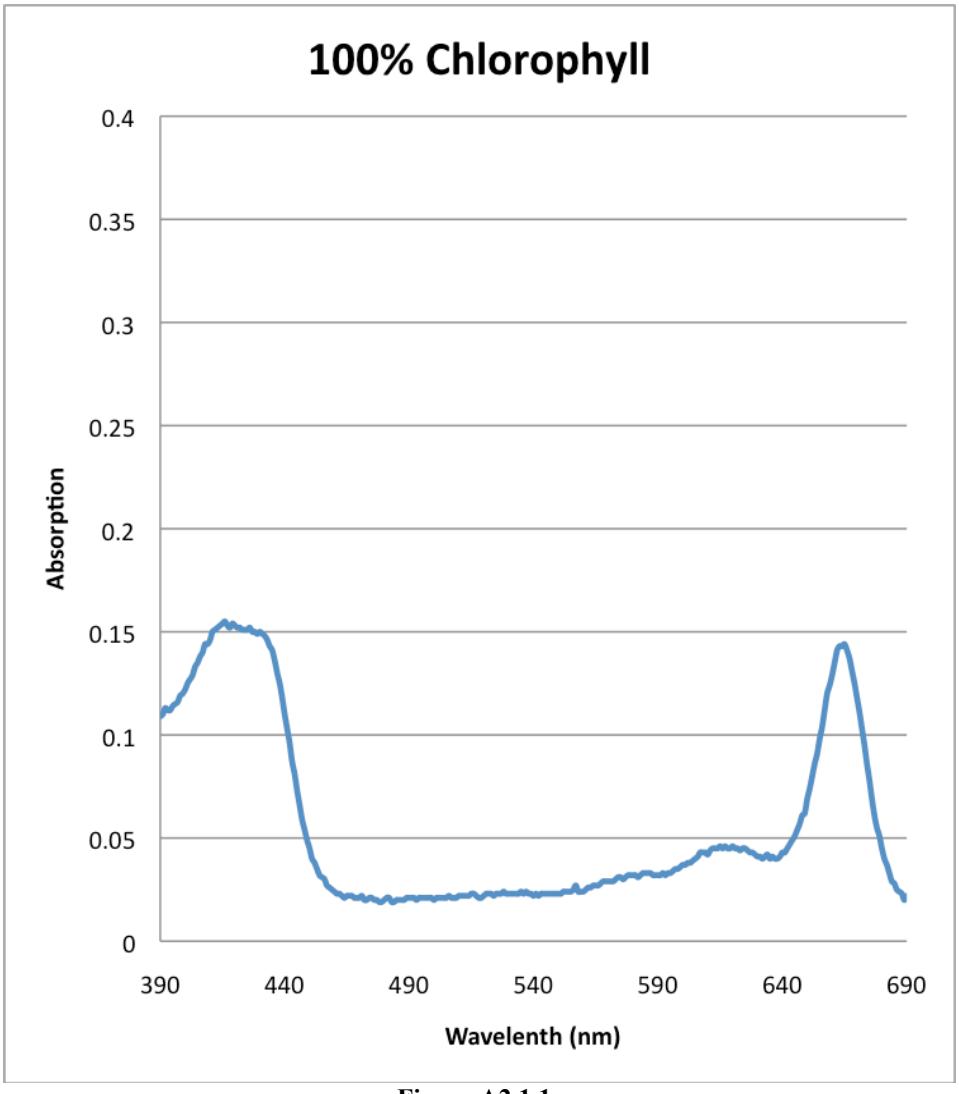

Figure A2.1.1.

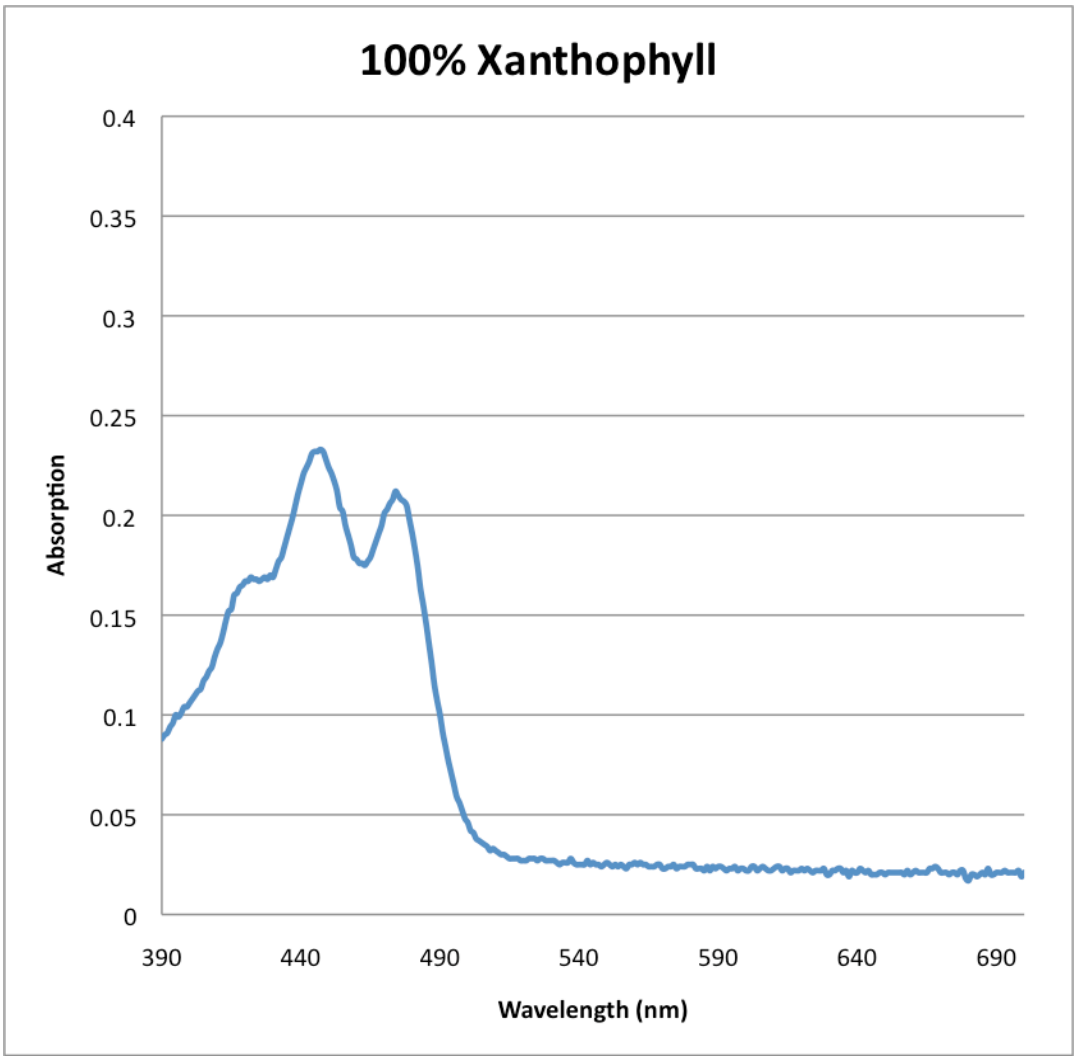
100% Xanthophyll
0.4
0.35
0.3
0.25
0.2
0.15
0.1
0.05
0
Absorption
390
440
490
540
590
640
690
Wavelength (nm)

Figure A2.1.2.

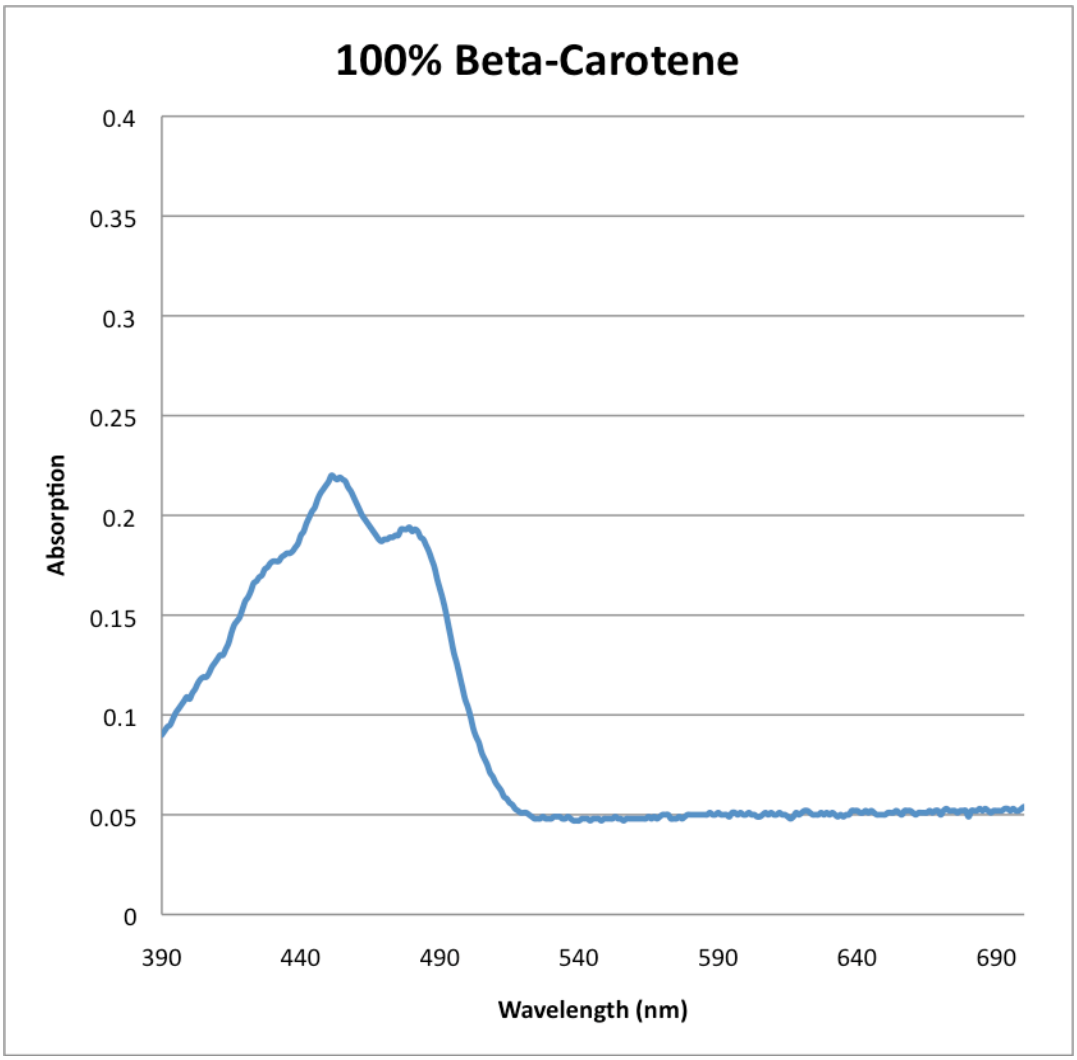
100% Beta-Carotene
0.4
0.35
0.3
0.25
0.2
0.15
0.1
0.05
0
Absorption
390
440
490
540
590
640
690
Wavelength (nm)

Figure A2.1.3.

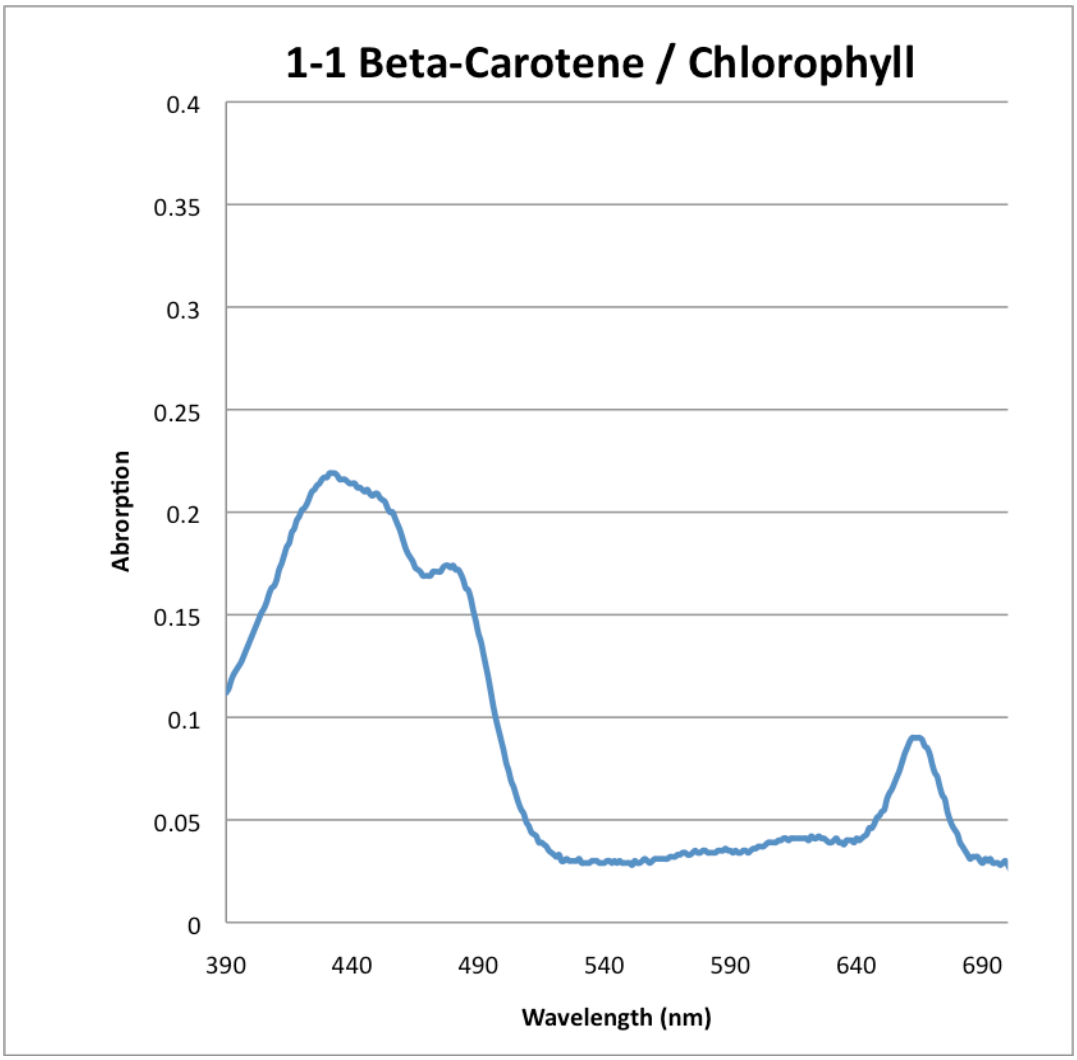
1-1 Beta-Carotene / Chlorophyll
0.4
0.35
0.3
0.25
0.2
0.15
0.1
0.05
0
Abrorption
390
440
490
540
590
640
690
Wavelength (nm)

Figure A2.1.4.

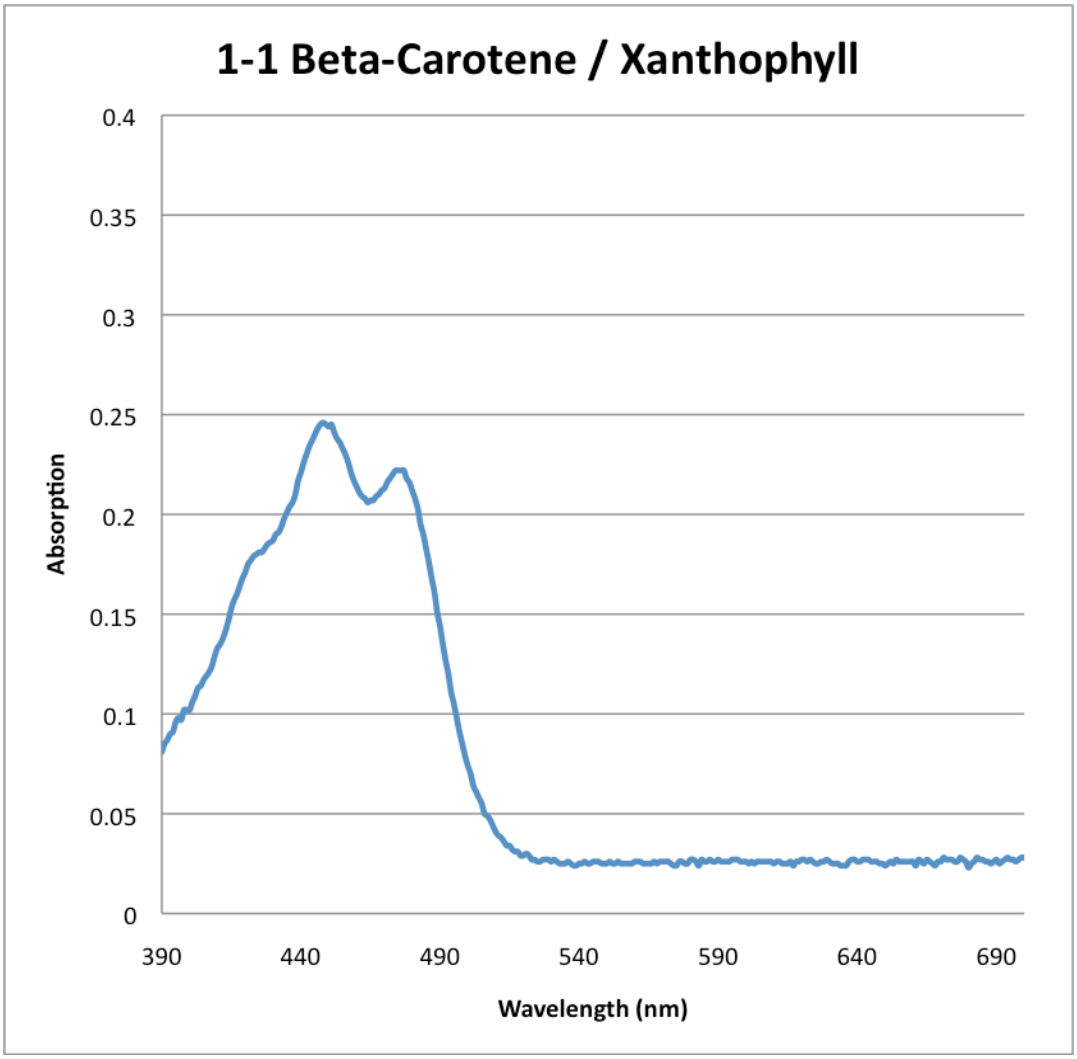
1-1 Beta-Carotene / Xanthophyll
0.4
0.35
0.3
0.25
0.2
0.15
0.1
0.05
0
Absorption
390
440
490
540
590
640
690
Wavelength (nm)

Figure A2.1.5.

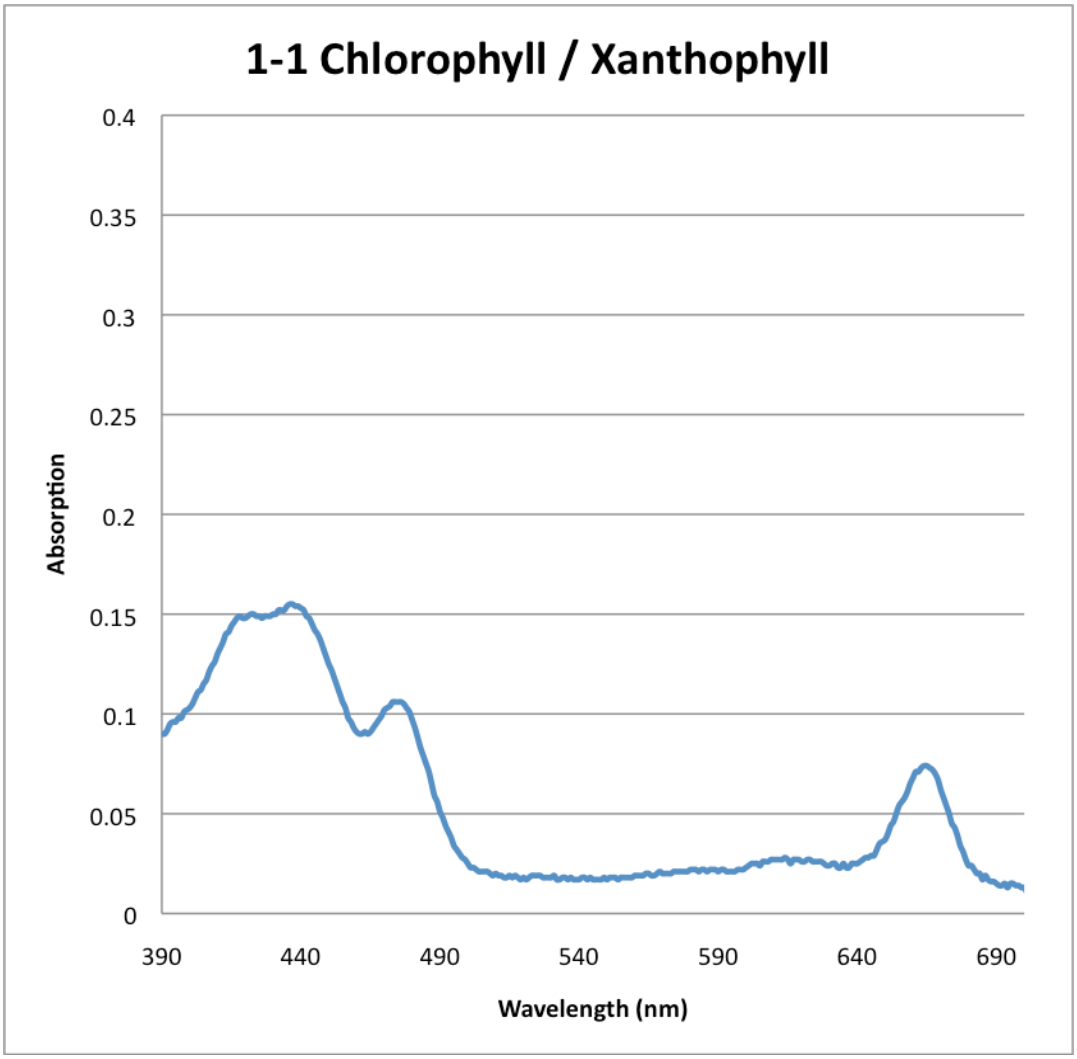
1-1 Chlorophyll / Xanthophyll
0.4
0.35
0.3
0.25
0.2
0.15
0.1
0.05
0
Absorption
390
440
490
540
590
640
690
Wavelength (nm)

Figure A2.1.6.

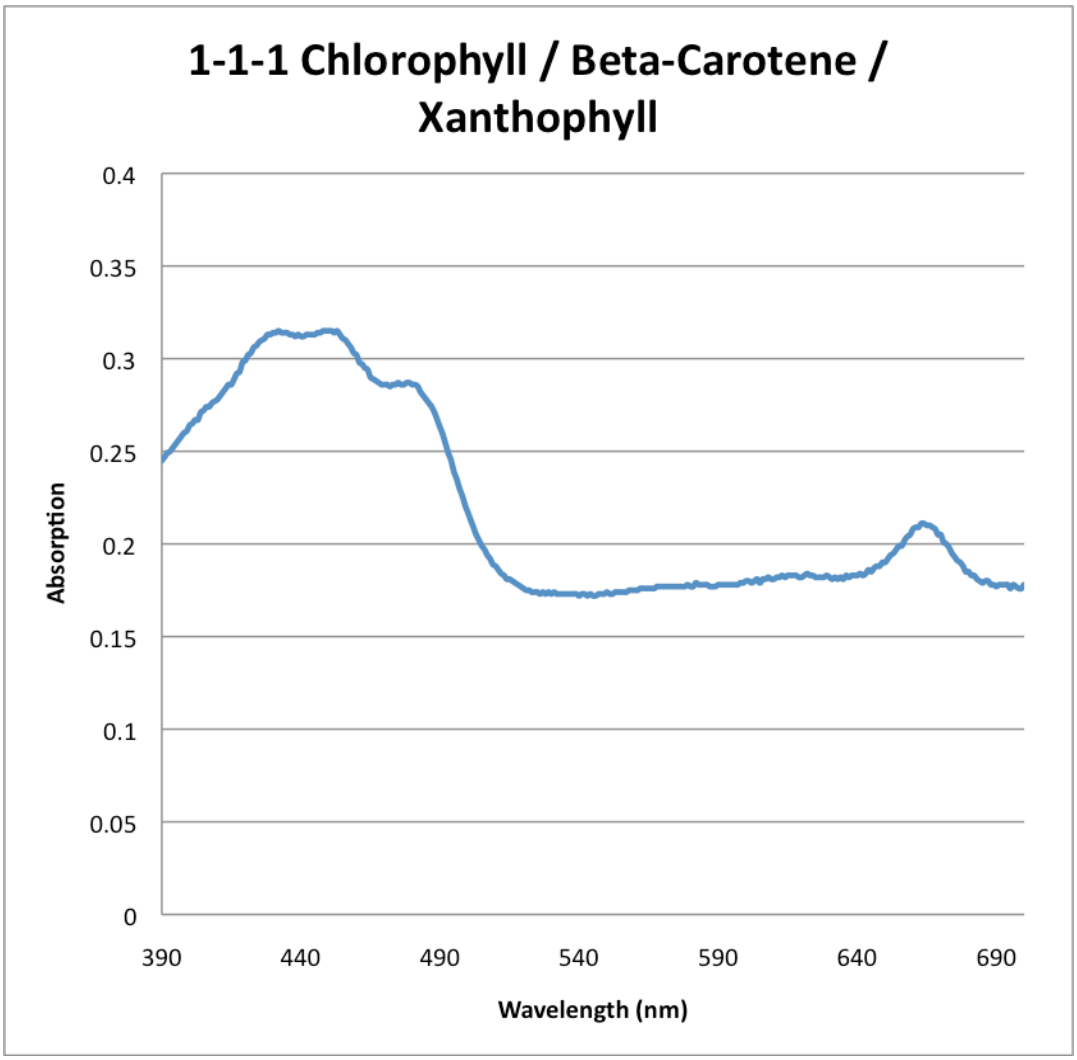
1-1-1 Chlorophyll / Beta-Carotene / Xanthophyll
0.4
0.35
0.3
0.25
0.2
0.15
0.1
0.05
0
Absorption
390
440
490
540
590
640
690
Wavelength (nm)

Figure A2.1.7.

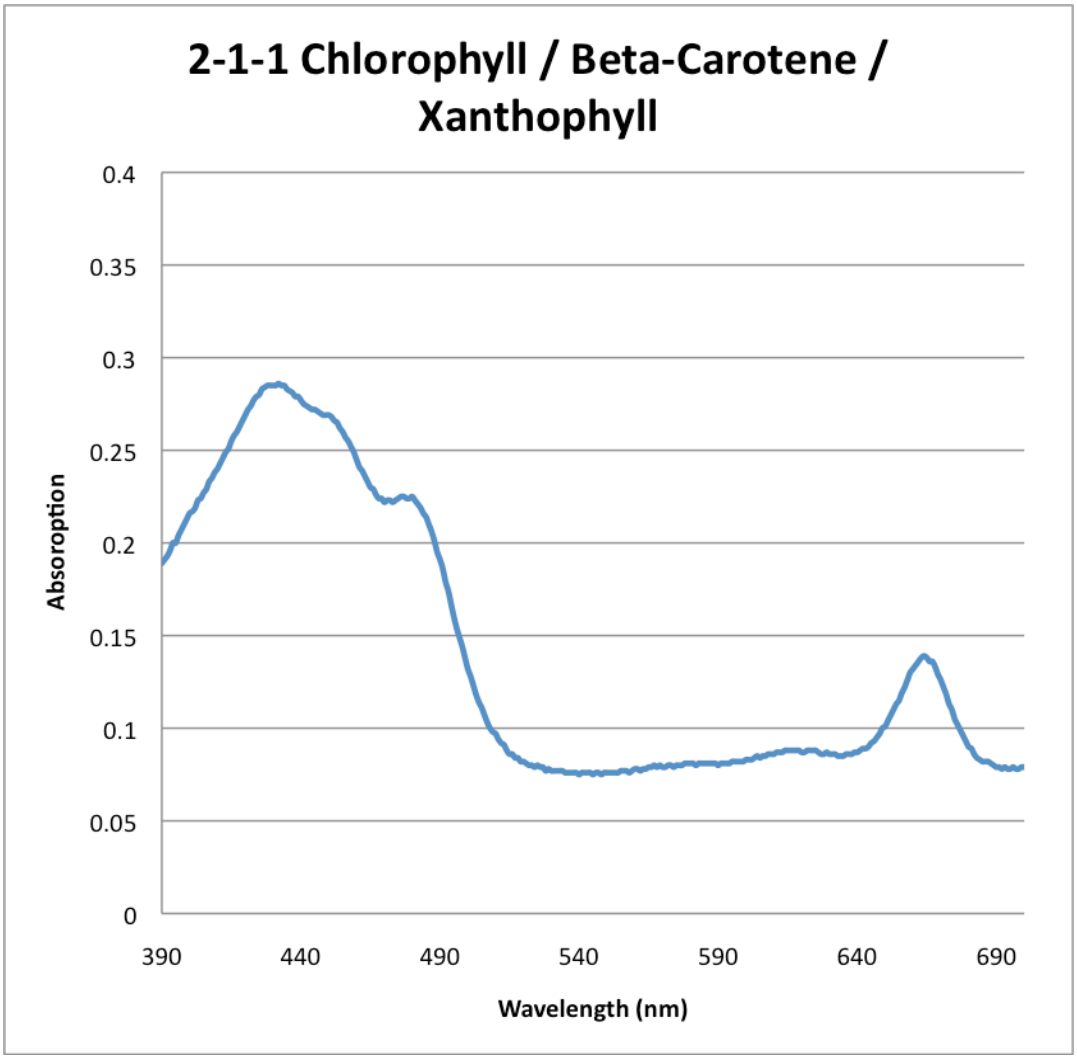
2-1-1 Chlorophyll / Beta-Carotene / Xanthophyll
Absoroption
0.4
0.35
0.3
0.25
0.2
0.15
0.1
0.05
0
390
440
490
540
590
640
690
Wavelength (nm)

Figure A2.1.8.

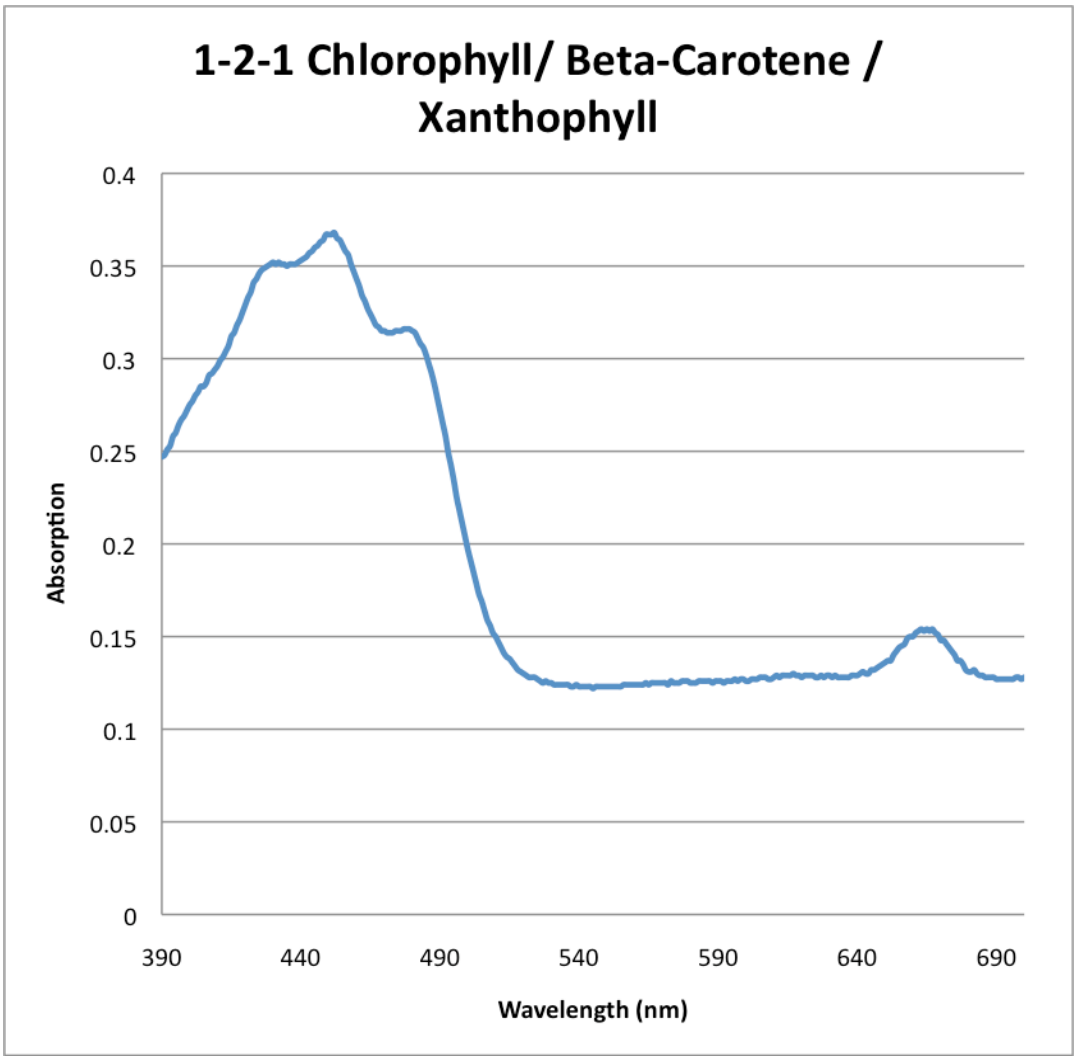
1-2-1 Chlorophyll/ Beta-Carotene / Xanthophyll
Absorption
0.4
0.35
0.3
0.25
0.2
0.15
0.1
0.05
0
390
440
490
540
590
640
690
Wavelength (nm)

Figure A2.1.9.

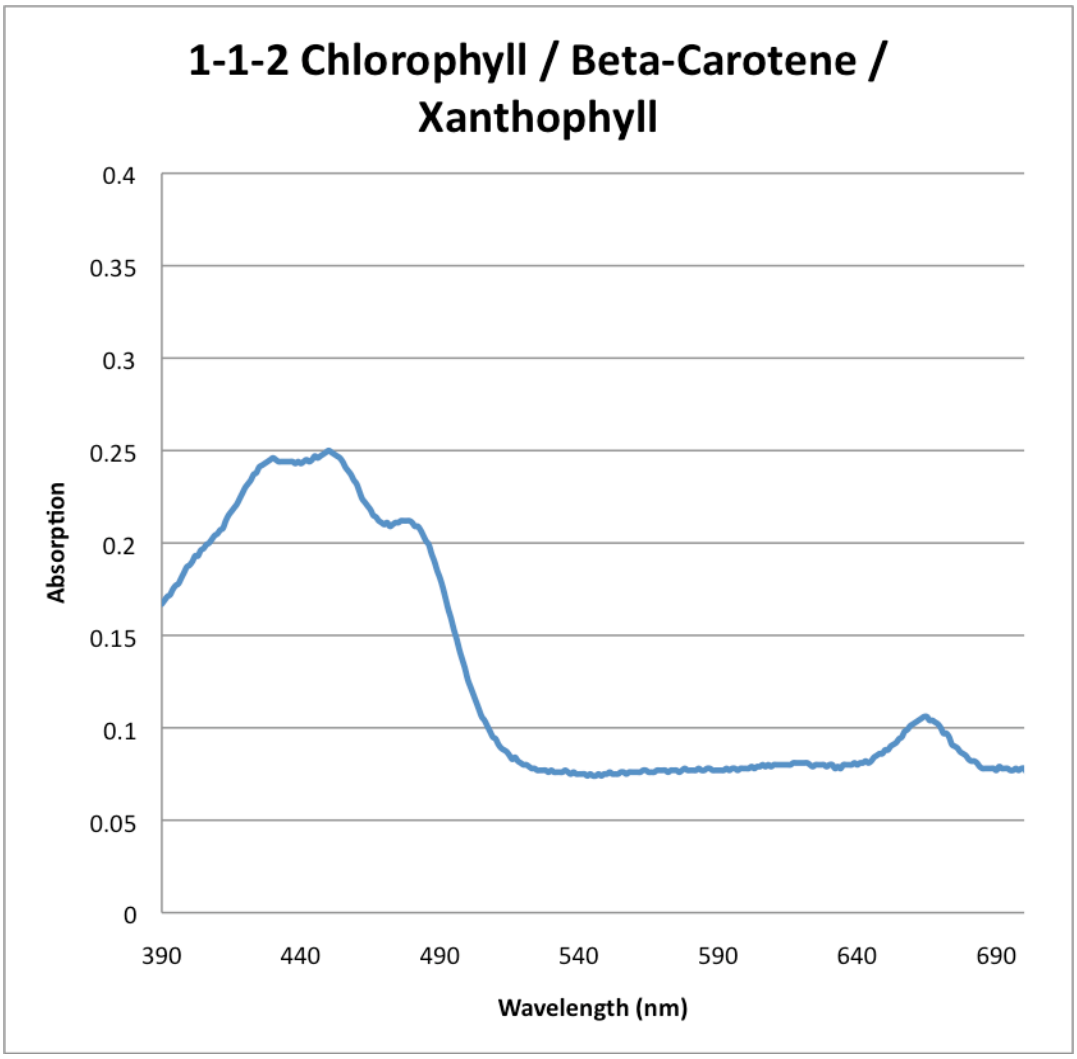

Figure A2.1.10.

A2.2. Cell Output Data

The following graphs are all Voltage versus Time graphs for DSSCs sensitized with the pigment combination described in the title of the graph. The Blank Cell contained no sensitizing solution, but all blank DSSCs we constructed produced a very low electrical output, as seen in the literature (*79*). The 3 colored lines correspond to the 3 cells, tested and constructed identically in triplicate.

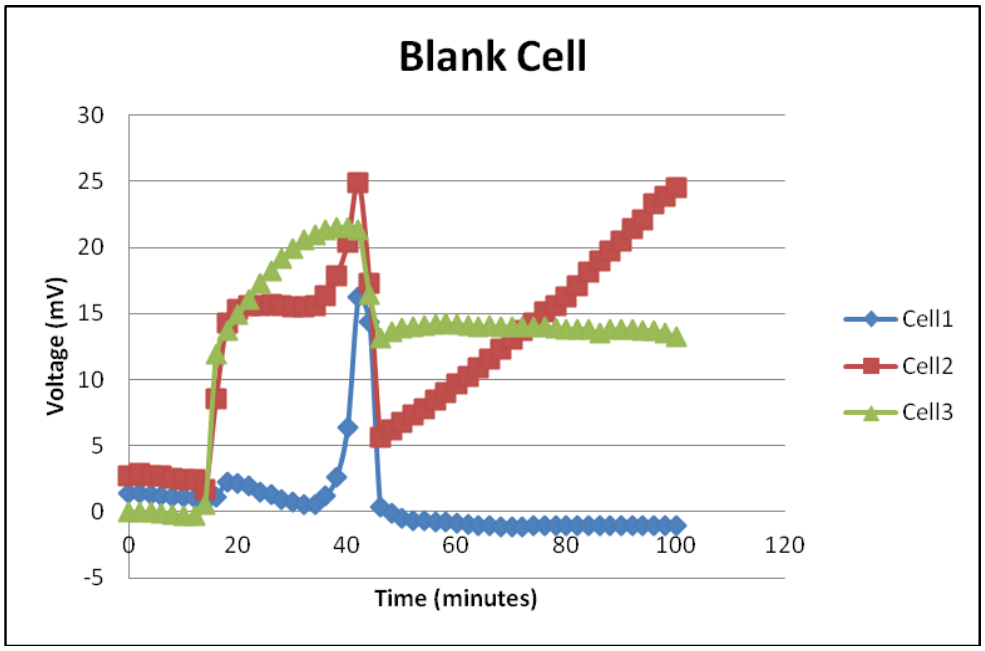

Figure A2.2.1

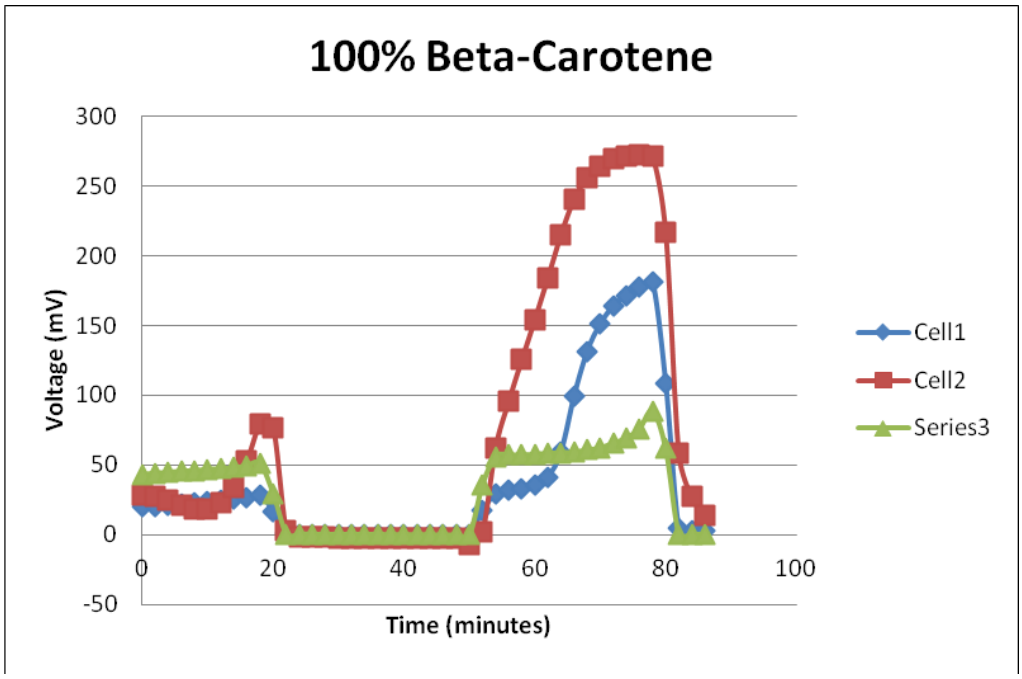

Figure A2.2.2.

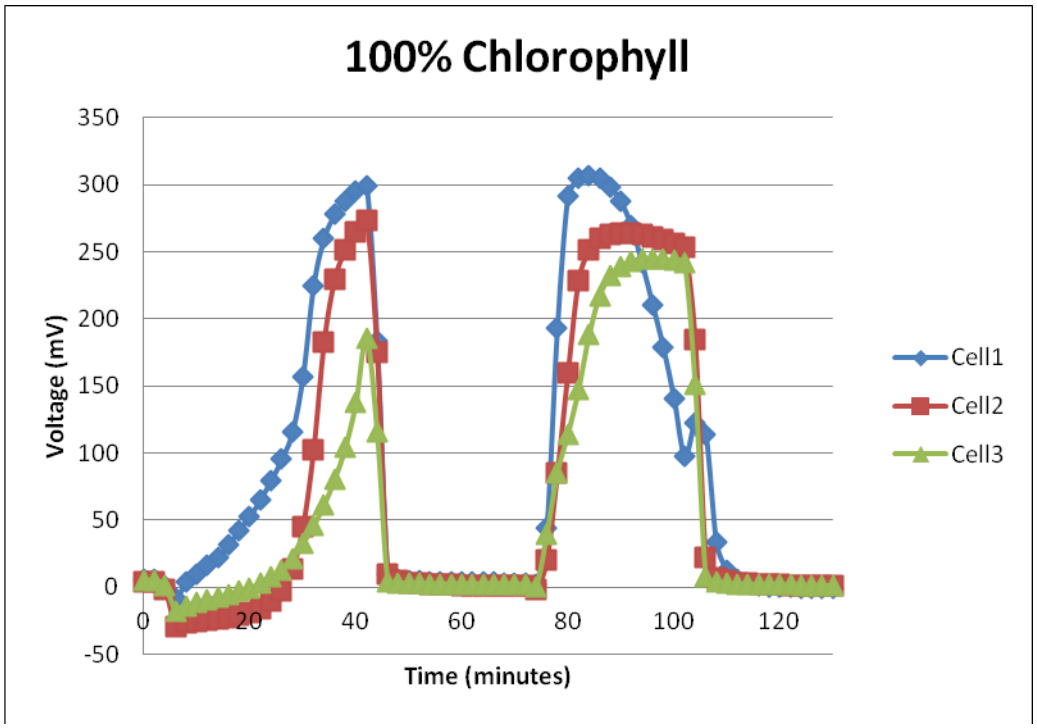

Figure A2.2.3.

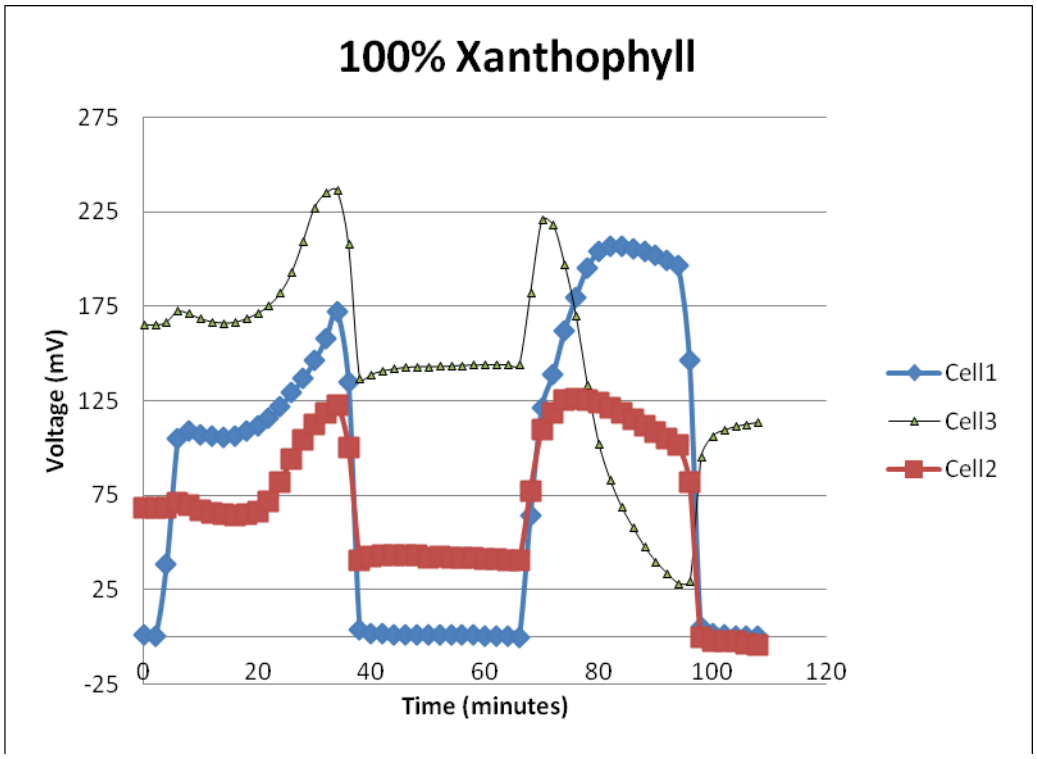

Figure A2.2.4.

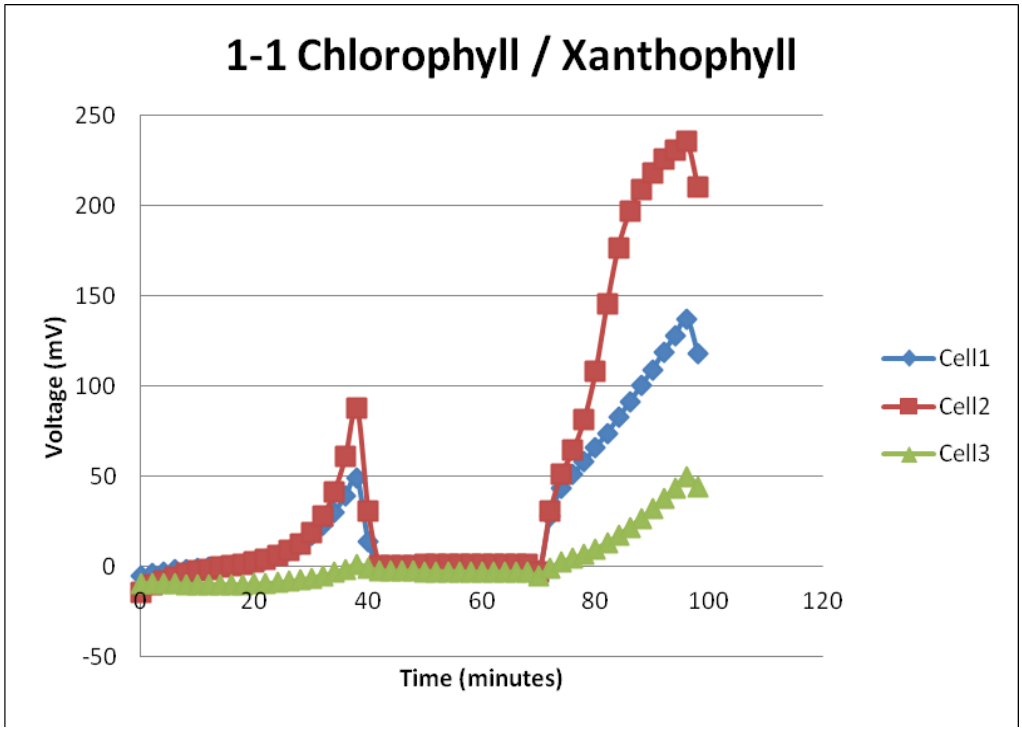

Figure A2.2.5.

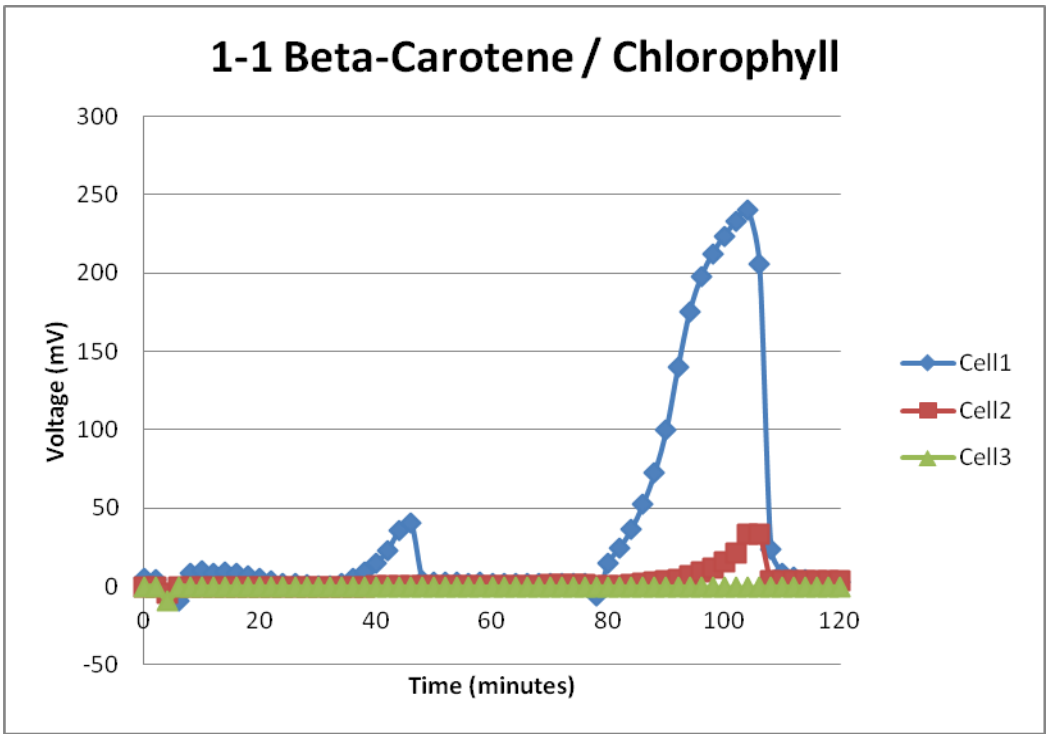

Figure A2.2.6.

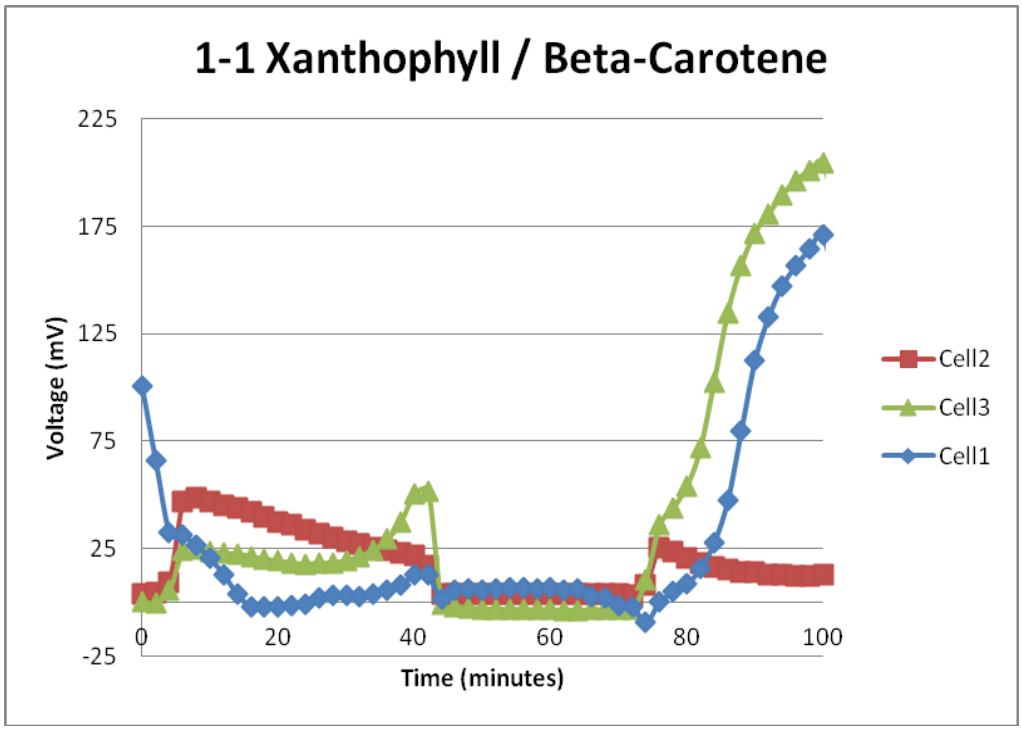

Figure A2.2.7.

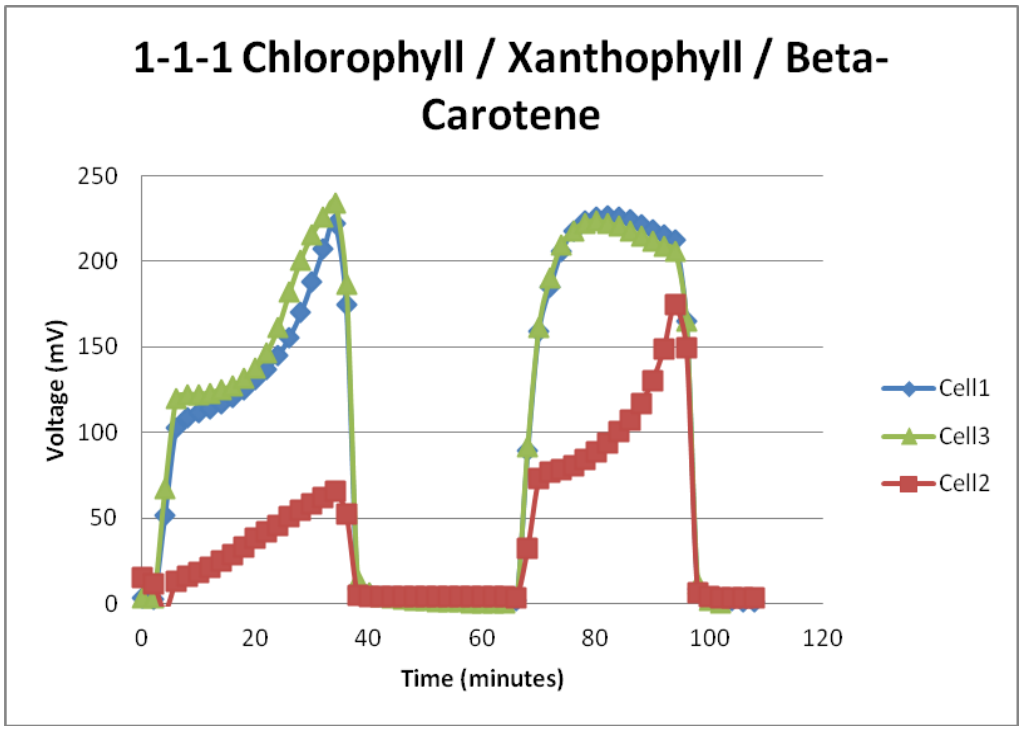

Figure A2.2.8.

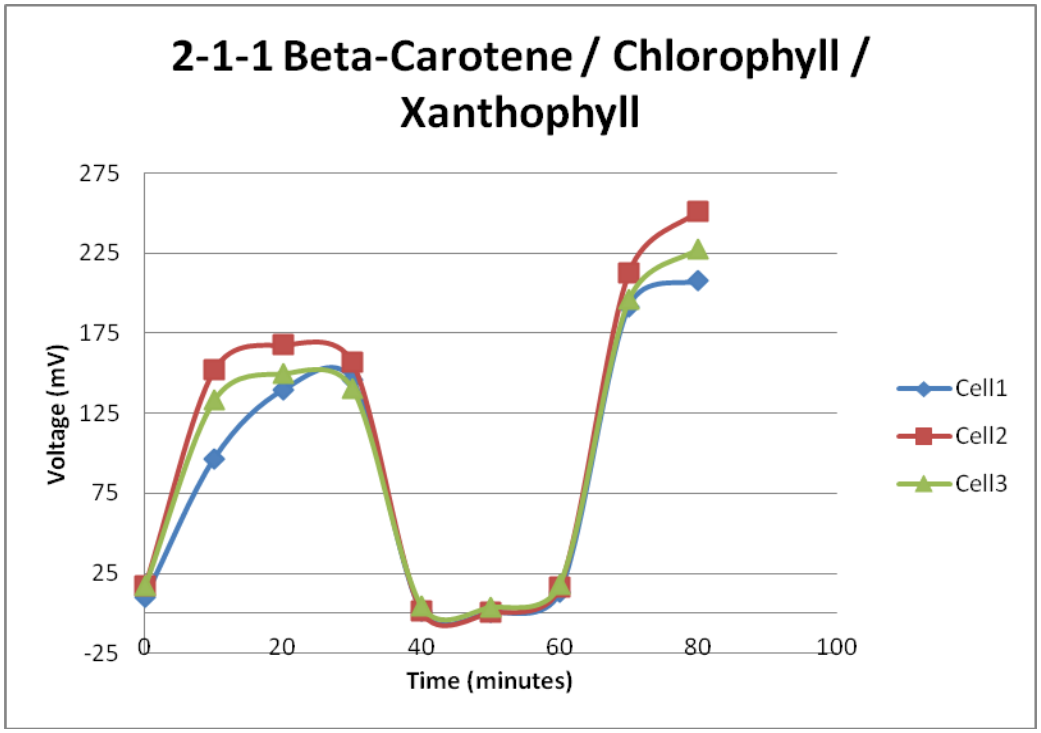

Figure A2.2.9.

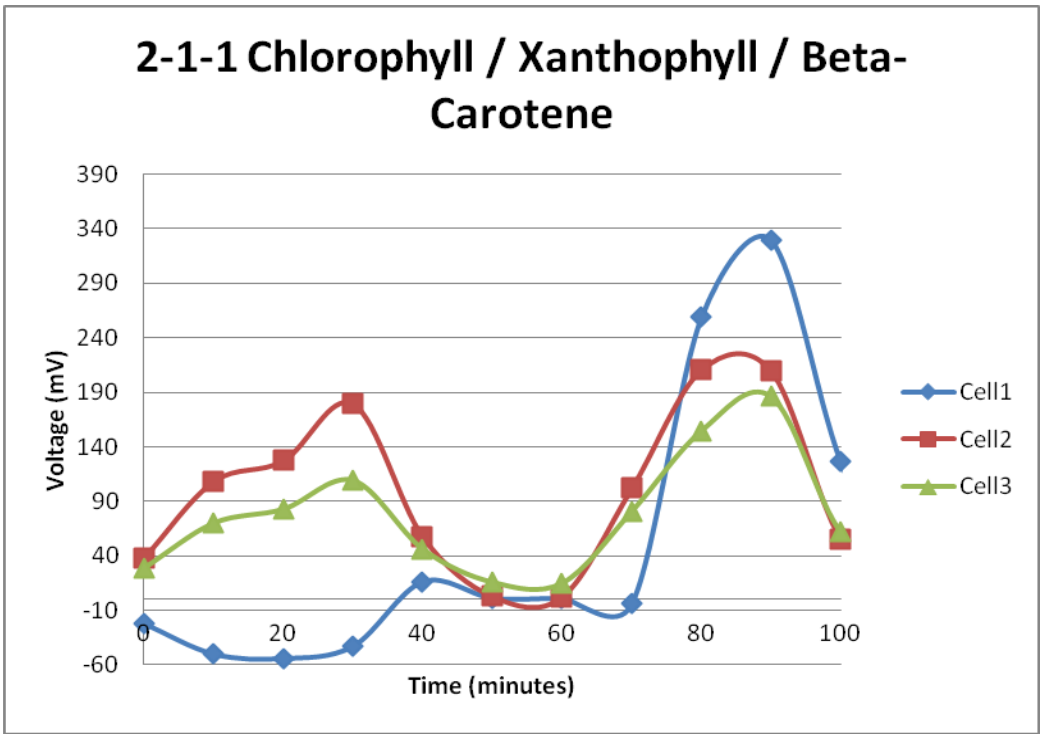

Figure A2.2.10.

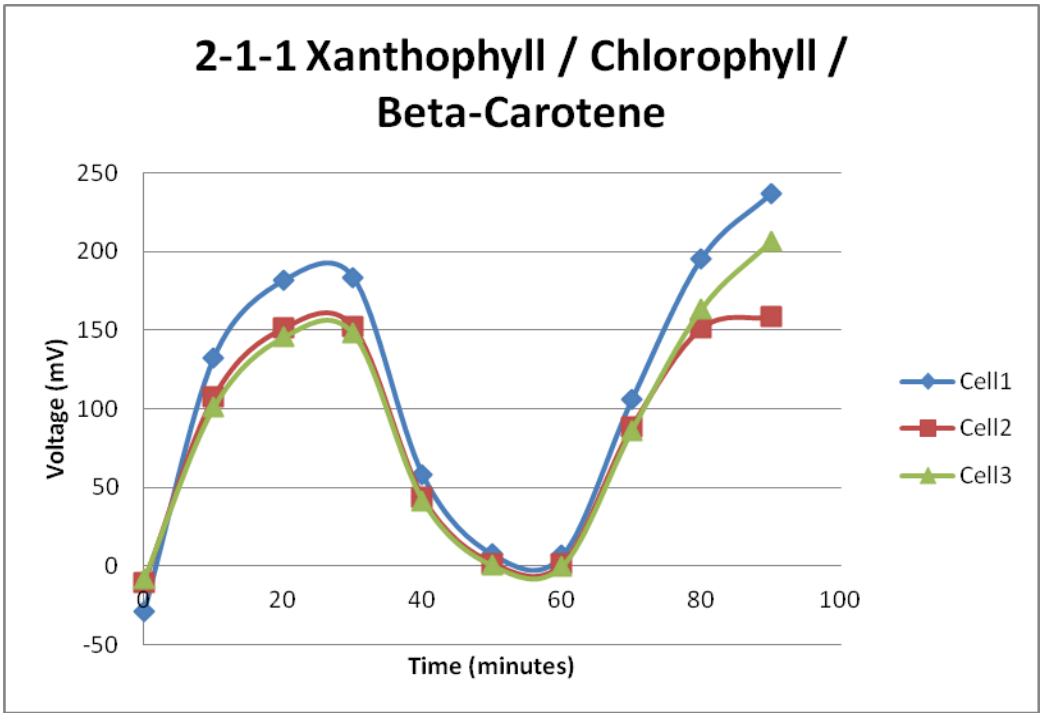

Figure A2.2.11.

ABBREVIATIONS

A – Amperes
AC – alternating current
AM – air mass
APCE – absorbed photon to current efficiency
ATP – adenosine triphosphate
BOS – balance of system
BP – British Petroleum
C – Celsius
CuI – Copper iodide
DOE – Department of Energy
DSSC – dye-sensitized solar cell
eV – electron volts
FF – fill factor
FTO – fluorine-doped tin oxide
ICAM – International Conference on Advance Manufacture
IPCE – incident photon to current efficiency
IR - infrared
ITO – tin-doped indium oxide
J_{sc} – short-circuit current
KI – Potassium iodide
kWh – kilowatt hour
LSD – Least Significant Differences
MW – megawatts
N3 - cis-bis(4,4-dicarboxy-2,2-bipyridine)dithiocyanato ruthenium(II)
NADPH – nicotinamide adenine dinucleotide phosphate
NASA – National Aeronautic and Space Administration
NREL – National Renewable Energy Laboratory
nm - nanometers
Ω – Ohms
OPEC – Organization of Petroleum Exporting Countries
PEDOT – poly(3,4-ethyl-enedioxythiophene)
PET-ITO - polyethylene terephthalate - tin-doped indium oxide
P_m – total solar power
Pmax – maximum power
PV - photovoltaic
Redox – reduction-oxidation
REPiS – Renewable Electric Plant Information System
SWCNT – single wall carbon nanotube
TEC – total electron content
TEMPO – 2,2,6,6-tetramethryl piperidine-N-oxyl
TiO_2 – titanium dioxide
TW – terawatts
UV - ultraviolet

V - Voltage
V_{oc} – open-current voltage
W_p – peak watts

REFERENCES

(1) *Climate Change 2001: The Scientific Basis*. Houghton, J.E.T.; Ding, Y.; Griggs, D.J.; Noguer, M.; van der Linden, P.J.; Dai, X.; Maskell, K.; Johnson, C.A, Eds.; Cambridge University Press: Cambridge, U.K., 2001

(2) U.S. Global Change Research Program. *Global Climate Change Impacts in the United States*; Cambridge University Press, New York, 2009.

(3) The Energy Information Association, The Department of Energy. http://www.eia.doe.gov/aer/eh/frame.html (accessed July 28, 2010).

(4) Action Forex. *1973 Oil Crisis*. http://www.actionforex.com/articles-library/financial-glossary/1973-oil-crisis-20041204320 (accessed July 28, 2010).

(5) U.S. Department of State, Office of the Historian. Milestones: 1969-1976, OPEC Oil Embargo, 1973-1973. http://history.state.gov/milestones/1969-1976/OPEC. (accessed July 24, 2010).

(6) The Wall Street Journal, The Rig Disaster Timeline. http://online.wsj.com/article/SB10001424052748704302304575213883555525958.html (accessed July 30, 2010).

(7) The Encyclopedia of Earth. Deepwater Horizon Oil Spill. http://www.eoearth.org/article/Deepwater_Horizon_oil_spill?topic=50364#gen31 (accessed Dec 22, 2010).

(8) Walsh, B. Going Green. *Time,* Dec 20, 2010. http://www.time.com/time/health/article/0,8599,2037876,00.html?amp&&& (accessed Dec 22, 2010)

(9) U.S. Energy Information Association, Independent Statistics and Analysis. Major Legislative and Regulatory Actions: The Energy Policy Act of 1992. http://www.eia.doe.gov/oil_gas/natural_gas/analysis_publications/ngmajorleg/enrgypolicy.html (accessed September 9, 2010).

(10) Demirbas, A. Political, economic and environmental impacts of biofuels: A review. *Applied Energy*. **2009**, *86*, S108-S117.

(11) Demirbas, A. Biofuels securing the planet's future energy needs. *Energy Conversion and Management*. **2009**, *50*, 2239-2249.

(12) Silva Lora, E.E.; Escobar Palacio, J.C.; Rocha, M.H.; Grillo Reno, M. L; Venturini, O.J.; Almazan del Olmo, O. Issues to consider, existing tools and constraints in biofuels sustainability assessments. *Energy*. **2010**, *Article In Press, Corrected Proof*.

(13) World Resources Institute. Biofuels Production and Policy: Implications for Climate Change, Water Quality, and Agriculture. http://www.wri.org/project/biofuels (accessed September 9, 2010).

(14) Crawford, R.H. Life cycle energy and greenhouse emissions analysis of wind turbines and the effect of size on energy yield. *Renewable and Sustainable Energy Reviews*. **2009**, *13*, 2653-2660.

(15) Sesto, E.; Casale, C. Exploitation of wind as an energy source to meet the world's electricity demands. *Journal of Wind Engineering and Industrial Aerodynamics*. **1998**, *74*, 375-387.

(16) Kunz, T.H.; Arnett, E.B.; Erickson, W.P.; Hoar, A.R., Johnson, G.D. Ecological impacts of wind energy development on bats; questions, research needs, and hypotheses. *Frontiers in Ecology and Environment*. **2007**, *5*, 315-324.

(17) Langhamer, O.; Haikonen, K.; Sundberg, J. Wave power-sustainable energy or environmentally costly? A review with special emphasis on linear wave energy converters. *Renewable and Sustainable Energy Reviews*. **2010**, *14*, 1329-1335.

(18) *Wave Energy Conversion: Volume 6;* Brooke, J., Ed.; Elsevier Ocean Engineering Series; Elsevier Science: Kidlington, 2003.

(19) Gill, A.B. Offshore renewable energy ecological implications of generating electricity in the coastal zone. *Journal of Applied Ecology.* **2005**, ***42*,** 605–615.

(20) World Nuclear Association. Another drop in nuclear generation. *World Nuclear News* (Online) May 5, 2010, http://www.world-nuclear-news.org/newsarticle.aspx?id=27665&terms=another+drop+ (accessed August 10, 2010).

(21) Findlay, T. *The Future of Nuclear Energy to 2030 and its Implications for Safety, Security and Nonproliferation: Overview*; The Centre for International Governance Innovation, Waterloo, Ontario, Canada, 2010, 10-12.

(22) Ciampichetti, A.; Rocco, P.; Zucchetti, M. Accidental and long-term safety assessment of fission and fusion power reactors. *Fusion Engineering and Design*. **2002**, *63-63*, 229-234

(23) The White House: Office of the Press Secretary. Remarks by President Barack Obama, April 5, 2009. http://www.whitehouse.gov/the_press_office/Remarks-By-President-Barack-Obama-In-Prague-As-Delivered/) (accessed August 1, 2010).

(24) Lewis, N.S. (ed.); Crabtree, G.W. (ed.); *Basic Research Needs for Solar Energy Utilization.*; Report of the United States Department of Energy Office of Basic Energy Sciences Workshop on Solar Energy Utilization (Online) **2005**;1-260.

www.er.doe.gov/bes/reports/files/SEU_rpt.pdf

(25) *The History of Solar*. U.S. Department of Energy (Online) **2006** www1.eere.energy.gov/solar/pdfs/solar_timeline.pdf

(26) Chen, Y.S.; Lee, J.; Tsai, S.; Ting, C. Manufacture of Dye-Sensitized Solar Cells and their I-V Curve Measurements. *Proceedings of ICAM 2007*, Taipei, Taiwan, November 26-28, 2007.

(27) Perlin, Josh. *The Silicon Solar Cell Turns 50;* DOE Report BR-520-33947 (Online); Department of Energy, National Renewable Energy Laboratory. http://www.nrel.gov//osti/\.pdf.

(28) Tesla, Nikola. "The problem of increasing human energy : with special references to the harnessing of the sun's energy." *The Century Illustrated Monthly Magazine* (Online) **1900**, 60, 175-211.

(29) Crabtree, G.W.; Lewis, N.S.; Solar Energy Conversion. *Phys. Today* (Online) **2007**, 60, 1-12. link.aip.org/link/PHTOAD/v60/i3/p37/s1/pdf

(30) Knier, Gil. How Do Photovoltaics Work?. NASA. http://science.nasa.gov/headlines/y2002/solarcells.htm (accessed July 18, 2010).

(31) "How Solar (Photovoltaic) Cells Work" AcetwAGL. http://www.acetewagl.com.au/education/energy/renewableenergy/solarenergy/howsolarcellswork.aspx km intro (accessed July 18, 2010).

(32) U.S. Department of Energy, Energy Efficiency and Renewable Energy, Solar Energy Technology Program. *Bandgap Energies of Semiconductors and Light* http://www1.eere.energy.gov/solar/bandgap_energies.html

(33) U.S. Department of Energy, Energy Efficiency and Renewable Energy, Solar Energy Technology Program *Semiconductors and the Built-In Electric Field for Crystalline Silicon Photovoltaic Cells* http://www.eere.energy.gov/basics/renewable_energy/semiconductors.html (Accessed July 18, 2010).

(34) Porter, K.; Trickett, D.; Bird, L. *REPiS: The Renewable Electric Plant Information System 1999 Ed*.; NREL Document TP-620-28674 (Online) Department of Energy, National Renewable Energy Laboratory 2000; 1-38. analysis.nrel.

(35) Joshi, P.; Xie, Y.; Ropp, M.; Galipeau, D.; Bailey, S.; Qiao, Q. Dye-Sensitized Solar Cells Based on Low Cost Nanoscale Carbon/TiO_2 Composite Counter Electrode. *Energy Environ. Sci.* **2009**, 2, 426-429.

(36) Boschloo, G.; Hagfeldt, A. Characteristics of the Iodide/Triiodide Redox Mediator

in Dye-Sensitized Solar Cells. *Acc. Chem. Res.* **2009**, 42, 1819-1826.

(37) Grätzel, M. Solar Energy Conversion by Dye-Sensitized Photovoltaic Cells. *Inorganic Chemistry.* **2005,** 44, 6841-6851.

(38) Liu, B.; Zhao, X.; Luo, W. The synergistic effect of two photosynthetic pigments in dye-sensitized mesoporous TiO2 solar cells. *Dyes Pigm.* **2008**, *76*, 327-331.

(39) Kumara, G.R.A.; Kaneko, S.; Okuya, M.; Onwona-Agyeman, B.; Konno, A., Tenakone, K. Shiso leaf pigments for dye-sensitized solid-state solar cell, *Sol. Energy Mater. Sol. Cells*. **2006**, *90,* 1220-1226.

(40) Vlachopoulos, N.; Liska, P.; Augustynski, J.; Grätzel, M. Very Efficient Visible Light Energy Harvesting and Conversion by Spectral Sensitization of High Surface Area Polycrystalline Titanium Dioxide Films. *J. Am. Chem. Soc.* **1988,** 110, 1216-1220.

(41) O'Regan, B.; Grätzel, M. A Low-Cost, High-Efficiency Solar Cell Based on Dye-Sensitized Colloidal TiO_2 Films. *Nature*. **1991,** 353, 737-740.

(42) Longo, C.; De Paoli, M-A. Dye-Sensitized Solar Cells: a Successful Combination of Materials. *J. Braz. Chem. Soc.* **2003,** 14, 889-901.

(43) Lenzmann, F.O.; Kroon, J.M. Recent Advances in Dye-Sensitized Solar Cells. *Advances in OptoElectronics.* **2007,** 2007, 1-10.

(44) Hamann, T. W.; Jensen, R. A.; Martinson, A. B. F.; Ryswyk, H. V.; Hupp, J. T. Advancing beyond current generation dye-sensitized solar cells. *Energy Environ. Sci*. **2008**, 1, 66–78.

(45) Grätzel, M. Swiss Federal Institute of Technology, Institute of Chemical Sciences and Engineering, Laboratory of Photonics and Interfaces, Zürich, Switzerland. Personal communication, November 2010.

(46) G24 Innovations. Personalizing Solar Power, 2011. www.g24i.com (accessed February 7, 2011).

(47) Lee, W. J.; Ramasamy, E.; Lee, D. Y.; Song, J. S. Dye-Sensitized Solar Cells: Scale Up and Current-Voltage Characterization. *Solar Energy Materials and Solar Cells.* **2007**, 91, 1676-1680.

(48) Park, J.; Koo, H.; Yoo, B.; Yoo, K.; Kim, K.; Choi, W.; Park, N. On the I-V Measurement of Dye Sensitized Solar Cells: Effect of Cell Geometry on photovoltaic parameters. *Solar Energy Materials and Solar Cells*. **2007**, 91, 1749-1754.

(49) Dai, S.; Wang, K.; Weng, J.; Sui, Y.; Huang, Y.; Xiao, S.; Chen, S.; Hu, L.; Kong, F.; Pan, X.; Shi, C.; Guo, L. Design of DSC Panel with Efficiency More than 6%. *Sol.*

Energy Mater. Sol. Cells. **2005**, 85, 447-455.

(50) Dai, S.; Weng, J.; Sui, Y.; Chen, S.; Xiao, S.; Huang, Y.; Kong, F.; Pan, X.; Hu, L.; Zhang, C.; Wang, K. The Design and Outdoor Application of Dye-Sensitized Solar Cells. *Inorg. Chim. Acta*. **2008**, 361, 786-791.

(51) Toivola, M.; Ahlskog, F.; Lund, P. Industrial Sheet Metals for Nanocrystalline Dye-Sensitized Solar Cell Structures. *Sol. Energy Mater. Sol. Cells.* **2006**, 90, 2881-2893.

(52) Kay, A.; Grätzel, M. Low Cost Photovoltaic Modules Based on Dye Sensitized Nanocrystalline Titanium Dioxide and Carbon Powder. *Sol. Energy Mater. Sol. Cells*. **1996,** *44*, 99-117.

(53) Kang, S.H; Kang, M.; Choi, S.; Kim, J.; Kim, H. Improved Charge Transport in Dye-Sensitized Solar Cells Employing Viscous Non-Volatile Electrolytes. *Electrochem. Commun.* (Online) **2008**, 10, 1326-1329.

(54) Khelashvili, G.; Behrens, S.; Weidenthaler, C.; Vetter, C.; Hinsch, A.; Kern, R.; Skupien, K.; Dinjus, E.; Bonnermann, H. Catalytic Platinum Layers for Dye Solar Cells: A Comparative Study. *Thin Solid Films.* **2006**, *511-512*, p. 342-348.

(55) Fang, X.; Ma, T.; Guan, G.; Akiyama, M.; Kida, T.; Abe, E. Effect of the Thickness of the Pt Film on a Counter Electrode on the Performance of a Dye-Sensitized Solar Cell. *J. Electroanal. Chem.* **2004**, *570*, 257-263.

(56) Burnside, S.; Winkel, S.; Brooks, K.; Shklover, V.; Grätzel, M.; Hinsch, A.; Kinderman, R.; Bradbury, C.; Hagfeldt, A. Deposition and Characterization of Screen-printed Porous Multi-layer Thick Film Structures from Semiconducting and Conducting Nanomaterials for Use in Photovoltaic Devices. *J. Mater. Sci.: Mater. Electron.* **2000**, 11, 355-362.

(57) Li, K.; Luo, Y.; Yu, Z.; Deng, M.; Li, D.; Meng, Q. Low Temperature Fabrication of Efficient Porous Carbon Counter Electrode for Dye-Sensitized Solar Cells. *Electrochem. Commun.* **2009**, 11, 1346-1349.

(58) Smestad, G.P.; Grätzel, M. Demonstrating Electron Transfer and Nanotechnology: A Natural Dye-Sensitized Nanocrystalline Energy Converter. *J. Chem. Educ* **1998**, 752-756.

(59) Bruecken, P.; Goates, W.; Kozlovsky, C. *Nanocrystalline Solar Cell Kit: Recreating Photosynthesis,* 2nd Ed.; Fanis, L.; Huseth, A.; Shanks, K. *Institute for Chemical Education:* Madison, WI, 2008.

(60) Suzuki, K.; Yamaguchi, M.; Kumagai, M.; Yanagida, S. Application of Carbon Nanotubes to Counter Electrodes of Dye-sensitized Solar Cells. *Chem. Lett.* **2003**, *32*, 28.

(61) Ramasamy, E.; Lee, W.J.; Lee, D.Y.; Song, J.S. Nanocarbon Counter electrode for Dye Sensitized Solar Cells. *Appl. Phys. Lett.* **2007**, *90*, 173103.

(62) Koo, B.K.; Lee, D.; Kim, H.; Lee, W.; Song, J.; Kim, H. Seasoning Effect of Dye-Sensitized Solar Cells with Different Counter Electrodes. *J. Electroceram.* **2006**, *17*, 79-82.

(63) Yanagida, S.; Yu, Y.; Manseki, K. Iodine/Iodine-Free Dye-Sensitized Solar Cells. *Acc. Chem. Res.* **2009**, 42 p. 1827-1838.

(64) Karim, M.A.; Song, M.; Park, J.S.; Kimg, Y.H.; Lee, M.J.; Lee, J.W.; Lee, C.W.; Cho, Y.; Gal, Y.; Lee, J.H.; Jin, S.H. Development of Liquid Crystal Embedded in Polymer Electrolytes Composed of Click Polymers for Dye-Sensitized Solar Cell Applications. *Dyes Pigm.* **2010**, *86*, 259-265.

(65) Wang, P.; Zakeeruddin, S.M.; Moser, J.E.; Grätzel, M. A New Ionic Liquid Electrolyte Enhances the Conversion Efficiency of Dye-Sensitized Solar Cells. *J. Phys. Chem. B.* **2003**, *107*, 13280-13285.

(66) Kubo, W.; Murakoshi, K.; Kitamura, T.; Yoshida, S.; Haruki, M.; Hanabusa, K.; Shirai, H.; Wada, Y.; Yanagida, S. Quasi-Solid-State Dye-Sensitized TiO_2 Solar Cells: Effective Charge Transport in Mesoporous Space Filled with Gel Electrolytes Containing Iodide and Iodine. *J. Phys. Chem. B.* **2001**, *105*,12809-12815.

(67) Wang, P.; Zakeeruddin, S.M.; Comte, P.; Exnar, I.; Grätzel, M. Gelation of Ionic Liquid-Based Electrolytes with Silica Nanoparticles for Quasi-Solid State Dye-Sensitized Solar Cells. *J. Am. Chem. Soc.* **2003**, *125*, 1166-1167.

(68) Wang, P.; Zakeeruddin, S.M.; Moser, J.E.; Nazeeruddin, M.K.; Sekiguchi, T.; Grätzel, M. A Stable Quasi-Solid-State Dye-Sensitized Solar Cell with an Amphiphilic Ruthenium Sensitizer and Polymer Gel Electrolyte. *Nat. Mater.* (Online) **2003**, *2*, 402-407 www.nature.com/naturematerials (Accessed July 7, 2010).

(69) Lehninger, A. *Biochemistry*, 2nd ed.; Worth Publishers, Inc.: 1975.

(70) Karp, G. *Cell and Molecular Biology: Concepts and Experiments*, 6th ed.; John Wiley and Sons: 2009.

(71) Taiz, L and E. Zeiger. 2006. Plant Physiology. 4th. Ed. Sinauer, Publishing.

(72) Farabee, M. http://www.emc.maricopa.edu/faculty/farabee/biobk/excitation.gif (accessed July 29, 2010), Estrella Mountain Community College online biology book.

(73) Govindjee. The Photosynthesis Page Govindjee. http://www.life.illinois.edu/govindjee/NewZScheme.jpg (accessed July 29, 2010), University of Illinois at Urbana-Champaign.

(74) Berg, S. http://course1.winona.edu/sberg/ILLUST/fig10-7.gif (accessed July 29, 2010), Dr. Steven Berg's Home Page, Winona State University.

(75) Kay, A.; Grätzel, M. Artificial Photosynthesis. 1. Photosensitization of TiO2 Solar Cells with Chlorophyll Derivatives and Related Natural Porphyrins. *J. phys. Chem*. **1993**, *97*, 6272-6277.

(76) Angelo State University. Professor Boudreaux's webpage. http://www.angelo.edu/faculty/ kboudrea/index.htm (accessed August 21, 2010).

(77) McQuarrie, D. A. *Quantum Chemistry*, 2nd ed.; University Science Books: Sausalito, 2008.

(78) Padova, P. D.; Lucci, M.; Olivieri, B.; Quaresima, C.; Priori, S.; Francini, R.; Grilli, A.; Hricovini, K.; Davoli, I. Natural hybrid organic-inorganic photovoltaic devices. *Superlattices Microstruct.*, **2009**, *45*, 555-563.

(79) Grätzel, M. Conversion of Sunlight to Electric Power by Nanocrystalline Dye-Sensitized Solar Cells. *J. Photochem. Photobiol.* **2004,** 164, 3-14.

(80) Yamazaki, E.; Murayama, M.; Nishikawa, N.; Hashimoto,N.; Shoyama, M.; Kurita, O. Utilization of natural carotenoids as photosensitizers for dye-sensitized solar cells. *Sol. Energy*, **2007**, *81* 512–516.

(81) Cherepy, N. J.; Smestad, G. P.; Grätzel, M.; Zhang, J. Z. Ultrafast Electron Injection: Implications for a Photoelectrochemical Cell Utilizing an Anthocyanin Dye-Sensitized TiO2 Nanocrystalline Electrode. *J. Phys. Chem. B* **1997**, *101,* 9342-9351.

(82) Tennakone, K.; Kumarasinghe, A. R.; Kumara, G. R. R. A; Wijayantha, K. G. U.; Sirimanne, P. M. Nanoporous TiO2 photoanode sensitized with the flower pigment cyaniding. *J. Photochem. Photobiol.,* **1997**, 108, 193-195.

(83) Dai, Q.; Rabani, J. Unusually efficient photosensitization of nanocrystalline TiO2 films by pomegranate pigments in aqueous medium. *New J. Chem*., *2002*, 26, 421–426.

(84) Calogero, G.; Marco, G. D. Red Sicilian orange and purple eggplant fruits as natural sensitizers for dye-sensitized solar cells. *Sol. Energy Mater. Sol. Cells*, **2008**, *92*, 1341– 1346.

(85) Zhang, D.; Yamamoto, N.; Yoshida, T.; Minoura, H. Natural dye sensitized solar cells, *Trans. MRS J.* **2002**, 27 811.

(86) Polo, A. S.; Iha, N. Y. M. Blue sensitizers for solar cells: Natural dyes from Calafate and Jaboticaba. *Sol. Energy Mater. Sol. Cells*, **2006**, *90*, 1936–1944.

(87) Hao, S.; Wu, J.; Huang, Y.; Lin, J., Natural dyes as photosensitizers for dye-sensitized solar cell, *Sol. Energy,* **2006**, **80,** 209-214.

(88) Chang,H.; Lo, Y.; Pomegranate leaves and mulberry fruit as natural sensitizers for dye-sensitized solar cells, *Sol. Energy*, *84*, 1833-1837.

(89) Wongcharee, K.; Meeyoo, V.; Chavadej, S.; Dye sensitized solar cell using natural dyes exracted from rosella and blue pea flowers. *Sol. Energy Mater. Sol. Cells* **2007**, *91* 566-571.

(90) Luque, A, Hegedus, S. Handbook of Photovoltaic Science and Engineering, 1st ed. Wiley: New York, 2003.